mαcrϕ@ufmg

UNIVERSIDADE FEDERAL DE MINAS GERAIS

Escola de Engenharia

Programa de Pós-Graduação em Engenharia Elétrica

Research group MACRO - Mechatronics, Control and Robotics

MODEL PREDICTIVE CONTROL SCHEMES WITH AVOIDANCE FEATURES

Marcelo Alves dos Santos

Belo Horizonte

2023

Marcelo Alves dos Santos

MODEL PREDICTIVE CONTROL SCHEMES WITH AVOIDANCE FEATURES

Ph.D thesis submitted to the Graduate Program in Electrical Engineering of the Engineering School at the Universidade Federal de Minas Gerais, in partial fulfillment of the requirements for the degree of Doctorate in Electrical Engineering.

Advisors: Guilherme Vianna Raffo
Antonio Ferramosca

Belo Horizonte
2023

Santos, Marcelo Alves dos.
S237m Model Predictive Control schemes with avoidance features [recurso eletrônico] / Marcelo Alves dos Santos. - 2023.
1 recurso online (138 f. : il., color.) : pdf.

Orientador: Guilherme Vianna Raffo.
Coorientador: Antonio Ferramosca.

Tese (doutorado) - Universidade Federal de Minas Gerais, Escola de Engenharia.

Apêndices: f. 132-138.

Bibliografia: f. 125-131.
Exigências do sistema: Adobe Acrobat Reader.

1. Engenharia elétrica - Teses. 2. Controle preditivo - Teses. 3. Estabilidade- Teses. I. Raffo, Guilherme Vianna. II. Ferramosca, Antonio. III. Universidade Federal de Minas Gerais. Escola de Engenharia. IV. Título.

CDU: 621.3(043)

Ficha catalográfica elaborada pelo bibliotecário Reginaldo César Vital dos Santos CRB/6 2165
Biblioteca Prof. Mário Werneck, Escola de Engenharia da UFMG

UNIVERSIDADE FEDERAL DE MINAS GERAIS
ESCOLA DE ENGENHARIA
PROGRAMA DE PÓS-GRADUAÇÃO EM ENGENHARIA ELÉTRICA

FOLHA DE APROVAÇÃO

"MODEL PREDICTIVE CONTROL SCHEMES WITH AVOIDANCE FEATURES"

MARCELO ALVES DOS SANTOS

Tese de Doutorado submetida à Banca Examinadora designada pelo Colegiado do Programa de Pós-Graduação em Engenharia Elétrica da Escola de Engenharia da Universidade Federal de Minas Gerais, como requisito para obtenção do grau de Doutor em Engenharia Elétrica. Aprovada em 08 de maio de 2023. Por:

Prof. Dr. Guilherme Vianna Raffo
DELT (UFMG) - Orientador

Prof. Dr. Antonio Ferramosca
DIGIP (University of Bergamo) - Coorientador

Prof. Dr. Leonardo Antônio Borges Torres
DELT (UFMG)

Prof. Dr. Luciano Cunha de Araújo Pimenta
DELT (UFMG)

Prof. Dr. Julio Elias Normey Rico
DAS (UFSC)

Prof. Dr. Tito Luís Maia Santos
DEE (UFBA)

---

sei! assinatura eletrônica

Documento assinado eletronicamente por **Guilherme Vianna Raffo**, **Professor do Magistério Superior**, em 09/05/2023, às 09:38, conforme horário oficial de Brasília, com fundamento no art. 5º do Decreto nº 10.543, de 13 de novembro de 2020.

sei! assinatura eletrônica

Documento assinado eletronicamente por **Antonio Ferramosca**, **Usuário Externo**, em 09/05/2023, às 10:07, conforme horário oficial de Brasília, com fundamento no art. 5º do Decreto nº 10.543, de 13 de novembro de 2020.

sei! assinatura eletrônica

Documento assinado eletronicamente por **Julio Elias Normey Rico**, **Usuário Externo**, em 09/05/2023, às 10:56, conforme horário oficial de Brasília, com fundamento no art. 5º do Decreto nº 10.543, de 13 de novembro de 2020.

sei! assinatura eletrônica

Documento assinado eletronicamente por **Leonardo Antonio Borges Torres**, **Professor do Magistério Superior**, em 09/05/2023, às 10:57, conforme horário oficial de Brasília, com fundamento no art. 5º do Decreto nº 10.543, de 13 de novembro de 2020.

sei! assinatura eletrônica

Documento assinado eletronicamente por **Luciano Cunha de Araujo Pimenta**, **Professor do Magistério Superior**, em 09/05/2023, às 13:48, conforme horário oficial de Brasília, com fundamento no art. 5º do Decreto nº 10.543, de 13 de novembro de 2020.

sei! assinatura eletrônica

Documento assinado eletronicamente por **Tito Luís Maia Santos**, **Usuário Externo**, em 10/05/2023, às 20:15, conforme horário oficial de Brasília, com fundamento no art. 5º do Decreto nº 10.543, de 13 de novembro de 2020.

A autenticidade deste documento pode ser conferida no site https://sei.ufmg.br/sei/controlador_externo.php?acao=documento_conferir&id_orgao_acesso_externo=0, informando o código verificador **2276229** e o código CRC **C1755751**.

To my beloved wife and parents

Acknowledgments

Entering such a long project is a mix of challenge and excitement. In the beginning, I could feel like the path was all figured out, but the world is indeed non-linear and time-variant. Some things went wrong, some other ones turned out to be surprisingly good. Some challenges were bigger than expected on a technical and personal level, while others were very fun to tackle. Now, at the end of this project, I can see how not only my research evolved but also how I evolved in the roles I play as a husband, son, brother, friend, researcher, teacher, advisee, and college. In this context, I can only thank everyone involved in this process for their support and understanding during this period.

I thank my beloved wife for always supporting me in pursuing my dreams. When I was hesitant, exhausted, or wanting to give up, you kept me on my toes and helped me to just keep going. For this, I cannot thank you enough. I also thank my dear parents for encouraging me to pursue my studies. Thanks for always being my safe harbor in the most difficult times and for giving me valuable advice and encouragement. It is impossible to measure the role you both have in my life and in my achievements. To my siblings, I will always keep you both in my heart. Despite the distance, you were always by my side. I also extend my gratitude to my other family members.

To my advisors, Prof. Guilherme Vianna Raffo and Prof. Antonio Ferramosca, I was fortunate to have had the opportunity to work with you in the past years. Without you, this work would not be possible. Thank you for all the support and understanding and for guiding me on this path that ended with this thesis and has opened numerous possibilities for future collaborations.

Moreover, I would like to thank all the colleagues from the MACRO team. Although the pandemic reduced our time together, collaborations and exchange of ideas were invaluable. Finally, in the person of Prof. Frederico Gadelha Guimarães and Prof. Carmela Maria Polito Braga, I thank all the professors and staff of the Graduate Program in Electrical Engineering and Department of Electronics Engineering.

Gratiam pro gratia

Resumo

Nos últimos anos, pode-se observar um movimento significativo em direção ao Controle Preditivo Baseado em Modelo (MPC, do inglês *Model Predictive Control*), principalmente devido à sua flexibilidade e aos avanços obtidos na garantia de estabilidade e robustez. Além disso, a capacidade do MPC de impor restrições e projetar funções de custo abriu novas possibilidades para aplicações que requerem múltiplos objetivos. Entre eles, o problema de se evitar regiões específicas do espaço (problema de evitação) é particularmente desafiador devido a não convexidades presentes no espaço admissível.

Na literatura de MPC, existem trabalhos teoricamente fundamentados que lidam com problemas não convexos buscando soluções que forneçam aproximações convexas, por exemplo, incorporando um homeomorfismo ao problema de otimização. No entanto, esses trabalhos não abordam o problema de não convexidades causadas por buracos no interior do espaço admissível, pois isso não é típico da maioria das aplicações e aparece principalmente ao lidar com problemas de evitação. A literatura de MPC para evitação é composta em sua maioria por trabalhos focados na aplicação, deixando de lado alguns fundamentos de MPC. Por exemplo, adicionar restrições diretamente ao problema de controle ótimo pode resultar em desafios em termos da factibilidade do algoritmo de controle. Da mesma forma, em formulações para regulação em aplicações que requerem rastreamento ou referências contínuas por partes, não se pode garantir estabilidade em malha-fechada. Além disso, os trabalhos que modificam o funcional de custo para incluir o problema de evitação geralmente não lidam com o impacto de perder as propriedades de decrescimento da função valor. Nesse contexto, esta tese investiga o problema de evitação dentro do arcabouço de controle preditivo baseado em modelo com o objetivo de formalizar conceitos e fornecer uma estrutura teórica sólida para um problema de controle que está cada vez mais presente na literatura.

Inspirados pelas formulações de *tracking* MPC, exploramos a ideia central de incorporar variáveis artificiais ao problema de controle ótimo. Essa abordagem nos permite introduzir capacidade de evitação nas formulações de *tracking* MPC, resultando em sistemas em malha fechada com um domínio de atração ampliado e com garantias de factibilidade recursiva para referências contínuas por partes. As variáveis artificiais são consideradas juntamente com uma penalidade para evitação, formando a base de nossas estratégias e garantindo a factibilidade recursiva mesmo na presença de um número desconhecido de regiões a serem evitadas. Além disso, ao considerar um problema convexo equivalente, esta abordagem supera os problemas de se trabalhar com espaços admissíveis não convexos. As estratégias de controle propostas são analisadas por meio do paradigma de estabilidade entrada-estado (ISS, do inglês *input-to-state stability*), permitindo provar que, sob a hipótese de que o custo de evitação é uniformemente limitado ao longo do tempo, o sistema em malha fechada é estável entrada-estado e recursivamente factível. Finalmente, esta tese propõe esquemas de controle lineares e não lineares para o problema de evitação e examina sua robustez na presença de distúrbios desconhecidos porém limitados.

Palavras-chave: mpc; evitação; rastreamento de referência; robustez.

Abstract

In recent years, there has been a significant movement towards Model Predictive Control (MPC), primarily due to its flexibility and advancements in ensuring stability and robustness. Furthermore, the MPC ability to impose constraints and design objective functions has opened new possibilities for applications that require multiple objectives. Amongst them, the problem of avoidance has become a prominent challenge due to the non-convexities of the admissible space.

In the MPC literature, there are theoretically grounded works that handle non-convex problems seeking solutions that provide convex approximations, for instance, incorporating a convexifying homeomorphism into the optimization problem. However, these works do not address the problem of non-convexity caused by holes inside the space, since this is not typical for most applications and mainly appears when handling avoidance problems. The literature for MPC with avoidance features is mostly composed of works focused on the application, leaving some MPC fundamentals aside. For instance, adding constraints directly to the optimal control problem can result in feasibility issues for the MPC algorithm. Similarly, in regulatory formulations for applications requiring tracking or changing targets, stability cannot be guaranteed. Additionally, works modifying the cost functional to include avoidance often do not deal with the impact of losing the value function's decreasing properties. In this context, this thesis investigates the problem of avoidance within the model predictive control framework aiming to formalize concepts and provide a solid theoretical framework for a control problem that is increasingly prevalent in the literature.

Inspired by the set-point tracking MPC framework, we explore the central idea of incorporating artificial variables into the optimal control problem. This approach enables us to introduce avoidance features into the set-point tracking MPC strategy, resulting in closed-loop systems with an enlarged domain of attraction and improved feasibility assurance against changing references. The artificial variables are considered together with an avoidance penalty, forming the basis of our strategies and ensuring recursive feasibility even in the presence of an unknown number of regions to avoid. Additionally, this approach overcomes the problems of working with non-convex admissible spaces, allowing us to consider an equivalent convex problem. We analyze the resulting control schemes using the input-to-state stability (ISS) paradigm and show that, under the mild assumption that the avoidance cost is uniformly bounded over time, the closed-loop system is input-to-state stable and recursively feasible. Finally, this thesis proposes both linear and non-linear control schemes for avoidance and examines the robustness of the approach in the face of unknown but bounded disturbances.

Keywords: mpc, avoidance, set-point tracking, robustness.

List of Figures

1.1 This figure exemplifies the problem of loss of feasibility during changing set-points. In Figure (a), the regulatory formulation is considered and the domain of attraction $X_3(s_i)$ (in light gray) and the invariant set $\Omega(s_i)$ (in dark gray) are presented for the set-point s_i, with $i = 1, 2$. In Figure (b), the tracking formulation is considered and the domain of attraction $X_3(\Omega^t)$ (in light gray) and the invariant set Ω^t (in yellow) are also presented. In both figures, the green set represents the set of equilibrium states X_s. . . . 26

1.2 This figure exemplifies the problem of loss of feasibility during changing set-points in a non-convex admissible space. In the figure, the tracking invariant set Ω^t (in yellow), and the invariant sets for the regulatory formulation $\Omega(s_1)$ and $\Omega(s_2)$ (in dark grey) are presented. Further, the set of equilibrium states X_s is depicted in green while the non-feasible region obstructing the space O is depicted in red. 33

3.1 Complete trajectory performed by the ball (blue line) over the non-convex plate composed by the union of two ellipses. In the figure, the black cross-mark denotes the desired set-point. 63

3.2 Absolute output tracking error with $e_{p_1} = p_1 - p_{1t}$ and $e_{p_2} = p_2 - p_{2t}$. In the figure, it is illustrated the relation between error reduction and avoidance. 64

3.3 Time evolution of the ball position (p_1 and p_2) and the plate angles (θ_1 and θ_2) during the tracking of the provided set-point. 64

3.4 Time evolution of the desired angular accelerations (a_1 and a_2), the manipulated variables of the system. 65

3.5 Trajectory performed by the UAV (black line) to safely complete a given task while avoiding nine previously unknown obstacles, which are denoted by the green rectangle-shaped objects. In the figure, the UAV is denoted as a black cross with blue and red spheres in its extremities and the light red sphere around the UAV denotes the range in which obstacles can be detected. 66

3.6 Absolute output tracking error illustrating the relation between error reduction and avoidance. In the figure, $e_x = x^{\mathcal{I}} - x_r$, $e_y = y^{\mathcal{I}} - y_r$, and $e_z = z^{\mathcal{I}} - z_r$. 67
3.7 Time evolution of the quadrotor UAV orientation (ϕ, θ, and ψ) during the execution of the provided task. 68
3.8 Time evolution of the applied lift forces to the quadrotor UAV, with f_i being the lift force of the i-th propeller. 68

4.1 The figure displays the nominal (dashed blue) and avoidance (solid green) trajectories for a disturbance-free case. Arrows depict the double integrator phase portrait, the red set represents the non-feasible region, the circle yellow marker identifies the target, and the square yellow marker indicates the initial condition. 86
4.2 The figure illustrates the evolution of the disturbed system for different disturbance realizations. The red set represents the non-feasible region, while the green set denotes the enlarged non-feasible region. The light blue sets depict the tubes containing the evolution of the disturbed system. . . 87
4.3 The figure displays the time evolution of the control inputs for a single simulation. The dashed blue line represents the nominal control law, while the solid black line depicts the dual feedback control law that incorporates a feedback term to reduce the prediction error (see equation (4.23)). . . . 87
4.4 Complete trajectory followed by the UAV as it safely navigates from the initial condition (bottom-left) to the target (upper-right), while avoiding three obstacles. The red sets in the figure represent the obstacles, while the green sets depict the enlarged non-feasible regions. 90
4.5 Time evolution of the quadrotor UAV position ($x^{\mathcal{I}}$, $y^{\mathcal{I}}$, and $z^{\mathcal{I}}$) alongside the considered disturbance profile during the execution of the provided task. 90
4.6 Time evolution of the quadrotor UAV attitude (ϕ, θ, and ψ) alongside the considered disturbance profile during the execution of the provided task. . 91
4.7 Time evolution of the quadrotor UAV linear velocity ($\dot{x}^{\mathcal{I}}$, $\dot{y}^{\mathcal{I}}$, and $\dot{z}^{\mathcal{I}}$) alongside with the considered disturbance profile during the execution of the provided task. 91
4.8 Time evolution of the quadrotor UAV angular velocity ($\dot{\phi}$, $\dot{\theta}$, and $\dot{\psi}$) alongside with the considered disturbance profile during the execution of the provided task. 92
4.9 Time evolution of the applied lift forces to the quadrotor UAV, with f_i being the lift force of the i-th propeller. 92

5.1 The trajectory of the differential mobile robot is shown in the figure for cases with and without terminal constraints. The desired set-point is denoted by a black star marker in the bottom-right, green squares represent obstacles, the triangle shape represents the robot pose, and the circle around the robot depicts the sensor range of detection. 110
5.2 Absolute position error with $e_x = x^{\mathcal{I}} - x_t$ and $e_y = y^{\mathcal{I}} - y_t$ for the cases with and without terminal constraint. In the figure, it is illustrated the relation between error reduction and avoidance. 111
5.3 Time evolution of the mobile robot states ($x^{\mathcal{I}}$ $y^{\mathcal{I}}$ θ) for the cases with and without terminal constraint during the tracking of the desired target. . . 112
5.4 Time evolution of the manipulated variables (forward and angular velocities) for the cases with and without terminal constraint. 112
5.5 Domains of attraction for the set-point tracking and set-point stabilization strategies considering formulations with terminal equality constraints. In the figure, the blue set represents the domain of attraction for the tracking approach, while the green set represents the domain of attraction for the regulatory approach. 113
5.6 Complete trajectory performed by the UAV to safely navigates from the initial condition (bottom-left) to the target (upper-right) while avoiding five obstacles (green sets). In the figure, the UAV is denoted as a black cross with blue and red spheres in its extremities. 114
5.7 X-Y view of the complete trajectory performed by the UAV to safely complete the given task. In the figure, the circles around the UAV denote the sensor range of detection. 115
5.8 X-Z view of the complete trajectory performed by the UAV to safely complete the given task. In the figure, the circles around the UAV denote the sensor range of detection. 116
5.9 Absolute output tracking error illustrating the relation between error reduction and avoidance for the cases with and without terminal constraint. In the figure, $e_x = x^{\mathcal{I}} - x_t$, $e_y = y^{\mathcal{I}} - y_t$, and $e_z = z^{\mathcal{I}} - z_t$. 116
5.10 Time evolution of the quadrotor UAV orientation (ϕ, θ, and ψ) for the cases with and without terminal constraint. 118
5.11 Applied lift forces to the quadrotor UAV for the cases with and without terminal constraint. In the figure, f_i denotes the lift force of the i-th propeller. 118

A.1 Ball-on-plate system frames and variables definition. 133
A.2 Differential mobile robot with non-holonomic constraints frames and variables definition. 134
A.3 Quadrotor UAV frames and variables definition. 136

Notation

Mathematical notation

$\exists$	there exists
$\in$	is an element of
$\forall$	for all
$\sum$	sum operator
$\prod$	product operator
$f(\cdot)$	function f
$f : X \mapsto Y$	f is a function that maps set X into Y
$f_1 \circ f_2$	composition of two functions f_1 and f_2
id	identity function from $\mathbb{R}$ onto $\mathbb{R}$
$\lvert x \rvert$	absolute value of x
$\lVert x \rVert$	Euclidean norm of x
$\lVert x \rVert_P$	weighted Euclidean norm of x
$\lvert x \rvert_X$	distance of a point x from the set X
$\boldsymbol{u}$	sequence of values of a signal $(u(0), u(1), \cdots)$
$\boldsymbol{u}(a)$	parameter-dependent signal
$u(i; a)$	i-th element of $\boldsymbol{u}(a)$
$\mathbb{I}$	integers
$\mathbb{I}_{\geq 0}$	non-negative integers
$\mathbb{I}_{n:m}$	integers in the interval $[n, m]$

$\mathbb{R}$	real numbers
$\mathbb{R}_{\geq 0}$	non-negative real numbers
$\mathbb{R}^n$	real-valued vectors with dimension n
$\mathbb{R}^{n\times m}$	real-valued matrices with dimension $m \times n$
$X \cup Y$	union of sets X and Y
$X \cap Y$	intersection of sets X and Y
$X \subseteq Y$	set X is a subset of set Y
$X \subset Y$	set X is a proper subset of set Y
$X \oplus Y$	Minkowski sum between sets X and Y
$X \ominus Y$	Pontryagin difference between sets X and Y
$\mathrm{Proj}_a(X)$	orthogonal projection of the set X onto the a space
$(\cdot)'$	transpose operator
$O_{n,m}$	matrix of zeros with dimension $n \times m$
I_n	identity matrix with dimension $n \times n$
$P > 0$	positive definite symmetric matrix P
$\mathrm{diag}\{\cdot\}$	diagonal matrix with diagonal composed by the elements of $\{\cdot\}$
max	maximum
min	minimum
sup	supremum or least upper bound
arg	argument or solution of an optimization

Symbols

x	state vector
u	input vector
y	output
w	process disturbance

n	state dimension
m	input dimension
p	output dimension
k	sample time
A, B, C, D	discrete time linear system matrices
f, h	discrete time non-linear system functions
$\phi(j; x, \boldsymbol{u})$	system solution at instant j for an initial condition x and control sequence $\boldsymbol{u}$
X	state constraint set
U	input constraint set
Y	output constraint set
W	process disturbance constraint set
Z	joint state and input constraint set
$O(i)$	i-th non-feasible output region
Ω	terminal set
Ω_t^a	terminal set for tracking
$X_N(\Omega)$	N-steps controllable set to Ω
$\mathcal{R}$	reachable set
$(\cdot)_s$	subscript s denotes steady state variables
$(\cdot)_t$	subscript t denotes a target condition
$(\cdot)_a$	subscript a denotes artificial variables
$(\cdot)^O$	superscript O denotes an optimal condition
$\tilde{x}$	tilde accent over a vector denotes a feasible solution to an optimization problem
$\tilde{X}$	tilde accent over a set denotes a space without non-feasible regions
$\bar{x}$	bar accent denotes nominal variables
N	horizon length

N_p	prediction horizon length
N_c	control horizon length
N_o	number of non-feasible output regions
Q	state penalty matrix
R	input penalty matrix
P	terminal penalty matrix
κ	offset cost penalty matrix
μ	avoidance penalty scalar
$V_N(\cdot)$	MPC value function with horizon N
$V_{N_c,N_p}(\cdot)$	MPC value function with horizons N_p and N_c
$\ell(\cdot)$	stage cost
$V_f(\cdot)$	terminal penalty
$V_{of}(\cdot)$	offset cost
$V_{av}(\cdot)$	avoidance cost
$V_s(\cdot)$	shifted value function
$F(\cdot)$	penalty function

Contents

1 Introduction **19**

1.1 Motivation . . . 19
1.2 Model Predictive Control . . . 21
1.3 Set-point Tracking Model Predictive Control . . . 24
1.4 Robustness in Model Predictive Control . . . 27
1.5 The Avoidance Problem . . . 29
1.6 Contributions . . . 33
1.6.1 Set-point tracking MPC with avoidance features . . . 33
1.6.2 Robust set-point tracking MPC with avoidance features . . . 34
1.6.3 Non-linear set-point tracking MPC with avoidance features . . . 34
1.7 List of Publications . . . 34
1.8 Structure of the Text . . . 35

2 Mathematical Preliminaries **37**

2.1 Set Methods in Control Theory . . . 37
2.1.1 General definitions . . . 37
2.1.2 Set operations . . . 38
2.1.3 Set representations . . . 38
2.1.4 Invariant sets . . . 39
2.2 Lyapunov Stability Theory . . . 42
2.3 Final Remarks . . . 45

3 Set-Point Tracking with Avoidance **46**

3.1 Introduction . . . 46
3.2 Problem Description . . . 46
3.3 Control Design . . . 49
3.4 Controller Properties . . . 60
3.4.1 Stability under changing references . . . 60
3.4.2 Unreachable references . . . 60
3.4.3 Enlarged domain of attraction . . . 61

3.4.4 Avoidance guarantees . . . 61
3.5 Numerical Examples . . . 61
3.5.1 Ball-on-plate with non-convex plate . . . 62
3.5.2 UAV navigation in cluttered environment . . . 65
3.6 Final Remarks . . . 69

4 Robust Set-Point Tracking with Avoidance 70
4.1 Introduction . . . 70
4.2 Problem Description . . . 71
4.3 Tube-Based Robust Approach . . . 72
4.4 Nominal Steady Conditions . . . 74
4.5 Control Design . . . 75
4.6 Numerical Examples . . . 84
4.6.1 Double integrator . . . 85
4.6.2 Quadrotor UAV . . . 88
4.7 Final Remarks . . . 93

5 Non-linear Set-Point Tracking with Avoidance 94
5.1 Introduction . . . 94
5.2 Problem Description . . . 95
5.3 Control Design . . . 96
5.3.1 Relaxed terminal equality constraint . . . 105
5.3.2 Weighted terminal cost . . . 107
5.4 Numerical Examples . . . 108
5.4.1 Control strategies setup . . . 108
5.4.2 Differential Mobile Robot . . . 109
5.4.3 Quadrotor UAV . . . 113
5.5 Final Remarks . . . 120

6 Conclusion 121
6.1 Continuity Proposals . . . 123

Bibliography 125

A Numerical Examples Models 132
A.1 Ball-on-plate . . . 132
A.2 Differential Mobile Robot . . . 134
A.3 Quadrotor UAV . . . 135

1
Introduction

This chapter describes the motivation behind working with avoidance within the Model Predictive Control (MPC) framework and introduces the research problem of this thesis. An overview of the MPC methodology together with a literature review is provided. Then, the state-of-the-art related to the avoidance problem is presented. Finally, the contributions of this work to the MPC literature are stated.

1.1 Motivation

Among numerous control techniques, MPC strategies have stood out due to their ability to control constrained multiple-input multiple-output systems. These controllers can deal in a simple way with multivariate underactuated systems, ensuring input-to-output stability and internal stability (Rawlings & Mayne, 2009). Moreover, their prediction-based nature allows for obtaining a control system capable of providing smoother signals, which results in smaller control efforts. MPC strategies have been mainly used as an advanced control technique for industrial processes and most of their advances have been made guided by the need to create systems that meet quality and uniformity standards. Two reasons justify this phenomenon: on one hand, to obtain systems subject to strict safety and quality controls; on the other hand, to promote sustainable growth by minimizing their environmental impact and the consumption of resources (Ellis et al., 2014). Therefore, it is desirable to design control techniques providing policies that optimize specific efficiency criteria and guarantee the satisfaction of the limits imposed on the systems.

In the last two decades, MPC strategies have achieved important theoretical progress regarding the guarantee of stability and robustness, the incorporation of secondary objectives to those of traditional dynamic control, the inclusion of stochasticity in its formulation, and efficient solution for optimization problems, among others (Mayne, 2014). Consequently, there is a movement towards MPC that seeks to benefit from these advances and from its flexibility alongside the increasing computational power of embedded systems, allowing this strategy to be considered for real-world applications. Particularly, as a receding horizon optimal control technique, the flexibility to impose constraints and to design the objective function has brought new possibilities for applications requiring multiple objectives.

The design of a multi-level control framework is a traditional way of solving multi-objective problems (Tatjewski, 2008). While this framework addresses objectives such as efficiency of operation, capacity, and profitability, among others, an underlying design assumption for low-level controllers is that the reference is feasible to execute. These goals are commonly addressed by upper-level systems, which are responsible for dictating feasible objective-oriented references (Ellis et al., 2014). However, this procedure is not trivial, since problems can appear either by the change of dynamics around the reference or by guaranteeing constraints satisfaction during the transition to a new reference. Therefore, the overall result might present performance deterioration in the case where the layers' coupling is not handled accordingly. In such conditions, approaches considering multi-objective problems in a unified non-decoupled scheme are of interest.

The problem of avoidance, investigated in this thesis, fits the previous description. Historically, researchers have resorted to multi-level frameworks that split reference generation from dynamic control. Nevertheless, in the past decade, there has been an increasing number of solutions proposing non-decoupled schemes within the MPC framework, aiming to exploit the optimization problem design through its objective function and constraints. This movement, however, is not limited to the avoidance problem. For instance, in robotics, MPC has typically been used to incorporate secondary tasks into the main control objective (Jacquet & Franchi, 2022).

Avoidance is a challenging problem in control because, ultimately, it involves non-convexity. In the MPC literature, for instance, there are theoretically grounded works that handle non-convex problems seeking solutions that provide convex approximations. However, the majority of these works do not tackle the problem of non-convexity caused by holes inside the space, since this is not typical for most applications and mainly appears when handling avoidance problems. In other communities, such as robotics, the problem of avoidance considering single-layer schemes with MPC is being addressed. However, these works often leave some MPC fundamentals aside, mainly focusing on the application. For instance, when constraints are directly added to the optimal control problem, the resulting MPC algorithm may present feasibility issues. Additionally, in the case of regulatory formulations for applications that require tracking or changing targets, no stability guarantee can be provided. In fact, the MPC community has developed theories and tools in the past decades that are not being used in these new applications to carefully handle some points that are important for MPC strategies in terms of feasibility and stability.

In this context, this thesis proposes MPC strategies with avoidance features that address some problems commonly found in the literature. The main motivation of this work is to formalize concepts and provide a solid theoretical background for a control problem that is becoming more prevalent in the literature.

1.2 Model Predictive Control

MPC is one of the few strategies that allow the control of constrained systems regarding an optimal criterium while ensuring constraint satisfaction, stability, and convergence to an equilibrium point with a potentially enlarged domain of attraction. Under certain assumptions, closed-loop stability can be demonstrated for any feasible initial condition (Mayne et al., 2000). For that reason, MPC has attracted the efforts of numerous researchers in recent years, which has led to notable theoretical advances in the understanding of the control problem, the study of its characteristics and limitations, and the design of stabilizing procedures (Rawlings & Mayne, 2009; Mayne, 2014).

All MPC formulations are in some way based on the idea of solving a finite horizon optimal control problem at each sampling time, such that, right after the problem is solved, the prediction horizon recedes and the initial conditions of the optimization problem are updated (Camacho & Bordons, 2004). Thus, regardless of the formulation, controllers following the MPC methodology present these three main ingredients: prediction, optimization, and receding horizon policy.

The prediction of the future evolution of the system can be obtained through prediction models of the form

$$x(k+1) = f(x(k), u(k)), \tag{1.1}$$

where $x(k)$ and $u(k)$ are, respectively, state and input vectors constrained as

$$(x(k), u(k)) \in X \times U, \;\; \forall k \in \mathbb{I}_{\geq 0}, \tag{1.2}$$

with X and U being, respectively, the sets of admissible states and inputs.

Based on the predictions, the following cost functional can be considered:

$$V_N(x; \boldsymbol{u}) = \sum_{j=0}^{N-1} \ell(x(j), u(j)) + V_f(x(N)), \tag{1.3}$$

with N being the horizon length, x being the initial condition, $\boldsymbol{u}$ being a control sequence, $u(j)$ being the j-th element of the control sequence computed at sample time k, $x(j)$ being the j-step ahead prediction at sample time k. The functions $\ell(x,u)$ and $V_f(x)$ are known, respectively, as stage cost and terminal cost.

An optimal control sequence, $\boldsymbol{u}^O(x)$, that minimizes the cost functional $V_N(x;\boldsymbol{u})$ for the nominal system while satisfying the constraints can be obtained by solving the following optimization problem:

$$
\begin{aligned}
\min_{\boldsymbol{u}}\ & V_N(x;\boldsymbol{u}) \\
\text{s.t. } & x(0) = x, && \text{(1.4a)}\\
& x(j+1) = f(x(j),u(j)), j \in \mathbb{I}_{0:N-1}, && \text{(1.4b)}\\
& (x(j),u(j)) \in X \times U, j \in \mathbb{I}_{0:N-1}, && \text{(1.4c)}\\
& x(N) \in \Omega, && \text{(1.4d)}
\end{aligned}
$$

with the terminal state constraint ensuring that the last predicted state will reach an admissible invariant set Ω under a terminal control law $\kappa_f(x)$, i.e., a control strategy that dictates how the system should behave as it approaches a specified terminal state.

The solution of the optimization problem, which is known as an open-loop optimal control problem, results in the control sequence $\boldsymbol{u}^O(x) = (u^O(0;x), u^O(1;x), \cdots, u^O(N-1;x))$. Based on the receding horizon policy of MPC and the fact that the optimization problem is solved at each sampling time using the current knowledge of the system parameters, an implicit optimal control law $\kappa_N(x) = u^O(0;x)$ can be obtained. This control law completes the feedback process of MPC when applied to the controlled system.

The terminal set Ω imposes an indirect constraint on the control sequence, $\boldsymbol{u} \in U_N(x)$, such that

$$U_N(x) = \{\boldsymbol{u} : (x,\boldsymbol{u}) \in Z_N\}, \tag{1.5}$$

where Z_N is defined by

$$Z_N = \{(x,\boldsymbol{u}) : u(j;x) \in U, \phi(j;x,\boldsymbol{u}) \in X, \forall j \in \mathbb{I}_{0:N-1}, \phi(N;x,\boldsymbol{u}) \in \Omega\}, \tag{1.6}$$

with $\phi(j;x,\boldsymbol{u})$ being the solution to (1.1) for a given sequence of control inputs $\boldsymbol{u}$ and initial state x. In other words, Z_N is the set of feasible pairs $(x,\boldsymbol{u})$. Therefore, the domain of attraction for the MPC can be defined as

$$X_N = \{x : \exists \boldsymbol{u} \text{ such that } (x,\boldsymbol{u}) \in Z_N\}. \tag{1.7}$$

Since not every optimization problem has a solution, the following assumptions are often made:

- The functions $f(x,u)$, $\ell(x,u)$, and $V_f(x)$ are continuous, $f(0,0) = 0$, $\ell(0,0) = 0$ and $V_f(0) = 0$.

- The sets X and Ω are closed, $\Omega \subseteq X$, and U is compact, with each set containing the origin in its interior.

Under such assumptions, it holds that (Rawlings & Mayne, 2009, Proposition 2.4)

1. The functional $V_N(x, \boldsymbol{u})$ is continuous in Z_N;
2. For each $x \in X_N$, the set $U_N(x)$ is compact;
3. For each $x \in X_N$, a solution to (1.4) exists.

The optimal performance in MPC would be achieved by solving an infinite horizon constrained control problem. However, in order to obtain tractable constrained optimization problems, MPC strategies consider a finite receding horizon approach at the cost of losing the properties of infinite horizon optimal controllers. Incorporating stabilizing ingredients into the controller design can help overcome this problem, but it involves considering extra conditions in the controller design (Mayne et al., 2000; Rawlings & Mayne, 2009).

The different ingredients included to ensure stability, feasibility, and optimality lead to the following stabilizing schemes of MPC:

- MPC with terminal inequality constraint: In this formulation, the terminal state is forced to reach an invariant set, $x(N) = \Omega$, which provides a larger domain of attraction when compared to the terminal equality formulation.

- MPC with terminal equality constraint: In this formulation, the terminal state is forced to reach a desired steady state, x_s, in N steps, in other words, $x(N) = x_s$. This condition is difficult to be obtained in real applications due to numerical issues.

- MPC with a terminal cost: In this formulation, the terminal state is penalized by a terminal cost functional $V_f(x)$ that, if sufficiently large, is able to ensure automatic satisfaction of a terminal constraint.

- MPC with terminal cost and constraint: This formulation combines the last two ideas to obtain recursive feasibility and convergence for any prediction horizon.

These formulations are well established in the literature (Mayne et al., 2000; Rawlings & Mayne, 2009) and, for the general case with terminal cost and constraint, the stabilizing conditions are set so the optimal cost is a Lyapunov function. Thus, the basic stability assumption takes the form

$$\min_{u \in U}\{V_f(f(x,u)) + \ell(x,u) | f(x,u) \in \Omega\} \leq V_f(x), \forall x \in \Omega, \tag{1.8}$$

which implies that the set Ω is a control invariant for the system $x(k+1) = f(x(k), u(k))$. Therefore, within this stabilizing scheme, the invariant condition on the terminal set Ω ensures feasibility of the closed-loop system, and the decreasing condition on the terminal function $V_f(x)$ guarantees convergence.

1.3 Set-point Tracking Model Predictive Control

The standard formulation presented in the previous section addresses the problem of regulating a system to a desired set-point. Specifically, without any loss of generality, the method described can be applied to the problem of regulation to the origin. However, if time-varying set-points are considered, there is no guarantee that the closed-loop system will maintain feasibility and stability properties (Pannocchia & Kerrigan, 2005). Besides, MPC strategies are often designed with the underlying assumption that the desired set-point is feasible, which may not be true since feasibility issues can come from the system dynamics limitations and constraints.

The problem of time-varying set-points has been addressed through different approaches (Mayne, 2014), for instance, switching strategies for feasibility recovery (Chisci & Zappa, 2003) and command governor-based strategies (Bemporad, 1998; Angeli & Mosca, 1999; Garone et al., 2017). In the command governor approach, the system is ensured to evolve in a feasible manner towards the desired set-point by incorporating a low-pass filter to smooth out the reference. A control law is then defined to stabilize the system based on an auxiliary reference, which is continuously adjusted by the command governor to converge towards the desired set-point. Inspired by the command governor ideas, predictive control schemes for tracking have been proposed seeking to deal with the problem of loss of recursive feasibility by formulating strategies with a greater domain of attraction when compared to the ones obtained with the predictive control schemes for regulation. These tracking strategies share with command governors the same central idea of adding an artificial reference to problem.

In Limon et al. (2008), a predictive control strategy for tracking of piecewise constant set-points has been proposed seeking to deal with the problem of loss of recursive feasibility in the presence of changing set-points. The authors have shown that the so-called tracking MPC has a larger domain of attraction when compared to the ones obtained with predictive controllers for regulation. In this strategy, the controller is designed to ensure asymptotic convergence for any admissible steady-state reference and, if not the case, to ensure convergence to an admissible steady-state. The control strategy is formulated using artificial state and input variables to describe the artificial steady-state for which asymptotic convergence is guaranteed. In addition, terminal conditions for stability are considered by including a terminal penalty term in the cost functional and a terminal constraint ensuring that the system reaches an invariant set for tracking.

In Ferramosca et al. (2009), the authors have analyzed the closed-loop performance for the controller proposed in Limon et al. (2008) and showed the importance of the offset cost in the overall controller performance. In that work, the offset cost functional has been extended to a convex, positive definite, and subdifferentiable function for which the convergence to an equilibrium point that minimizes this cost is demonstrated. Further, the authors have established conditions for the terminal cost and the offset cost functional for which it is possible to ensure local optimality, which leads to optimal closed-loop performance locally.

The formulation obtained for the tracking predictive control of constrained linear systems has been first extended in Ferramosca (2011) for the case of constrained non-linear systems and further analyzed in Limon et al. (2018). In that work, the authors have shown that the tracking formulation for the investigated class of non-linear systems maintains the properties of closed-loop stability and recursive feasibility for any set-point if proper choices of terminal cost and constraints are made. Besides, two simplified formulations have been presented for which the properties of the controller still hold. In the first formulation, the terminal constraint to an invariant set for tracking has been simplified and defined as a relaxed equality constraint. In the second formulation, the terminal constraint has been removed and a weighted terminal cost has been used to guarantee stability.

The MPC for regulation as presented in (1.4) can be easily adapted into the tracking MPC framework as proposed in Limon et al. (2008, 2018). For that let x_a and u_a be, respectively, the stationary artificial state and input such that $x_a = f(x_a, u_a)$. Moreover, let Z_s be the set of joint steady-states and inputs defined by

$$Z_s = \{(x_s, u_s) : x_s = f(x_s, u_s), x_s \in X, u_s \in U\}. \tag{1.9}$$

Now, lets define an offset cost functional $V_{of}(\cdot)$ as a continuous, convex, and positive definite function, such that

$$\arg \min_{x_a \in Z_s} V_{of}\left(x_a, x_t\right), \tag{1.10}$$

is unique with x_t being the set-point. Therefore, the cost functional for tracking can be defined as

$$V_N^t(x, x_t; \boldsymbol{u}) = \sum_{j=0}^{N-1} \ell(x(j) - x_a, u(j) - u_a) + V_f(x(N) - x_a) + V_{of}(x_a - x_t). \tag{1.11}$$

Finally, a tracking MPC strategy can be obtained by solving the following optimization problem at each sampling time in a receding horizon fashion:

$$\begin{aligned}
&\min_{\boldsymbol{u}} \; V_N^t(x, x_t; \boldsymbol{u}) \\
&\text{s.t. } x(0) = x, && (1.12a)\\
&\quad x(j+1) = f(x(j), u(j)), j \in \mathbb{I}_{0:N-1}, && (1.12b)\\
&\quad (x(j), u(j)) \in X \times U, j \in \mathbb{I}_{0:N-1}, && (1.12c)\\
&\quad (x_a, u_a) \in \lambda Z_s, && (1.12d)\\
&\quad x(N) \in \Omega^t, && (1.12e)
\end{aligned}$$

with Ω^t being an invariant set for tracking, as proposed in Limon et al. (2018), and with $\lambda \in (0, 1)$ and possibly very close to 1.

Example 1.1. Aiming to illustrate the benefits of set-point tracking MPC over regulatory approaches, consider a double integrator system of the form

$$x(k+1) = \begin{bmatrix} 1 & 0.3 \\ 0 & 1 \end{bmatrix} x(k) + \begin{bmatrix} 0.3 & 0.15 \\ 0 & 0.3 \end{bmatrix} u(k),$$

with $x = [x_1 \ x_2]' \in X$ and $u = [u_1 \ u_2]' \in U$. The states and inputs constraint sets are defined, respectively, by $X = \{x \in \mathbb{R}^2 : |x| \leq [10 \ 4]'\}$ and $U = \{u \in \mathbb{R}^2 : |u| \leq [1 \ 1]'\}$. Furthermore, in terms of the nominal MPC parameters, the horizon length is $N = 3$ and the states and inputs weighting matrices are $Q = I_2$ and $R = 5I_2$.

Figure 1.1 (a) illustrates the problem of feasibility due to non-admissible terminal conditions or short horizons in the regulatory formulation of MPC. In the figure, X_s is the set of steady-states defined by $X_s = \text{Proj}_x(Z_s)$, s_1 and s_2 are set-points, and $x(0)$ is the initial condition. For the set-point s_1, the initial condition is inside the domain of attraction $X_3(s_1)$ and the terminal control invariant set $\Omega(s_1)$ is admissible. However, if the set-point change to s_2, the initial condition does not belong to the domain of attraction $X_3(s_2)$ and the terminal control invariant set $\Omega(s_2)$ is not admissible. In this example, a

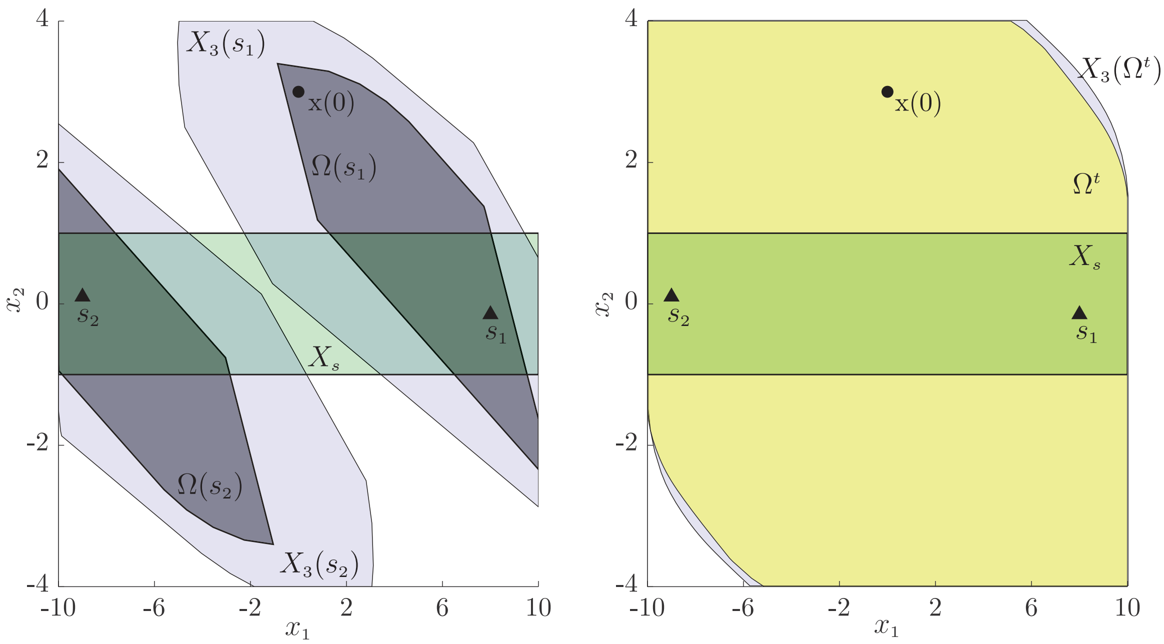

(a) Regulatory formulation.

(b) Tracking formulation.

Figure 1.1: This figure exemplifies the problem of loss of feasibility during changing set-points. In Figure (a), the regulatory formulation is considered and the domain of attraction $X_3(s_i)$ (in light gray) and the invariant set $\Omega(s_i)$ (in dark gray) are presented for the set-point s_i, with $i = 1, 2$. In Figure (b), the tracking formulation is considered and the domain of attraction $X_3(\Omega^t)$ (in light gray) and the invariant set Ω^t (in yellow) are also presented. In both figures, the green set represents the set of equilibrium states X_s.

set-point changing from s_1 to s_2 can cause loss of feasibility and, consequently, stability. Increasing the horizon length is a possible solution to this issue, although limited. In this context, Figure 1.1 (b) illustrates the same problem considering the tracking formulation of MPC. Notice that for the same horizon length, the domain of attraction, $X_3(\Omega^t)$, and the terminal control invariant for tracking, Ω^t, are enlarged. In fact, the set-point change from s_1 to s_2 does not imply any loss of feasibility since the domain of attraction contains the set-points and the initial condition, and the terminal control invariant Ω^t is admissible.

1.4 Robustness in Model Predictive Control

Robust control deals with uncertain systems that have a known predicted dynamic behavior distinct from the real state evolution. The uncertainties can come from distinct sources of disturbances, uncertainties about the knowledge of the states, and inaccurate dynamic models. Moreover, these can be described as additive or multiplicative uncertainties and may be of deterministic or stochastic nature (Rawlings & Mayne, 2009; Kouvaritakis & Cannon, 2016). Despite closed-loop nominal MPC methods having some degree of inherited robustness due to the feedback process and an appropriate choice of the terminal control law and penalties, the presence of disturbances and model uncertainties may lead to performance deterioration or even loss of stability (Yu et al., 2014; Lucia et al., 2020). In this context, control strategies that consider the effect of uncertainties by design concept are required to maintain stability and performance specifications in presence of uncertainties (Bemporad & Morari, 1999).

The problem of robustness in MPC has been addressed through different strategies, among them the most popular is the open-loop min-max MPC, introduced in Campo & Morari (1987), for which the optimization problem is solved for the worst-case of the expected disturbances while the constraints most hold for all possible values of uncertainties. In Skokaert & Mayne (1998), the min-max approach is extended to include feedback in the receding-horizon control algorithm. Thus, considering the feedback approach, a different control sequence can be obtained for each realization of the disturbance. Further, in Lee & Yu (1997), the closed-loop properties for both approaches are analyzed.

Since the min-max schemes are based on the minimization of the worst-case cost for all possible uncertainties, they may lead to excessively conservative control policies. Therefore, an alternative approach to the min-max strategy is the tube-based MPC, as proposed in the works of Chisci et al. (2001); Langson et al. (2004); Mayne et al. (2006). In this formulation, a semi-feedback control scheme is considered with a standard open-loop predictive controller with tight constraints being used to handle the nominal system while a secondary feedback control policy is considered to increase the system robustness. In Limon et al. (2009), both strategies have been analyzed under the Input-to-State Stability (ISS) framework.

When it comes to set-point tracking problem in presence of uncertainties, in Limon et al. (2010), the formulation presented in Limon et al. (2008) has been extended to the case of uncertain systems considering a tube-based approach for robustness. By means of artificial stationary states, a built-in steady-state target optimizer, and invariant sets, the authors have designed a control strategy that is feasible for any changing set-point and capable of steering the uncertain system asymptotically to a neighborhood of an admissible set-point. Similarly, but in the context of economic predictive control for uncertain linear systems, in D'Jorge et al. (2018), the authors have considered the ideas of Limon et al. (2008) and Limon et al. (2010) to ensure asymptotic convergence for any admissible set-point. In D'Jorge et al. (2020), the stochastic nature of the uncertainties and their statistical properties have been considered to obtain the tight constraints. The authors have shown that the proposed control strategy maintains the main characteristics of tracking predictive controllers, but with an even greater domain of attraction.

Despite the tube-based MPC formulations be a computationally efficient way to provide the closed-loop system with robustness, often, the computation of the robust invariant sets requires the execution of costly set-operations. Thus, mainly for high-dimensional systems and formulations where these sets need to be obtained online, it is important to tackle the problem of how low-cost tube-based controllers can be formulated. In that context, in Paulson & Mesbah (2020), polyhedral control Lyapunov functions have been used to obtain low complexity controllers capable of guaranteeing recursive feasibility and robust stability for uncertain linear systems. To reduce the computational cost of the traditional tube-based strategy, the authors have proposed to avoid the online solution of an optimization problem to choose the center of the tubes by generating a central tube path with suitable polyhedral control Lyapunov functions using contractive invariant sets. In Darup & Mönnigmann (2018), on the other hand, the idea of dual control, well known in classical formulations of predictive controllers, has been extended to the robust case. This strategy is based on obtaining a set in the vicinity of a terminal set for which it is not necessary to solve any optimization problem because there is an explicit control law that is already optimal in that region. In Morato et al. (2023), a robust nonlinear tracking model predictive control is proposed for tracking of piecewise constant references. The idea of using quasi-Linear Parameter Varying (LPV) embeddings is employed to obtain linear predictions at each sampling time, resulting in a computationally efficient approach.

Although there are works looking for new formulations with lower computational cost, there are also those seeking efficient set representations in order to perform the required operations for the robust tube-based control strategy implementation with a low computational burden. For example, in Raimondo et al. (2013), a zonotopic set representation has been used in the context of a robust fault-tolerant model predictive controller. Also, in Le et al. (2013), a controller based on Mayne et al. (2006) has been formulated using zonotopes to achieve a tube-based MPC with output feedback.

1.5 The Avoidance Problem

In some applications, besides being able to track set-points, avoiding specific regions in some known admissible space is an important requirement. For instance, in autonomous navigation, the ability to ensure collision avoidance against obstacles is paramount. Moreover, problems that have inherently non-convex admissible spaces, such as the problem of charging Li-ion batteries (Goldar et al., 2020), may also benefit from it by going from a non-convex control problem to an equivalent convex one. In the literature, optimization-based control strategies have been used to add avoidance features into the control problem due to the freedom of using the cost functional and the constraints for such purpose. In fact, the avoidance problem is often solved through optimal control by considering either the space to be avoided as a modified constraint in an equivalent problem or by adding relaxed avoidance constraints. Such solutions can be formulated into single-layer frameworks, which, unlike multi-layer strategies, avoid suboptimal solutions, loss of feasibility, and lack of stability guarantees (Limon et al., 2012).

Among those works considering constraints in an equivalent problem, in Raković et al. (2021), an MPC strategy for collision avoidance has been proposed to the regulation problem with deterministic linear systems. The authors have considered a strategic-tactical decision-making architecture to obtain a resulting convex MPC for collision avoidance, allowing the problem to be solved with quadratic programming. The resulting convex MPC has been shown to be asymptotic stable, feasible, and positively invariant. In Zhang et al. (2021), the authors have considered avoidance in an n-dimensional space by reformulating the collision avoidance constraints as smooth non-convex constraints under the assumption that obstacles can be described as convex sets. Based on the resulting smooth constraints, the optimization problem can be solved with a gradient or Hessian-based approach. In Thirugnanam et al. (2022), the problem of avoidance between polytopes has been approached using control barrier function constraints to generate dynamically collision-free feasible trajectories. In Cotorruelo et al. (2021), the authors have extended the set-point tracking MPC framework by incorporating a convexifying homeomorphism into the optimization problem so that non-convex admissible output sets could be handled. If the convexifying homeomorphism exists, the proposed approach is suitable for applications with non-convex output space. In Nascimento et al. (2019); Pereira et al. (2019); Small et al. (2019); Kloeser et al. (2020); Pereira et al. (2021c), single-layer schemes considering MPC have addressed the avoidance problem by designing additional constraints. Nonetheless, depending on how the optimization problem is formulated, it is difficult to guarantee recursive feasibility in environments with a large number of obstacles. Additionally, by considering the obstacles as constraints, the search-space for the optimization problem may become excessively small leading to suboptimal or unfeasible solutions.

Among those works relaxing avoidance constraints, in Shim et al. (2003), a framework based on a non-linear model predictive controller has been proposed to achieve decentralized autonomous flight for multiple unmanned aerial vehicles subject to constraints and flying in an environment obstructed by fixed and moving obstacles. The trajectory generation problem has been formulated by including potential functions into an optimization problem solved with a gradient-descent method. Further, in Kamel et al. (2017), a decentralized non-linear MPC scheme, similar to the one proposed by Shim et al. (2003), has been considered for trajectory tracking with collision avoidance during multi-agent flights. In Hermans et al. (2018), the authors have considered non-linear MPC within a penalty method framework designed to satisfy collision-avoidance while calculating the trajectory to be followed by the system. In Pereira et al. (2021a) and Pereira et al. (2021b), an ellipsoidal representation of obstacles has been incorporated into a non-linear model predictive controller as relaxed avoidance constraints. The proposed formulation is obtained considering the Special Euclidean group SE(3) to allow for aggressive navigation in cluttered environments with previously unknown obstacles. In Sánchez et al. (2021), artificial variables have been used to integrate the obstacle avoidance feature to MPC. In the work, obstacles have been represented as soft constraints in the optimization problem, and the artificial variables helped solving the path-following problem while avoiding obstacles. Furthermore, in Santos et al. (2021), the first results of set-point tracking considering artificial variables, an offset cost, and an avoidance cost have been presented. However, despite tracking set-points while avoiding undesirable regions, the proposed controller lacks formal guarantees of stability and recursive feasibility.

To approach the avoidance problem through an equivalent problem that either convexifies the space or changes the constraints to achieve some given properties may require prior knowledge of the regions to be avoided. In addition, in the presence of changing set-points, feasibility issues must be addressed. When considering a previously unknown number of regions to be avoided, the inclusion of penalty functions into the optimization problem allows avoiding online computation of equivalent constraints. Likewise, the stability analysis can be performed without any assumptions on the convexity of the admissible space, but at the price of possibly invalidating the decreasing property of the value function commonly used to derive stability. A similar problem appears in economic MPC schemes, where the value function is generally non-decreasing as the system approaches the economically optimal steady-state (Alessandretti et al., 2017). Nevertheless, under this condition, asymptotic stability for the resulting closed-loop system can still be demonstrated. For instance, in Diehl et al. (2011), a decreasing rotated value function has been designed using dissipativity theory, and in Alessandretti et al. (2017), it has been shown that any additional cost acting as a disturbance to the standard stabilizing cost presents ISS property as long as it is uniformly bounded over time.

Aiming to exemplify the above concepts, consider again a system described by a non-linear discrete-time model of the form

$$\begin{aligned} x(k+1) &= f(x(k), u(k)), \\ y(k) &= h(x(k), u(k)), \end{aligned} \tag{1.13}$$

with $x(k)$, $u(k)$, and $y(k)$ being, respectively, the state, input, and output vectors. Furthermore, the evolution of the system is constrained by

$$(x(k), u(k)) \in Z,\ \forall k \in \mathbb{I}_{\geq 0}, \tag{1.14}$$

where $Z = X \times U$ with $X = \text{Proj}_x(Z)$ and $U = \text{Proj}_u(Z)$ being the sets of admissible states and inputs.

Now, let O denotes the space obstructed by a finite number of non-feasible output regions to be avoided. The admissible output set becomes then a (possibly) non-convex set defined by

$$\tilde{Y} = Y - O, \tag{1.15}$$

with Y being the set of admissible outputs obtained considering the output-state map $h(\cdot)$.

Assuming that the inverse map $h^{-1} : \tilde{Y} \mapsto \tilde{Z}$ exists, the evolution of the system in the obstructed space must satisfy the constraint

$$(x(k), u(k)) \in \tilde{Z},\ \forall k \in \mathbb{I}_{\geq 0}. \tag{1.16}$$

The first obvious approach to provide avoidance can be obtained by modifying the standard regulatory MPC strategy (1.4) to enforce the avoidance constraint (1.16) directly. Therefore, an MPC strategy with avoidance features can be obtained by solving the following optimization problem:

$$\begin{aligned} \min_{\boldsymbol{u}}\ & V_N(x; \boldsymbol{u}) \\ \text{s.t. }\ & x(0) = x, && \text{(1.17a)} \\ & x(j+1) = f(x(j), u(j)), j \in \mathbb{I}_{0:N-1}, && \text{(1.17b)} \\ & (x(j), u(j)) \in \tilde{Z}, j \in \mathbb{I}_{0:N-1}, && \text{(1.17c)} \\ & x(N) \in \tilde{\Omega}, && \text{(1.17d)} \end{aligned}$$

where $\tilde{\Omega} = \Omega - \text{Proj}_x(\tilde{Z})$.

The second approach follows the idea of using the relaxation of the avoidance constraints, which aims to avoid imposing constraint (1.16) directly into the optimal control problem. Thus, consider the cost functional

$$\tilde{V}_N(x, O; \boldsymbol{u}) = V_N(x; \boldsymbol{u}) + V_{av}(\boldsymbol{y}, O), \tag{1.18}$$

which modifies the cost functional (1.3) by adding an avoidance term $V_{av}(\boldsymbol{y}, O)$. Moreover, let $V_{av}(\boldsymbol{y}, O)$ be a function that is inversely proportional to the distance between the predicted output $\boldsymbol{y}$ and the non-feasible region so that moving towards O increases the cost functional value. Therefore, an MPC strategy with avoidance features can be obtained by solving the following optimization problem:

$$\begin{aligned}
\min_{\boldsymbol{u}} \ & \tilde{V}_N(x, O; \boldsymbol{u}) \\
\text{s.t. } & x(0) = x, && (1.19a) \\
& x(j+1) = f(x(j), u(j)), j \in \mathbb{I}_{0:N-1}, && (1.19b) \\
& (x(j), u(j)) \in Z, j \in \mathbb{I}_{0:N-1}, && (1.19c) \\
& x(N) \in \Omega. && (1.19d)
\end{aligned}$$

Ultimately, the problem of avoidance comes down to how one can solve a control problem in a non-convex space. Particularly, the non-convexity brought by the avoidance problem is difficult to handle since typically there is no direct topological transformation resulting in a convex space. Clearly, on one hand, formulation (1.17) presents feasibility and stability problems due to the constraints added in the admissible space and, mainly, on the control invariant set. Further, the resultant optimization problem has a non-convex search space, which makes it particularly hard to solve. On the other hand, formulation (1.19) avoids the use of hard constraints keeping the search space convex. However, the decreasing property of the optimal cost is lost and different approaches to analyze stability must be proposed. Finally, applications requiring avoidance capacity commonly have changing set-points. In such conditions, since formulations like (1.17) and (1.19) use a regulatory MPC approach, they can present stability and feasibility issues.

Example 1.2. Assume Example 1.1 to better illustrate the avoidance problem. Thus, consider the admissible state-space X obstructed by a non-feasible reagion defined as $O = \{x \in \mathbb{R}^2 : [4 \ \ -2.5]' \leq x \leq [6 \ \ 2.5]'\}$. Figure 1.2 depicts the set of steady-states X_s, the control invariant set for tracking Ω^t, and the terminal control invariant sets for the regulatory case $\Omega(s_1)$ and $\Omega(s_2)$. In addition to the problem of loss of feasibility during changing set-points, already discussed in Example 1.1, the presence of non-feasible regions makes the admissible invariant set for the regulatory problem, $\tilde{\Omega}(s_1) = \Omega(s_1) - O$, to be a non-convex disconnected set. Therefore, it is not possible to guarantee that the terminal ingredients in this case will provide the system with stability and feasibility. Even if the tracking formulation of MPC is considered, the admissible invariant set for tracking $\tilde{\Omega}^t = \Omega^t - O$ is a non-convex set. Therefore, the enlarged domain of attraction provided in the tracking formulation is not sufficient to endow the system with stability and feasibility properties.

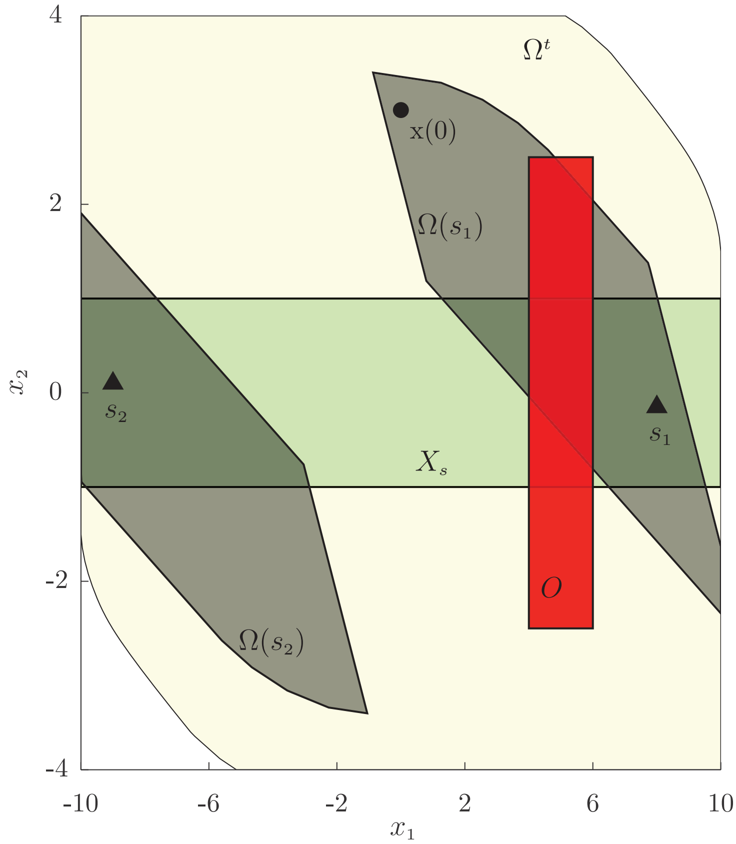

Figure 1.2: This figure exemplifies the problem of loss of feasibility during changing set-points in a non-convex admissible space. In the figure, the tracking invariant set Ω^t (in yellow), and the invariant sets for the regulatory formulation $\Omega(s_1)$ and $\Omega(s_2)$ (in dark grey) are presented. Further, the set of equilibrium states X_s is depicted in green while the non-feasible region obstructing the space O is depicted in red.

1.6 Contributions

This thesis's main contribution relies on how to solve MPC problems with non-convex admissible spaces by adding penalties and showing that the resulting equivalent convex problem is input-to-state stable. Based on this central idea, this work proposes several frameworks that address issues commonly found in the literature when using MPC strategies for avoidance.

1.6.1 Set-point tracking MPC with avoidance features

In Chapter 3 we analyse the avoidance problem under the tracking MPC formulation proposed in Limon et al. (2008). For that, the avoidance constraints are added to the optimal control problem as penalty functions working as an avoidance function in the MPC cost functional. The contributions are threefold:

1. A novel linear set-point tracking MPC strategy with avoidance features;

2. Demonstration of recursive feasibility for changing targets and previously unknown

non-feasible output regions to be avoided within the system admissible states;

3. Demonstration of ISS property with respect to the avoidance cost.

1.6.2 Robust set-point tracking MPC with avoidance features

In Chapter 4 we analyse the proposed set-point tracking MPC with avoidance features when the controlled system is subjected to unknown but bounded disturbances. The notion of tube of trajectories is used for robustification, and the proposed avoidance strategy is analyzed in terms of input-to-state stability. The contributions are threefold:

1. A novel robust linear set-point tracking MPC strategy with avoidance features;

2. Demonstration of recursive feasibility and robust constraint satisfaction for changing set-points, previously unknown non-feasible output regions, and unknown but bounded disturbances.

3. Demonstration of input-to-state stability with respect to the disturbances and the avoidance cost.

1.6.3 Non-linear set-point tracking MPC with avoidance features

In Chapter 5 we extend the proposed set-point tracking MPC with avoidance features to non-linear systems. Ultimately, it extends the results of Limon et al. (2018) to add avoidance features. Besides, formulations considering distinct terminal ingredients are analyzed under the ISS framework. The contributions are twofold:

1. Novel non-linear set-point tracking control schemes for obstacle avoidance;

2. Analysis, in terms of stability and feasibility, of the effect of including avoidance as additional cost into non-linear tracking MPC schemes.

1.7 List of Publications

During the development of this Ph.D. thesis, the following results were obtained:

Conference papers:

1. Santos, M. A., Ferramosca, A., & Raffo, G. V. (2018). Tube-based MPC with Nonlinear Control for Load Transportation using a UAV. In *Proceedings of the 9th IFAC Symposium on Robust Control Design* (pp. 649 - 655).

2. Dulce-Galindo, J.A., Santos, M. A., Raffo, G. V., & Pena, P. N. (2019). Autonomous Navigation of Multiple Robots using Supervisory Control Theory. In *Proceedings of the 18th European Control Conference* (pp. 3198 - 3203).

3. Santos, M. A., Ferramosca, A., & Raffo, G. V. (2021). Tracking Nonlinear Model Predictive Control for Obstacle Avoidance. In *Proceedings of the Latin American Robotics Symposium* (pp. 30 - 35).

4. Santos, M. A., Ferramosca, A., & Raffo, G. V. (2021). Energy-aware Model Predictive Control with Obstacle Avoidance. In *Proceedings of the International Conference on Unmanned Aircraft Systems* (pp. 647 - 655).

5. Trevas, A. C., Santos, M. A., & Raffo, G. V. (2022). Controle Preditivo Não-Linear Baseado em Modelo Obtido via Aprendizado de Máquina. *Anais do XXIV Congresso Brasileiro de Automática* (pp. 1 - 8).

6. Miranda, T. C., Pereira, M. C., Santos, M. A., & Raffo, G. V. (2022). Model Predictive Control for Attitude Maneuvers of a Nanosatellite. In *Proceedings of the 5th IAA Latin American CubeSat Workshop and 3rd IAA Latin American Symposium on Small Satellites* (pp. 1 - 10).

Journal papers:

1. Dulce-Galindo, J.A., Santos, M. A., Raffo, G. V., & Pena, P. N. (2022). Distributed Supervisory Control for Multiple Robot Autonomous Navigation Performing Single-robot Tasks. *Mechatronics*, v. 86, pp. 102848.

2. Santos, M. A., Ferramosca, A., & Raffo, G. V. (2023). Nonlinear Model Predictive Control Schemes for Obstacle Avoidance. Journal of Control Automation and Electrical Systems, v. 34, pp. 891 - 906.

3. Santos, M. A., Ferramosca, A., & Raffo, G. V. (2024). Set-Point Tracking MPC with Avoidance Features. Automatica, v. 159, pp. 111390.

1.8 Structure of the Text

The remaining of the text is organized as follow:

- Chapter 2: presents the mathematical background required for the understanding of this thesis;
- Chapter 3: introduces a model predictive control approach that utilizes artificial variables and penalty functions to solve the set-point tracking problem with avoidance features;
- Chapter 4: explores the issue of robustness for the set-point tracking model predictive control approach with avoidance features by employing the concept of tube of trajectories;

- Chapter 5: extends the set-point tracking model predictive control with avoidance features to address non-linear systems;

- Chapter 6: concludes the work and outlines potential areas for future research.

2

Mathematical Preliminaries

This chapter presents the background on the mathematical tools used throughout this thesis, which are: set methods in control theory, Lyapunov stability theory, and optimization.

2.1 Set Methods in Control Theory

This section presents basic definitions about sets, their representations, operations, and applications in control theory. All definitions presented here can be found with further details in Kerrigan & Maciejowski (2000), Kerrigan (2000), Blanchini & Miani (2007), Nguyen (2014), and Le et al. (2013).

2.1.1 General definitions

The notation $A \subseteq B$ is used to denote that A is a subset of B, $A \subset B$ denotes that A is a proper subset of B, and $a \in A$ denotes that a belongs to A. Further, $\mathbb{I}$ is the set of integer numbers, and $\mathbb{R}$ is the set of real numbers.

Definition 2.1 (Closed set (Nguyen, 2014))**.** A set $S \subset \mathbb{R}^n$ is closed if it contains its own boundary.

Definition 2.2 (Bounded set (Nguyen, 2014))**.** A set $S \subset \mathbb{R}^n$ is said to be bounded if it is contained in some ball $B_R = \{x \in \mathbb{R}^n : \|x\|_2 \leq \epsilon\}$ with finite radius $\epsilon > 0$.

Definition 2.3 (Compact set (Nguyen, 2014))**.** A set $S \subset \mathbb{R}^n$ is compact if it is closed and bounded.

A set is said to be convex if, given two points, every point on the line segment joining these two points is also a member of the set. This geometric interpretation of a convex set can be formally stated by the follow definition.

Definition 2.4 (Convex set (Nguyen, 2014)). A set $S \subset \mathbb{R}^n$ is said to be convex if for every $x_1, x_2 \in S$ and every number $\alpha \in \mathbb{R}$, $0 < \alpha < 1$, the point $\alpha x_1 + (1-\alpha)x_2 \in S$.

Definition 2.5 (Linear variety (Nguyen, 2014)). A set $H \subset \mathbb{R}^n$ is said to be a linear variety, if for every $x_1, x_2 \in H$ and every $\alpha \in \mathbb{R}$, the point $\alpha x_1 + (1-\alpha)x_2 \in H$.

2.1.2 Set operations

Set operations are useful tools in control theory, hence three of them are defined in this subsection, while the well-known operations, such as union ($\bigcup$), intersection ($\bigcap$), difference ($-$), and Cartesian product ($\times$) are disregarded.

Definition 2.6 (Affine transformation (Nguyen, 2014)). Consider the set $S \subset \mathbb{R}^n$. An affine transformation of S is given by

$$AS + b = \{Ax + b : x \in S\},$$

with $A \in \mathbb{R}^{m\times n}$ and $b \in \mathbb{R}^m$.

Definition 2.7 (Minkowski sum (Nguyen, 2014)). The Minkowski sum of two sets $S_1, S_2 \subset \mathbb{R}^n$ is given by

$$S_1 \oplus S_2 = \{x_1 + x_2 : x_1 \in S_1, x_2 \in S_2\}.$$

Definition 2.8 (Pontryagin difference (Nguyen, 2014)). The Pontryagin difference of two sets $S_1, S_2 \subset \mathbb{R}^n$ is given by

$$S_1 \ominus S_2 = \{x_1 \in S_1 : x_1 + x_2 \in S_1, \forall\ x_2 \in S_2\}.$$

Definition 2.9 (Hausdorff distance (Blanchini & Miani, 2007)). The Hausdorff distance between two sets S_1 and S_2 is given by

$$\delta_H(S_1, S_2) = \min\{\alpha \geq 0 : S_2 \subseteq S_1 + \alpha B, S_1 \subseteq S_2 + \alpha B\},$$

with B denoting the unit ball of any norm.

2.1.3 Set representations

Definition 2.10 (Hyperplane (Nguyen, 2014)). A hyperplane $H(f, g)$ is a set of the form

$$H(f, g) = \{x \in \mathbb{R}^n : f'x = g\},$$

where $f \in \mathbb{R}^n$ and $g \in \mathbb{R}$.

From the geometric perspective, a hyperplane in $\mathbb{R}^n$ can be defined as an $(n-1)$-dimensional linear variety. For instance, in $\mathbb{R}^3$, a plane, which is a 2-dimensional linear variety, is a hyperplane.

Definition 2.11 (Half-spaces (Nguyen, 2014))**.** From the definition of hyperplane, a closed half-space $\mathcal{H}(f,g)$ is a set of the form

$$\mathcal{H}(f,g) = \{x \in \mathbb{R}^n : f'x \leq g\},$$

where $f \in \mathbb{R}^n$ and $g \in \mathbb{R}$.

Definition 2.12 (Polyhedral set (Blanchini & Miani, 2007))**.** A convex polyhedral set $P(F,g)$ is a set of the form

$$P(F,g) = \{x \in \mathbb{R}^n : F'x \leq g\},$$

where $F = \begin{bmatrix} f_1' & f_2' & \cdots & f_m' \end{bmatrix}$ and $g = \begin{bmatrix} g_1 & g_2 & \cdots & g_m \end{bmatrix}'$ with $f_i \in \mathbb{R}^n\ \forall i$, and $g_i \in \mathbb{R}\ \forall i$. In other words, a convex polyhedral is expressed as the intersection of a finite number of half-spaces.

Definition 2.13 (Zonotope - Generator Representation (Le et al., 2013))**.** Given a center $c \in \mathbb{R}^n$ and a set of generator vectors $\{g_1, g_2, \cdots, g_m\} \subset \mathbb{R}^n$, $m \geq n$, a m-zonotope $Z \subset \mathbb{R}^n$ with order $o = m/n$ is defined as

$$Z = \left\{ x \in \mathbb{R}^n : x = c + \sum_{i=1}^{m} \alpha_i g_i,\ -1 \leq \alpha_i \leq 1 \right\},$$

which can be shortly written as $Z = \{G, c\}$, with $G = [g_1 \cdots g_m]$ being the generator matrix.

Definition 2.14. For every $Z = \{G_z, c_z\} \subset \mathbb{R}^n$, $W = \{G_w, c_w\} \subset \mathbb{R}^n$, and $R \in \mathbb{R}^{m \times n}$, the two identities hold:

$$Z \oplus W = \{[G_z\ G_w], c_z + c_w\},$$
$$RZ = \{RG_z, Rc_z\}.$$

Proposition 2.1. (Raimondo et al., 2013, Proposition 3) Let $Z = \{G, c\} \subset \mathbb{R}^n$ and $T = \{z \in \mathbb{R}^n : h_i'z \leq k_i, i = 1, \cdots, m\}$, where $k_i \in \mathbb{R}$, $h_i \in \mathbb{R}^n$, and $h_i \neq O_{n,1}$, being $O_{n,1}$ a vector of zeros. Then, $T \ominus Z = \{z \in \mathbb{R}^n : h_i'z \leq k_i^*, i = 1, \cdots, m\}$, where $k_i^* = k_i - h_i'c - \|h_i'G\|_1$.

2.1.4 Invariant sets

The invariant set theory results are fundamental to design controllers for constrained systems and to understand some of their properties, for instance, stability and feasibility.

Therefore, the following definitions describe these sets for systems with and without uncertainties. Moreover, let $U \subset \mathbb{R}^m$, $X \subset \mathbb{R}^n$, and $W \subset \mathbb{R}^n$ denote compact sets, and let Ω denotes any arbitrary subset in $\mathbb{R}^n$.

Definition 2.15 (Positively invariant set (Kerrigan & Maciejowski, 2000))**.** The set $\Omega \subset \mathbb{R}^n$ is said to be positively invariant for the system $x(k+1) = f(x(k))$ if, $\forall x(0) \in \Omega$, the system evolution satisfies $x(k) \in \Omega$, $\forall k \in \mathbb{I}_{\geq 0}$. In other words, if a system reaches a positively invariant set, it will stay inside this set indefinitely.

Definition 2.16 (Maximal positively invariant set (Kerrigan & Maciejowski, 2000))**.** The set $O_\infty(\Omega)$ is said to be the maximal positively invariant set contained in Ω for the system $x(k+1) = f(x(k))$ if $O_\infty(\Omega)$ is positively invariant and contains all positively invariant sets contained in Ω. Therefore, if Φ is a positively invariant set, $\Phi \subseteq O_\infty(\Omega) \subseteq \Omega$.

The concept of positively invariant set can be extended to closed-loop systems through the definition of the control invariant set.

Definition 2.17 (Control invariant set (Kerrigan & Maciejowski, 2000))**.** The set $\Omega \subset \mathbb{R}^n$ is said to be a control invariant set for the system $x(k+1) = f(x(k), u(k))$ with $x(k) \in X$ and $u(k) \in U$, if, for all $x(0) \in \Omega$, there exists a state-dependent control law $u(k) = \kappa(x(k))$ such that $x(k+1) \in \Omega$, $\forall k \in \mathbb{I}_{\geq 0}$.

Definition 2.18 (Maximal control invariant set (Kerrigan & Maciejowski, 2000))**.** The set $C_\infty(\Omega)$ is said to be the maximal control invariant set contained in Ω for the system $x(k+1) = f(x(k), u(k))$ if $C_\infty(\Omega)$ is the union of all control invariant sets contained in Ω. Thus, if Φ is a control invariant set, $\Phi \subseteq C_\infty(\Omega) \subseteq \Omega$.

The control invariant set can be obtained through the admissible set.

Definition 2.19 (Admissible set (Kerrigan & Maciejowski, 2000))**.** The i-th step admissible set $C_i(\Omega)$ is the set of states for which exists an admissible control sequence able to keep the state evolution inside Ω during i steps, i.e.,

$$C_i(\Omega) = \{x(0) \in \Omega : \exists u(k) \in U, \forall k = 0, \cdots, i-1, \text{ such that } x(k+1) \in \Omega\}.$$

The admissible set has some properties useful for numerical implementation of control invariant sets.

Proposition 2.2. (Kerrigan & Maciejowski, 2000) The sequence $C_i(\Omega)$ satisfies the properties:

(i) Each set $C_{i+1}(\Omega) \subseteq C_i(\Omega)$;

(ii) Each set $C_i(\Omega) = \bigcap_{j=0}^{i} C_j(\Omega)$;

(iii) $C_\infty(\Omega)$ is finitely determined if $\exists i \in \mathbb{I}_{\geq 0}$ such that $C_{i+1}(\Omega) = C_i(\Omega)$. Therefore, $C_i(\Omega) = C_\infty(\Omega)$.

Definition 2.20 (The one-step set (Kerrigan & Maciejowski, 2000))**.** The one-step set $Q(\Omega)$ is defined as the set of $x \in \mathbb{R}^n$ for which an admissible control input exists and can drive the system to Ω in one-step, i.e.,

$$Q(\Omega) = \{x \in \mathbb{R}^n : \exists u(k) \in U \text{ such that } f(x(k), u(k)) \in \Omega, \forall k \in \mathbb{I}_{\geq 0}\}.$$

Using the definition of the one-step operator it is possible to state a geometric condition for invariance.

Theorem 2.1. (Geometric condition for invariance (Kerrigan & Maciejowski, 2000, Theorem 2.2)) The set $\Omega \in \mathbb{R}^n$ is a control invariant set if and only if $\Omega \subseteq Q(\Omega)$.

This theorem gives a geometric interpretation for invariant sets making the one-step set a standard tool for computing invariant sets through iterative algorithms.

Definition 2.21 (Robust positively invariant set (Kerrigan, 2000))**.** The set Ω is said to be robust positively invariant for the uncertain system $x(k+1) = f(x(k), w(k))$ if, $\forall x(0) \in \Omega$ and $\forall w(k) \in W$, the system evolution satisfies $x(k) \in \Omega$, $\forall k \in \mathbb{I}_{\geq 0}$. In other words, if a system reaches a robust positively invariant set, it will stay inside this set despite the uncertainties, i.e., $x(k) \in \Omega \Rightarrow x(k+1) \in \Omega, \forall w(k) \in W$.

Definition 2.22 (Maximal robust positively invariant set (Kerrigan, 2000))**.** The set $O_\infty(\Omega)$ is said to be the maximal robust positively invariant set contained in Ω for the uncertain system $x(k+1) = f(x(k), w(k))$ if $O_\infty(\Omega)$ is robust positively invariant and contains all the robust positively invariant sets contained in Ω. Therefore, if Φ is a robust positively invariant set, $\Phi \subseteq O_\infty(\Omega) \subseteq \Omega$.

Definition 2.23 (Robust control invariant set (Kerrigan, 2000))**.** The set $\Omega \subset \mathbb{R}^n$ is said to be a robust control invariant set for the uncertain system $x(k+1) = f(x(k), u(k), w(k))$ with $x(k) \in X$, $u(k) \in U$, and $w(k) \in W$; if, $\forall x(0) \in \Omega$, there exists a state-dependent control law $u(k) = \kappa(x(k)), \forall x(k) \in \Omega, \forall k \in \mathbb{I}_{\geq 0}$, such that $x(k+1) \in \Omega$, $\forall w(k) \in W$.

Definition 2.24 (Maximal robust control invariant set (Kerrigan, 2000))**.** The set $C_\infty(\Omega)$ is said to be the maximal robust control invariant set contained in Ω for the uncertain system $x(k+1) = f(x(k), u(k), w(k))$ if $C_\infty(\Omega)$ is robust control invariant and contains all the robust control invariant sets contained in Ω. Therefore, if Φ is a robust control invariant set, $\Phi \subseteq C_\infty(\Omega) \subseteq \Omega$.

As for the case without uncertainties, the useful one-step set can be defined in order to provide an operator to deal with the set invariance for uncertain systems.

Definition 2.25 (The robust one-step set (Kerrigan, 2000)). The robust one-step set $Q(\Omega)$ is defined as the set of $x \in \mathbb{R}^n$ for which an admissible control input exists and can drive the system to Ω in one step, for all considered disturbances, i.e,

$$Q(\Omega) = \{x \in \mathbb{R}^n : \exists u(k) \in U \text{ such that } f(x(k), u(k), w(k)) \in \Omega, \forall w(k) \in W, \forall k \in \mathbb{I}_{\geq 0}\}.$$

Theorem 2.2. (Geometric condition for robust invariance (Kerrigan, 2000, Theorem 2.1)) The set $\Omega \in \mathbb{R}^n$ is a robust control invariant set if and only if $\Omega \subseteq Q(\Omega)$.

Definition 2.26 (Reachable set (Kerrigan & Maciejowski, 2000)). The reachable set of Ω, $\mathcal{R}(\Omega)$, is the set of states to which the system can evolve from Ω through an admissible input in one-step, i.e.,

$$\mathcal{R}(\Omega) = \{x \in \mathbb{R}^n : \forall x(k) \in \Omega, \forall u(k) \in U, \forall w(k) \in W \text{ such that } x = f(x(k), u(k), w(k)) \forall k \in \mathbb{I}_{\geq 0}\}.$$

Although definitions 2.25 and 2.26 seem similar, notice that definition 2.25 is related to the concept of controllability to the set Ω, while 2.26 is the reachability from Ω. Moreover, the reachable set has some properties useful for the numerical implementation of robust control invariant sets.

Proposition 2.3. (Kerrigan, 2000) The sequence $\mathcal{R}_i(\Omega)$ satisfies the properties:

(i) $\mathcal{R}_j(\Omega) \subseteq \mathcal{R}_{j+1}(\Omega)$, $\forall j \in \mathbb{I}_{\geq 0}$;

(ii) The sequence of sets $\mathcal{R}_j(\Omega)$ has a limit $\mathcal{R}_\infty(\Omega)$ as $j \to \infty$;

(iii) $\mathcal{R}_\infty(\Omega)$ is the minimal robust positive invariant set.

2.2 Lyapunov Stability Theory

The Lyapunov stability theory results are used to analyze the properties of the controllers designed in this work. By using this theory, it is possible to determine if the controllers are stable or unstable, and to assess their robustness and performance under various conditions. All definitions presented here can be found with further details in Khalil (2002), Vidyasagar (2002), and Rawlings & Mayne (2009).

Definition 2.27. (Equilibrium point (Rawlings & Mayne, 2009)) A state $x_s \in X$ is an equilibrium point of the system $x(k+1) = f(x(k))$ if once the state is equal to x_s, it remains equal to x_s for all future time, i.e., $x_s = f(x_s)$.

Definition 2.28. (Control equilibrium set (Rawlings & Mayne, 2009)) A set $\Omega \subseteq X$ is a control equilibrium set of the closed-loop system $x(k+1) = f(x(k), \kappa(x(k)))$ with $\kappa(x(k)) \in U$ if for every point $x \in \Omega$ it follows that $x = f(x, \kappa(x))$.

Definition 2.29. (Stability (Khalil, 2002)) The equilibrium point $x_s = 0$ is said to be stable if, for each $\epsilon > 0$, there exists $\delta > 0$, such that $\|x(0)\| < \delta$ implies $\|x(k)\| < \epsilon$, for all $k \in \mathbb{I}_{\geq 0}$. Otherwise, the equilibrium point is unstable.

Definition 2.30. (Local stability (Rawlings & Mayne, 2009)) The (closed and invariant) set Ω is locally stable for the system $x(k+1) = f(x(k))$ if, for all $\epsilon > 0$, there exists a $\delta > 0$ such that $|x(k)|_\Omega < \delta$ implies $|x(k+i)|_\Omega < \epsilon$, for all $i \in \mathbb{I}_{\geq 0}$.

Definition 2.31. (Attraction (Rawlings & Mayne, 2009)) The (closed and invariant) set Ω is attractive for the system $x(k+1) = f(x(k))$ if $|x(k+i)|_\Omega \to 0$ as $i \to \infty$, for all $x \in X$.

Definition 2.32. (Global attraction (Rawlings & Mayne, 2009)) The (closed and invariant) set Ω is globally attractive for the system $x(k+1) = f(x(k))$ if $|x(k+i)|_\Omega \to 0$ as $i \to \infty$, for all $x \in \mathbb{R}^n$.

Definition 2.33. (Asymptotic stability (Rawlings & Mayne, 2009)) The (closed and invariant) set Ω is asymptotically stable for the system $x(k+1) = f(x(k))$ if it is locally stable and attractive.

Definition 2.34. (Global asymptotic stability (Rawlings & Mayne, 2009)) The (closed and invariant) set Ω is globally asymptotically stable for the system $x(k+1) = f(x(k))$ if it is locally stable and globally attractive.

Definition 2.35. (Positive definite function (Rawlings & Mayne, 2009)) A continuous function $\alpha(\cdot) : \mathbb{R}_{\geq 0} \to \mathbb{R}_{\geq 0}$ is positive definite ($\mathcal{PD}$) if $\alpha(s) > 0$ for all $s > 0$, and $\alpha(0) = 0$.

Definition 2.36. (Comparison functions - $\mathcal{K}$-functions (Khalil, 2002)) A continuous function $\alpha(\cdot) : \mathbb{R}_{\geq 0} \to \mathbb{R}_{\geq 0}$ is said to belong to a class $\mathcal{K}$ if it is positive definite and strictly increasing. It is said to belong to a class $\mathcal{K}_\infty$ if it is of class $\mathcal{K}$ and it is not bounded above, i.e., $\alpha(s) \to \infty$ as $s \to \infty$.

Definition 2.37. (Comparison functions - $\mathcal{KL}$-functions (Khalil, 2002)) A function $\beta(\cdot) : \mathbb{R}_{\geq 0} \times \mathbb{R}_{\geq 0} \to \mathbb{R}_{\geq 0}$ is a $\mathcal{KL}$-function if, for each fixed $t \geq 0$, the mapping $\beta(s,t)$ is a $\mathcal{K}$-function with respect to s and, for each fixed s, the mapping $\beta(s,t)$ is decreasing with respect to t, that is, $\beta(s,t) \to 0$ as $t \to \infty$.

Proposition 2.4. (Properties of comparison functions (Khalil, 2002)) Let α_1 and α_2 be class $\mathcal{K}$-functions on $[0,a)$, α_3 and α_4 be class $\mathcal{K}_\infty$-functions, and β be a class $\mathcal{KL}$-function. Denote the inverse of α_i by α_i^{-1}. Then,

- α_1^{-1} is defined on $[0, \alpha_1(a))$ and belongs to class $\mathcal{K}$.
- α_3^{-1} is defined on $[0, \infty)$ and belongs to class $\mathcal{K}_\infty$.
- $\alpha_1 \circ \alpha_2$ belongs to class $\mathcal{K}$.

- $\alpha_3 \circ \alpha_4$ belongs to class $\mathcal{K}_\infty$.
- $\sigma(s,t) = \alpha_1(\beta(\alpha_2(s),t))$ belongs to class $\mathcal{KL}$.

Theorem 2.3. (Lyapunov stability (Vidyasagar, 2002)) Let $x_s = 0$ be an equilibrium point for the system $x(k+1) = f(x(k))$ for a domain Ω containing $x_s = 0$. Let $V(\cdot) : \Omega \to \mathbb{R}_{\geq 0}$ be a continuous function such that for all $k \in \mathbb{I}_{\geq 0}$

$$
\begin{aligned}
V(0) = 0 \text{ and } V(x(k)) > 0 \in \Omega - \{0\}, \\
V(x(k+1)) - V(x(k)) \leq 0 \in \Omega.
\end{aligned}
$$

Then, $x_s = 0$ is stable. Moreover, if

$$
V(x(k+1)) - V(x(k)) < 0 \in \Omega - \{0\},
$$

then $x_s = 0$ is asymptotically stable.

Definition 2.38. (Lyapunov function (Rawlings & Mayne, 2009)) A function $V(\cdot) : \mathbb{R}^n \to \mathbb{R}_{\geq 0}$ is said to be a Lyapunov function for the system $x(k+1) = f(x(k))$ and set Ω if there exist functions $\alpha_i \in \mathcal{K}_\infty$, $i = 1, 2$ and $\alpha_3 \in \mathcal{PD}$ such that for any $x \in \mathbb{R}^n$,

$$
\begin{aligned}
V(x(k)) &\geq \alpha_1 \left(|x(k)|_\Omega \right), \\
V(x(k)) &\leq \alpha_2 \left(|x(k)|_\Omega \right), \\
V(f(x(k))) - V(x(k)) &\leq -\alpha_3 \left(|x(k)|_\Omega \right).
\end{aligned}
$$

Theorem 2.4. (Lyapunov functions and global asymptotic stability (Rawlings & Mayne, 2009)) Suppose $V(\cdot)$ is a Lyapunov function for $x(k+1) = f(x(k))$ and set Ω, with $\alpha_3(\cdot)$ a $\mathcal{K}_\infty$-function. Then Ω is globally asymptotically stable.

Theorem 2.5. (Converse theorem for asymptotic stability (Rawlings & Mayne, 2009)) Let Ω be compact and $f(\cdot)$ continuous. Suppose that the set Ω is globally asymptotically stable for the system $x(k+1) = f(x(k))$. Then there exists a smooth Lyapunov function for the system $x(k+1) = f(x(k))$ and set Ω.

Theorem 2.6. (Lyapunov function and asymptotic stability (Rawlings & Mayne, 2009)) Suppose $X \subset \mathbb{R}^n$ is positively invariant for $x(k+1) = f(x(k))$, that Ω is closed and positively invariant for $x(k+1) = f(x(k))$, and that Ω lies in the interior of X. If there exists a Lyapunov function in X for the system $x(k+1) = f(x(k))$ and set Ω with $\alpha_3(\cdot)$ a $\mathcal{K}_\infty$-function (see Definition (2.38)), then Ω is asymptotically stable with a region of attraction X.

Definition 2.39. (Domain of attraction (Rawlings & Mayne, 2009)) The domain of attraction of an asymptotically stable set Ω for the system $x(k+1) = f(x(k))$ is the set of all initial states x such that $|x(k+i)|_\Omega \to 0$ as $i \to \infty$.

Definition 2.40. (Input-to-state stable (Jiang & Wang, 2001)) The system $x(k+1) = f(x(k), w(k))$ is input-to-state stable if there exists a $\mathcal{KL}$-function $\beta(\cdot)$ and a $\mathcal{K}$-function $\sigma(\cdot)$ such that for all initial state $x(0) \in \mathbb{R}^n$ and disturbance $w(k) \in W$

$$\|x(k)\| \leq \beta(\|x(0)\|, k) + \sigma\left(\|w(k)\|\right), \tag{2.1}$$

for all $k \in \mathbb{I}_{\geq 0}$.

Definition 2.41. (ISS-Lyapunov function (Jiang & Wang, 2001)) A continuous function $V(\cdot) : \mathbb{R}^n \to \mathbb{R}_{\geq 0}$ is called an ISS-Lyapunov function for system $x(k+1) = f(x(k), w(k))$ if there exist $\mathcal{K}_\infty$-functions $\alpha_1(\cdot), \alpha_2(\cdot), \alpha_3(\cdot)$ and a $\mathcal{K}$-function $\sigma(\cdot)$ such that for all $x(k) \in \mathbb{R}^n$ and $w(k) \in \mathbb{R}^p$

$$\begin{aligned} V(x(k)) &\geq \alpha_1(\|x(k)\|), \\ V(x(k)) &\leq \alpha_2(\|x(k)\|), \\ V(f(x(k), w(k))) - V(x(k)) &\leq -\alpha_3(\|x(k)\|) + \sigma(\|w(k)\|), \end{aligned}$$

for all $k \in \mathbb{I}_{\geq 0}$.

Lemma 2.1. (ISS-Lyapunov function implies ISS (Jiang & Wang, 2001)) If system $x(k+1) = f(x(k), w(k))$ admits a continuous ISS-Lyapunov, then it is ISS.

It is noteworthy that the above definitions can easily be adapted to encompass controlled systems as well.

2.3 Final Remarks

In this chapter the main mathematical concepts used in this work were formally defined aiming to provide a better understanding of this thesis. In the next chapters, model predictive controllers will be designed with the help of the mathematical tools presented in this chapter.

3

Set-Point Tracking with Avoidance Features

3.1 Introduction

This chapter proposes a finite-horizon optimal control strategy to solve the tracking control problem while providing avoidance features to the closed-loop system. Inspired by the set-point tracking model predictive control (MPC) framework of Limon et al. (2008), the problem of feasibility while tracking changing set-points is solved using artificial variables and an offset cost functional. Afterward, the avoidance feature is included in the set-point tracking MPC strategy through an avoidance cost functional, which allows the utilization of convex admissible sets even in the presence of a previously unknown number of regions to be avoided. This approach allows us to add avoidance features into the set-point tracking MPC strategy without losing the properties of an enlarged domain of attraction and feasibility insurances in the face of any changing reference. Finally, it is shown that the closed-loop system is recursively feasible and input-to-state stable under the mild assumption that the avoidance cost is uniformly bounded over time.

3.2 Problem Description

Consider a finite-dimensional linear time-invariant dynamical system of the form

$$\begin{aligned} x(k+1) &= Ax(k) + Bu(k), \\ y(k) &= Cx(k) + Du(k), \end{aligned} \tag{3.1}$$

with $x(k) \in \mathbb{R}^n$, $u(k) \in \mathbb{R}^m$, and $y(k) \in \mathbb{R}^p$ being, respectively, the state, input, and output vectors. The Jacobians linear model matrices related to the state, $A \in \mathbb{R}^{n\times n}$, and the input, $B \in \mathbb{R}^{n\times m}$, describe the dynamics of the states. Besides, matrices $C \in \mathbb{R}^{p\times n}$ and $D \in \mathbb{R}^{p\times m}$ define the controlled output as a linear combination of the states and the inputs. The solution of the system for a given sequence of control inputs $\boldsymbol{u}$ and initial state x is denoted as $x(j) = \phi(j; x, \boldsymbol{u})$, $j \in \mathbb{I}_{\geq 0}$, where $x = \phi(0; x, \boldsymbol{u})$. It is worth mentioning that non-square systems might be considered.

Assumption 3.1. The dynamical system (3.1) is controllable, observable, and the states are available at each sampling time.

The evolution of the system must be such that the constraint

$$(x(k), u(k)) \in Z \tag{3.2}$$

holds for all $k \geq 0$, defined by the sets of admissible states and inputs as $Z = X \times U$. In addition, there exists an invertible linear map $f : Z \mapsto Y$ defining the set of admissible output Y. Although this assumption is restrictive, it will be relaxed later on.

Assumption 3.2. The set $Z \subset \mathbb{R}^{n+m}$ is a compact convex polyhedron containing the origin in its interior.

If a finite previously unknown number N_o of non-feasible output regions $O(i)$ strictly contained in Y are considered, the admissible output set might become a non-convex compact set defined by

$$\tilde{Y} = Y - \bigcup_{i=1}^{N_O} O(i). \tag{3.3}$$

Thus, assuming that the inverse map $f^{-1} : \tilde{Y} \mapsto \tilde{Z}$ exists, the evolution of the system must be such that the constraint

$$(x(k), u(k)) \in \tilde{Z} \tag{3.4}$$

is satisfied for all $k \geq 0$, where $\tilde{Z}$ may not be a convex set fulfilling Assumption 3.2.

Set-point tracking MPC aims to make the error between the target output and the actual output tend to zero. Without the presence of non-feasible output regions $O(i)$, for asymptotic stabilization, a target output y_t must be a steady-output associated with an admissible equilibrium point (x_s, u_s). If this condition is satisfied, the target output is said to be reachable; otherwise, the tracking control problem fails since it is not possible to stabilize the system with the desired output (Limon et al., 2008). Therefore, any target output must satisfy

$$\begin{bmatrix} A - I_n & B \\ C & D \end{bmatrix} \begin{bmatrix} x_s \\ u_s \end{bmatrix} = \begin{bmatrix} O_{n,1} \\ y_t \end{bmatrix}, \tag{3.5}$$

with $(x_s, u_s) \in Z$ and $O_{n,1}$ being a n-dimensional zero vector.

For any given target output y_t, there exists an associated equilibrium point (x_s, u_s) if and only if (Rawlings & Mayne, 2009)

$$\text{rank}\left(\begin{bmatrix}(A-I_n) & B\\ C & D\end{bmatrix}\right) = n + p. \tag{3.6}$$

For a square system, i.e. $p = m$, if condition (3.6) is satisfied, every y_t can be tracked and there is a unique equilibrium point (x_s, u_s) associated to it. For a flat system, i.e. $p < m$, if condition (3.6) holds, every y_t can be tracked and there is an infinite number of equilibrium points (x_s, u_s) whose output is y_t. Finally, if the system is thin, i.e. $p > m$, or the condition (3.6) does not hold, y_t can be only partially tracked or the system can be steered to a target zone (Ferramosca et al., 2010).

Considering that condition (3.6) is satisfied, it is possible to define the set of joint steady-states and inputs, Z_s, and the set of reachable outputs, Y_r, respectively, as

$$Z_s = \{(x_s, u_s) : x_s = Ax_s + Bu_s, (x_s, u_s) \in Z\}, \tag{3.7}$$

$$Y_r = \{y_t : y_t = Cx_s + Du_s, (x_s, u_s) \in Z_s\}. \tag{3.8}$$

Two main sources of feasibility and stability issues are present when handling set-point tracking MPC with avoidance features. First, since the feasibility region for the closed-loop system is reference-dependent, unknown variations on the target outputs may compromise recursive feasibility and asymptotic stability, leading the controller to fail tracking the reference (Pannocchia & Kerrigan, 2005). Second, the existence of previously unknown non-feasible regions in the known admissible output space (3.3) might make the target output unfeasible ($y_t \notin \tilde{Y}$) or unreachable in the obstructed space (there is no evolution of the system output towards y_t that fulfill $y(k) \in \tilde{Y}, \forall k \geq 0$).

Therefore, within this context, the following problem is posed:

Problem 3.1. Design an MPC law $\kappa_N^o(x(k), y_t, O(i))$ to track any prior reachable target output $y_t \in Y_r$ ensuring that the evolution of the system output lies outside any non-feasible output region $O(i)$. Also, by considering that a global solution to the problem can be obtained, if the target is feasible and reachable in the obstructed space ($y_t \in Y_r \cap \tilde{Y}$), and there is no non-feasible region in the neighborhood of the target, the tracking error must tend to zero asymptotically

$$\lim_{k\to\infty} \|y(k) - y_t\| = 0.$$

Otherwise, the system output must converge asymptotically to a bounded set around a reachable steady-output $y_s \in Y_r \subset \tilde{Y}$ that minimizes a given performance index.

3.3 Control Design

The controller proposed in this section is designed to ensure Input-to-State Stability (ISS) in the Lyapunov sense for any reachable target in the obstructed space $\tilde{Y}$ while avoiding any non-feasible output region $O(i)$. For that, we consider the system (3.1) subject to the constraint (3.2). Besides, to avoid loss of controllability related to active constraints (Rao & Rawlings, 1999), we remove from Y_r those reachable targets that are associated with equilibrium points lying at active constraints. For that, the condition $(x_s, u_s) \in Z_s$ of (3.8) is replaced by $(x_s, u_s) \in \lambda Z_s$ with $\lambda \in (0, 1)$ and possibly very close to 1.

Avoidance features can be obtained enforcing $y(k) \in \tilde{Y}$ for all $k > 0$, implying that the closed-loop system satisfies constraint (3.4). However, since $\tilde{Z}$ is possibly a non-convex set priory unknown, enforcing constraint (3.4) directly may be impractical from the optimization problem point-of-view. Besides, there is no guarantee that the inverse map $f^{-1} : \tilde{Y} \mapsto \tilde{Z}$, required to obtain constraint (3.4), exists. A possible solution to work around those issues considers an equivalent strictly convex optimization problem that constrains the closed-loop system to the known admissible convex set Z by enforcing (3.2) while taking into consideration non-feasible regions $O(i)$ through penalty functions. Following this procedure, set-point tracking MPC with avoidance features can be obtained by extending the formulation proposed in Limon et al. (2008) by considering an avoidance cost functional in addition to the offset functional.

For that, let y_a be an artificial steady-output, which is an extra decision variable in the optimal control problem to avoid issues related to the loss of feasibility. Moreover, let (x_a, u_a) be an artificial equilibrium point associated with y_a.

Assumption 3.3. Any output non-feasible set $O(i)$ is available at each sampling time either by measurement and estimation or, if available, by previous knowledge on the sets. Also, they are considered constant throughout the prediction horizon.

Remark 3.1. Modeling, measurement, and estimation errors can be accounted considering an enclosure for each set $O(i)$, such as $\sigma O(i)$ with $\sigma > 1$.

Given a value function $V(y)$ and the non-convex constraint $y \in \tilde{Y}$ with the constraint set being represented as $\tilde{Y} = \{y : g_j(y, O(i)) \leq 0, j \in \mathbb{I}_{1:q}, \forall i\}$, the optimization problem

$$\begin{aligned} \text{minimize} \quad & V(y) \\ \text{subject to} \quad & y \in \tilde{Y}, \end{aligned} \tag{3.9}$$

can be rewritten as the unconstrained problem

$$\text{minimize} \quad V(y) + \mu F(y, O(i)), \tag{3.10}$$

where μ is a positive constant, and $F(y, O(i))$ is a continuous function such that $F(y, O(i)) \geq 0$ if $y \notin \tilde{Y}\ \forall i$, and $F(y, O(i)) = 0$ otherwise (Luenberger & Ye, 2008). A general class of penalty functions is

$$F(y, O(i)) = \sum_{j=1}^{q} (\max\{0, g_j(y, O(i))\})^{\epsilon}, \tag{3.11}$$

for some $\epsilon > 0$. As $\mu \to \infty$, the solution of the penalty problem converges to the solution of the constrained problem. Besides, if $\epsilon = 1$, exact penalization can be obtained if μ is chosen to be greater than the biggest corresponding Lagrange multiplier, meaning that the problems will be equivalent (Luenberger & Ye, 2008; Ferramosca et al., 2011).

Following the presented penalty method, the proposed controller is based on the solution at each sampling time of an optimal control problem having as parameters $(x, y_t, O(i))$ and as decision variables $(\boldsymbol{u}, x_a, u_a)$. The cost functional is composed of three terms: i) a dynamic term, which is a combination of a stage cost with respect to the artificial steady-state and input (x_a, u_a) and a terminal cost; ii) a stationary term, which is the offset cost functional penalizing the deviation of the artificial steady-output y_a to the target output y_t; and iii) another stationary term, which is the avoidance cost functional penalizing the artificial steady-output y_a and the system predicted output $\boldsymbol{y}$. Considering the horizon length $N \in \mathbb{I}_{>0}$, this cost functional is defined as

$$\begin{aligned} V_N(x, y_t, O(i); \boldsymbol{u}, x_a, u_a) = &\sum_{j=0}^{N-1} \|x(j) - x_a\|_Q^2 + \|u(j) - u_a\|_R^2 + \|x(N) - x_a\|_P^2 + V_{of}(y_a, y_t) + \\ &\sum_{i=1}^{N_o} \Big[\mu F(y_a, O(i)) + \sum_{j=0}^{N} \mu F(y(j), O(i))\Big]. \end{aligned} \tag{3.12}$$

Assumption 3.4. The following assumptions, standard in the tracking MPC literature, are sufficient conditions to ensure asymptotic stability for the closed-loop system without non-feasible regions $O(i)$ (Limon et al., 2008; Ferramosca et al., 2009):

1. Let $R \in \mathbb{R}^{m \times m}$ be a positive definite matrix and $Q \in \mathbb{R}^{n \times n}$ a positive semidefinite matrix such that the pair $(Q^{1/2}, A)$ is observable;
2. Let $K \in \mathbb{R}^{m \times n}$ be a stabilizing control gain such that $A_K = A + BK$ is Schur;
3. Let $P \in \mathbb{R}^{n \times n}$ be a positive definite matrix, solution of the Lyapunov equation $P = A_K' P A_K + Q + K'RK$;
4. Let $\Omega_t^a \subseteq \mathbb{R}^{n+n+m}$ be an admissible polyhedral invariant set for tracking for system (3.1) subject to (3.2), under the local control law $u = K(x - x_a) + u_a$. That is, the following constraints hold for all $(x, x_a, u_a) \in \Omega_t^a$:

$$\begin{aligned} &(x, K(x - x_a) + u_a) \in Z, \\ &(x_a, u_a) \in \lambda Z_s, \\ &(Ax + B(K(x - x_a) + u_a), x_a, u_a) \in \Omega_t^a; \end{aligned} \tag{3.13}$$

5. Let the offset cost $V_{of}(\cdot) : \mathbb{R}^{2p} \mapsto \mathbb{R}_{\geq 0}$ be a continuous, convex, and positive definite function with $V_{of}(0,0) = 0$ for $k = 0$, such that

$$\arg \min_{y_a \in Y_r} V_{of}(y_a, y_t) \tag{3.14}$$

is unique for any y_t.

Defining $\Omega_t = \mathrm{Proj}_x(\Omega_t^a)$, the feasible region $X_N(\Omega_t)$ is defined as the N-steps controllable set to Ω_t. Notice that $X_N(\Omega_t)$ is by definition the domain of attraction for the proposed controller. Furthermore, to provide the controller with avoidance features and to later derive the ISS property with respect to the avoidance cost, consider the following assumption.

Assumption 3.5. Let the continuous function $V_{av}(\cdot) : \mathbb{R}^p \mapsto \mathbb{R}_{\geq 0}$ be given by $V_{av}(\cdot) = \sum_{i=1}^{N_o} [\mu F(y_a, O(i)) + \sum_{j=0}^{N} \mu F(y(j), O(i))]$. Moreover, let the bound of the avoidance function be defined as $S = \sup(V_{av}(\cdot))$, such that V_{av} tends to S if $y_a \notin \tilde{Y}$ or $y(j) \notin \tilde{Y}$ for any $j \in \mathbb{I}_{0:N}$, with $V_{av}(\cdot) = 0$ whenever $y_a \in \tilde{Y}$ and $y(j) \in \tilde{Y}$ for all $j \in \mathbb{I}_{0:N}$.

The controller is derived from the solution of the optimal control problem $P_N^O(x, y_t, O(i))$ given by

$$V_N^O(x, y_t, O(i)) = \min_{\boldsymbol{u}, x_a, u_a} V_N(x, y_t, O(i); \boldsymbol{u}, x_a, u_a)$$

$$\text{s.t.}\ x(0) = x, \tag{3.15a}$$

$$x(j+1) = Ax(j) + Bu(j), \tag{3.15b}$$

$$y(j) = Cx(j) + Du(j), \tag{3.15c}$$

$$(x(j), u(j)) \in Z,\ \ j \in \mathbb{I}_{0:N-1}, \tag{3.15d}$$

$$y_a = Cx_a + Du_a, \tag{3.15e}$$

$$(x(N), x_a, u_a) \in \Omega_t^a, \tag{3.15f}$$

with constraints (3.15a)-(3.15d) subjecting the predicted trajectory to the system dynamics and constraints, and with constraints (3.15e) and (3.15f), respectively, defining the artificial steady-output related to an artificial equilibrium and enforcing the terminal state to be in a region where the system can be stabilized by a local control law $u = K(x - x_a) + u_a$. Notice that the constraints of the optimal control problem $P_N^O(x, y_t, O(i))$ do not depend on y_t, making it feasible for any changing set-point. Additionally, the resulting optimization problem has a known convex output space because the inclusion of the previously unknown non-feasible regions $O(i)$ as penalties allowed the use of the known admissible set Z in constraint (3.15d). Furthermore, the penalty approach makes the set Ω_t^a time-invariant, which allows it to be obtained through offline computation.

Considering the receding policy of MPC controllers and the fact that the optimization problem (3.15) is solved at each sampling time based on the current knowledge of the optimization parameters, the optimal control law is given by

$$\kappa_N^O(x, y_t, O(i)) = u^O(0; x, y_t, O(i)). \tag{3.16}$$

Theorem 3.1. (Asymptotic stability (Ferramosca et al., 2009, Theorem 1)) Consider that Assumptions 3.1, 3.2, and 3.4 hold for the system (3.1) constrained by (3.2) without the presence of non-feasible output regions $O(i)$. For a given target y_t and for any feasible initial state $x \in X_N(\Omega_t)$, the closed-loop system with $\kappa_N^O(x, y_t)$ is stable, fulfills the constraints throughout the time and, besides

(i) If $y_t \in Y_r$, then the closed-loop system asymptotically converges to y_t.

(ii) If $y_t \notin Y_r$, then the closed-loop system asymptotically converges to a reachable steady-output that minimizes

$$\arg \min_{y_a \in Y_r} V_{of}\left(y_a, y_t\right).$$

Theorem 3.2. (ISS-based avoidance) Consider that Assumptions 3.1 to 3.5 hold, then the closed-loop system with $\kappa_N^o(x, y_t, O(i))$ is ISS with respect to the avoidance cost $V_{av}(\cdot)$, i.e., there exist a $\mathcal{KL}$-function $\beta(\cdot)$ and a $\mathcal{K}$-function $\gamma(\cdot)$ such that for any feasible initial state $x(0) \in X_N(\Omega_t)$, steady-state $x_s \in \text{Proj}_x(Z_s)$, and bound S, the solution $\phi(k; x(0), \boldsymbol{u})$ exists and satisfies

$$\|\phi(k; x(0), \boldsymbol{u}) - x_s\| \leq \beta(\|x(0) - x_s\|, k) + \gamma(S), \tag{3.17}$$

for all $k \in \mathbb{I}_{>0}$.

Theorem 3.2 can be interpreted as follows. In presence of non-feasible output regions, the avoidance cost acts as disturbance and only ISS can be ensured. Therefore, the closed-loop system converges asymptotically to a bounded set around a steady state, either desired or feasible. Besides, depending on the penalties obtained, which in last analysis depends on the non-feasible output regions $O(i)$, only local convergence might be achieved. In this context, asymptotic stability in the terms of Theorem 3.1 is only recovered when the avoidance cost goes to zero, i.e, S goes to zero.

To demonstrate Theorem 3.2, first, we prove that the controlled system is recursively feasible. Afterward, as proposed in Alessandretti et al. (2017), a shifted value function is defined to account for the effect of the avoidance cost. Then, upper and lower bounds are obtained, as well as a bound on the shifted value function decrease. Finally, inspired by Alessandretti et al. (2017) and following the procedure presented in Jiang & Wang

(2001), it is shown that the closed-loop system is ISS with respect to the bound S and, consequently, to the avoidance cost functional.

Lemma 3.1. (Steady condition convergence) Consider that Assumptions 3.1 to 3.5 hold for the system (3.1) constrained by (3.2). For any feasible initial state $x \in X_N(\Omega_t)$, target y_t, and bound S, let the optimal solution to $P_N^O(x, y_t, O(i))$ be such that $x = x_a^O$, $u = u_a^O$, and $y = y_a^O$. Moreover, let (x_s, u_s, y_s) be the optimal triplet satisfying (3.5), such that function $V_{of}(y_a, y_t) + V_{av}(\boldsymbol{y}, y_a, O(i))$ is minimized. Then, $x = x_s$, $u = u_s$, and $y = y_s$.

Proof.

Consider that (x_a^O, u_a^O, y_a^O) is the optimal solution to $P_N^O(x, y_t, O(i))$. Then

$$V_N^O(x, y_t, O(i)) = V_{of}(y_a^O, y_t) + V_{av}(\boldsymbol{y}, y_a^O, O(i)). \tag{3.18}$$

This Lemma will be proved by contradiction, extending the results of Limon et al. (2018, Lemma 1) for the case with avoidance considering a linear system. For that, assume now that the stationary point is not optimal, i.e., $(x_a^O, u_a^O) \neq (x_s, u_s)$. Let us define

$$(\tilde{x}_a, \tilde{u}_a) = \gamma(x_a^O, u_a^O) + (1 - \gamma)(x_s, u_s) \tag{3.19}$$

with $\gamma \in [0, 1]$. Since both (x_s, u_s) and (x_a^O, u_a^O) are in Z_s, and this set is convex, then a convex combination of these points, $(\tilde{x}_a, \tilde{u}_a)$, is also in Z_s.

Considering Assumptions 3.4.5 and 3.5, it is possible to obtain a convex cost functional that superiorly bounds the non-convex cost $V_{of}(y_a, y_t) + V_{av}(\boldsymbol{y}, y_a, O(i))$. Then, we can define

$$V_B(y_a, y_t) = V_{of}(y_a, y_t) + S, \tag{3.20}$$

for any bound S, such that

$$V_B(\tilde{y}_a, y_t) \leq V_B(y_a^O, y_t) \tag{3.21}$$

for every γ. In other words, since the system is not at the optimal point (x_s, u_s), it is more convenient to move towards $(\tilde{x}_a, \tilde{u}_a)$ than to remain in (x_a^O, u_a^O).

Let $\tilde{\boldsymbol{u}}$ be a feasible control sequence that drives the system from (x_a^O, u_a^O) to $(\tilde{x}_a, \tilde{u}_a)$. This sequence is such that the j-th element is given by $\tilde{u}(j) = K(\tilde{x}(j) - \tilde{x}_a) + \tilde{u}_a$ and $\tilde{x}(j+1) = A\tilde{x}(j) + B\tilde{u}(j)$, with $\tilde{x}(0) = x_a^O$. Then, the cost to drive the system to $(\tilde{x}_a, \tilde{u}_a)$ in N steps is

$$\begin{aligned} V_N(x_a^O, y_t, O(i)) = \sum_{j=0}^{N-1} \|\tilde{x}(j) - \tilde{x}_a\|_Q^2 + \|K(\tilde{x}(j) - \tilde{x}_a)\|_R^2 + \|\tilde{x}(N) - \tilde{x}_a\|_P^2 + \\ V_{of}(\tilde{y}_a, y_t) + V_{av}(\tilde{\boldsymbol{y}}, \tilde{y}_a, O(i)) \end{aligned}$$

$$
\begin{aligned}
&\leq \sum_{j=0}^{N-1} \|\tilde{x}(j) - \tilde{x}_a\|_Q^2 + \|K(\tilde{x}(j) - \tilde{x}_a)\|_R^2 + \|\tilde{x}(N) - \tilde{x}_a\|_P^2 + V_{of}(\tilde{y}_a, y_t) + S \\
&\leq \|x_a^O - \tilde{x}_a\|_P^2 + V_{of}(\tilde{y}_a, y_t) + S \\
&\leq (1-\gamma)^2 \|x_a^O - x_s\|_P^2 + V_{of}(\tilde{y}_a, y_t) + S.
\end{aligned}
\tag{3.22}
$$

Now define $W(\gamma) = (1-\gamma)^2\|x_a^O - x_s\|_P^2 + V_B(\tilde{y}_a, y_t)$ and notice that for $\gamma = 1$, $W(1) = V_B(y_a^O, y_t)$. Taking the partial derivative of this function with respect to γ and evaluating it for $\gamma = 1$, we obtain

$$
\left.\frac{\partial W}{\partial \gamma}\right|_{\gamma=1} = g^{O'}(y_a^O, y_t), \tag{3.23}
$$

with $g^{O'}(y_a^O, y_t) \in \partial V_B(y_a^O, y_t)$, where $\partial V_B(y_a^O, y_t)$ is defined as the subdifferential of $V_B(y_a^O, y_t)$.

From convexity and from (3.21),

$$
\left.\frac{\partial W}{\partial \gamma}\right|_{\gamma=1} = g^{O'}(y_a^O, y_t) \geq V_B(y_a^O, y_t) - V_B(\tilde{y}_a, y_t) > 0. \tag{3.24}
$$

This means that there exists a value of $\gamma \in [0, 1)$ such that $V_B(\tilde{y}_a, y_t)$ is smaller than the value of the cost $V_B(\tilde{y}_a, y_t)$ for $\gamma = 1$, which is $V_B(y_a^O, y_t)$. This contradicts the optimality of the solution of $P_N^O(x, y_t, O(i))$. Then, it has to be $(x_a^O, u_a^O) = (x_s, u_s)$, with (x_s, u_s) being the minimizer of $V_{of}(y_a, y_t) + V_{av}(\boldsymbol{y}, y_a, O(i))$, which concludes the proof. $\square$

Lemma 3.2. (Artificial error boundedness) Consider that the Assumptions 3.1 to 3.5 hold. Let x_s be the optimal steady-state associated with the optimal target y_s, such that function $V_N(x, y_t, O(i))$ is minimized. For all $x \in X_N(\Omega_t)$ and $x_a^O \in \mathrm{Proj}_x(Z_s)$, define the function $e(x) = x - x_a^O$. Then, there exists a $\mathcal{K}$-function $\alpha_e(\cdot)$ such that

$$
\|e(x)\| \geq \alpha_e(\|x - x_s\|). \tag{3.25}
$$

Proof.

This lemma extends the results of D'Jorge et al. (2020, Lemma 4) for the case with avoidance. Thus, following a similar analysis, due to convexity, $e(x)$ is a continuous function (Rawlings & Mayne, 2009, Theorem A.23). Moreover, let us consider these two cases.

1. $\|e(x)\| = 0$ if and only if $x = x_s$. In fact,
   (i) if $e(x) = 0$, then $x = x_a^O$, and from Lemma 3.1, this implies that $x_a^O = x_s$;
   (ii) if $x = x_s$, then by optimality $x_a^O = x_s$, and then $x = x_a^O$. Therefore, $\|e(x)\| = 0$.
2. $\|e(x)\| > 0$ for all $\|x - x_s\| > 0$. In fact, for any $x \neq x_s$, $\|e(x)\| \neq 0$ and moreover $\|x - x_s\| > 0$. Then, $\|e(x)\| > 0$.

Therefore, since $X_N(\Omega_t)$ is compact (Vidyasagar, 1993, Chapter 5 - Lemma 6), there exists a $\mathcal{K}$-function $\alpha_e(\cdot)$ such that $\|e(x)\| \geq \alpha_e(\|x - x_s\|)$ on $X_N(\Omega_t)$, which concludes the proof. $\square$

Lemma 3.3. (Recursive feasibility) Consider that Assumptions 3.1 to 3.4 hold, then the closed-loop system with the optimal control law $\kappa_N^o(x, y_t, O(i))$ is recursively feasible for any feasible state $x \in X_N(\Omega_t)$.

Proof.

For a feasible state $x \in X_N(\Omega_t)$ at time k, the optimal cost functional is $V_N^O(x, y_t, O(i))$, with the decision variables $(\boldsymbol{u}^O, x_a^O, u_a^O)$ being the optimal solution of the optimization problem $P_N^O(x, y_t, O(i))$. The optimal control sequence $\boldsymbol{u}^O = (u^O(0), \cdots, u^O(N-1))$ is associated with the optimal predicted state sequence $\boldsymbol{x}^O = (x^O(0), \cdots, x^O(N-1), x^O(N))$ with $x^O(N) \in \Omega_t$. Defining an auxiliary feasible input sequence, an auxiliary feasible artificial state, and an auxiliary feasible artificial input, respectively,

$$\begin{aligned} \tilde{\boldsymbol{u}} &= (u^O(1), \cdots, u^O(N-1), K(x^O(N) - x_a^O) + u_a^O), \\ \tilde{x}_a &= x_a^O, \\ \tilde{u}_a &= u_a^O, \end{aligned} \tag{3.26}$$

the state sequence associated to $(\tilde{\boldsymbol{u}}, \tilde{x}_a, \tilde{u}_a)$ starting from $x(k+1) = Ax(k) + Bu^O(0)$ is given by

$$\tilde{\boldsymbol{x}} = (x^O(1), \cdots, x^O(N), x(N+1)), \tag{3.27}$$

with $x(N+1) = Ax^O(N) + B(K(x^O(N) - x_a^O) + u_a^O)$.

Since $(x^O(N), x_a^O, u_a^O) \in \Omega_t^a$, the control action $K(x^O(N) - x_a^O) + u_a^O$ is admissible and the terminal state $x(N+1)$ is feasible due to the positive invariance of Ω_t^a, i.e., $(x(N+1), \tilde{x}_a, \tilde{u}_a) \in \Omega_t^a$. Therefore, $x(k+1) \in X_N(\Omega_t)$, proving that the closed-loop system is recursively feasible. □

Consider the shifted value function defined by

$$V_s(x, y_t, O(i)) = V_N(x, y_t, O(i)) - S, \tag{3.28}$$

as a Lyapunov candidate for the problem $P_N^O(x, y_t, O(i))$.

Lemma 3.4. (Upper bound) Consider that Assumptions 3.1 to 3.5 hold, then the shifted value function $V_s(\cdot)$ satisfies

$$V_s(x, y_t, O(i)) \leq \alpha_c(\|x - x_s\|), \tag{3.29}$$

with $\alpha_c(\cdot)$ being a $\mathcal{K}_\infty$-function.

Proof.

From the shifted value function definition and based on the suboptimality of the feasible law $\boldsymbol{u}_f$, i.e., $u_f(j) \in U \ \forall j \geq 0$, it holds that

$$\begin{aligned}
&\sum_{j=0}^{N-1} \|x^O(j) - x_a^O\|_Q^2 + \|u^O(j) - u_a^O\|_R^2 + \|x^O(N) - x_a^O\|_P^2 + V_{of}(y_a^O, y_t) + V_{av}(\boldsymbol{y}^O, y_a^O, O(i)) - S \\
\leq &\sum_{j=0}^{N-1} \|x(j) - x_a\|_Q^2 + \|u_f(j) - u_a\|_R^2 + \|x(N) - x_a\|_P^2 + V_{of}(y_a, y_t) + V_{av}(\boldsymbol{y}, y_a, O(i)) - S \quad (3.30)
\end{aligned}$$

Since $V_{av}(\boldsymbol{y}, y_a, O(i)) - S \leq 0$ based on the boundedness of the avoidance function, we have

$$\begin{aligned}
&\sum_{j=0}^{N-1} \|x(j) - x_a\|_Q^2 + \|u_f(j) - u_a\|_R^2 + \|x(N) - x_a\|_P^2 + V_{of}(y_a, y_t) + V_{av}(\boldsymbol{y}, y_a, O(i)) - S \\
\leq &\sum_{j=0}^{N-1} \|x(j) - x_a\|_Q^2 + \|u_f(j) - u_a\|_R^2 + \|x(N) - x_a\|_P^2 + V_{of}(y_a, y_t) \\
= \ &J(x). \qquad (3.31)
\end{aligned}$$

Since $J(x)$ is a locally bounded continuous function with $J(x_s) = 0$ (Lemma 3.1), then there exists a $\mathcal{K}_\infty$-function $\alpha_c(\cdot)$ such that $J(x) \leq \alpha_c(\|x - x_s\|)$, for all $x \in X_N(\Omega_t)$ (Rawlings & Mayne, 2009). □

Lemma 3.5. (Lower bound) Consider that Assumptions 3.1 to 3.5 hold, then the shifted value function $V_s(\cdot)$ satisfies

$$V_s(x, y_t, O(i)) \geq \alpha_b(\|x - x_s\|) - S \qquad (3.32)$$

with $\alpha_b(\cdot)$ being a $\mathcal{K}_\infty$-function.

Proof.

From Assumptions 3.4.1 to 3.4.3, there is a $\mathcal{K}_\infty$-function $\alpha(\|x - x_a\|)$ such that

$$\|x - x_a\|_Q^2 + \|u - u_a\|_R^2 + \|x - x_a\|_P^2 \geq \alpha(\|x - x_a\|). \qquad (3.33)$$

Following the definition of the shifted value function (3.28), we have

$$\begin{aligned}
&\sum_{j=0}^{N-1} \|x(j) - x_a\|_Q^2 + \|u(j) - u_a\|_R^2 + \|x(N) - x_a\|_P^2 + V_{of}(y_a, y_t) + V_{av}(\boldsymbol{y}, y_a, O(i)) - S \\
\geq &\sum_{i=0}^{N-1} \alpha(\|x - x_a\|) + V_{of}(y_a, y_t) + V_{av}(\boldsymbol{y}, y_a, O(i)) - S \\
\geq &\sum_{i=0}^{N-1} \alpha(\|x - x_a\|) + V_{av}(\boldsymbol{y}, y_a, O(i)) - S \\
\geq &\sum_{i=0}^{N-1} \alpha(\|x - x_a\|) - S. \qquad (3.34)
\end{aligned}$$

Finally, based on Lemma 3.2 and on the optimality principle, we have

$$\sum_{i=0}^{N-1} \alpha(\|x - x_a\|) - S \geq \hat{\alpha}_b(\|x - x_a^O\|) - S \geq \alpha_b(\|x - x_s\|) - S, \tag{3.35}$$

with $\alpha_b(r) = \hat{\alpha}_b \circ \alpha_e(r)$. □

Lemma 3.6. (Decreasing property) Consider that Assumptions 3.1 to 3.5 hold, then the shifted function $V_s(\cdot)$ satisfies

$$V_s^O(x(k+1), y_t, O(i)) - V_s^O(x(k), y_t, O(i)) \leq -\alpha(\|x - x_s\|) + S, \tag{3.36}$$

with $\alpha(\cdot)$ being a $\mathcal{K}_\infty$-function.

Proof.

Let the optimal control sequence, the auxiliary feasible input sequence, the optimal output sequence, the auxiliary feasible output sequence, the auxiliary feasible artificial state, the auxiliary feasible artificial output, and the auxiliary feasible artificial input be given, respectively, by

$$\begin{aligned}
\boldsymbol{u}^O &= (u^O(0), u^O(1), \cdots, u^O(N-1)),\\
\tilde{\boldsymbol{u}} &= (u^O(1), \cdots, u^O(N-1), K(x^O(N) - x_a^O) + u_a^O),\\
\boldsymbol{y}^O &= (y^O(0), y^O(1), \cdots, y^O(N)),\\
\tilde{\boldsymbol{y}} &= (y^O(1), \cdots, y^O(N), y(N+1)),\\
\tilde{x}_a &= x_a^O,\\
\tilde{y}_a &= y_a^O,\\
\tilde{u}_a &= u_a^O,
\end{aligned} \tag{3.37}$$

with the triplet $(\tilde{x}_a, \tilde{u}_a, \tilde{y}_a)$ being the feasible solution to the one-step ahead optimization problem. Besides, $x(k+1) = Ax(k) + Bu^O(0)$ is the successor state.

Comparing, at $k+1$, $V_s(x(k+1), y_t, O(i); \tilde{\boldsymbol{u}}, \tilde{x}_a, \tilde{u}_a)$ and $V_s^O(x(k), y_t, O(i))$, it is possible to obtain

$$\begin{aligned}
V_s(x(k+1), y_t, &O(i);\ \tilde{\boldsymbol{u}}, \tilde{x}_a, \tilde{u}_a) - V_s^O(x(k), y_t, O(i)) =\\
&\|x^O(N) - \tilde{x}_a\|_Q^2 + \|K(x^O(N) - \tilde{x}_a)\|_R^2 + \|x(N+1) - \tilde{x}_a\|_P^2 + V_{of}(\tilde{y}_a, y_t) +\\
&V_{av}(\tilde{\boldsymbol{y}}, \tilde{y}_a, O(i)) - S - \|x(0)^O - x_a^O\|_Q^2 - \|u^O(0) - u_a^O\|_R^2 - \|x^O(N) - x_a^O\|_P^2 -\\
&V_{of}(y_a^O, y_t) - V_{av}(\boldsymbol{y}^O, y_a^O, O(i)) + S\\
\leq\ & V_{av}(\tilde{\boldsymbol{y}}, \tilde{y}_a, O(i)) - V_{av}(\boldsymbol{y}^O, y_a^O, O(i)) - \|x(0)^O - x_a^O\|_Q^2 - \|u^O(0) - u_a^O\|_R^2.
\end{aligned} \tag{3.38}$$

Based on the boundedness of the avoidance function, $V_{av}(\tilde{\boldsymbol{y}}, \tilde{y}_a, O(i)) - V_{av}(\boldsymbol{y}^O, y_a^O, O(i)) \leq S$, on the optimality principle, $V_s^O(x(k+1), y_t, O(i)) \leq V_s(x(k+1), y_t, O(i); \tilde{\boldsymbol{u}}, \tilde{x}_a, \tilde{u}_a)$, and on

Lemma 3.2, there is a $\mathcal{K}_\infty$-function $\alpha(\|x - x_s\|)$ such that

$$\begin{aligned} V_s^O(x(k+1), y_t, O(i)) - V_s^O(x(k), y_t, O(i)) &\leq -\hat{\alpha}(\|x - x_a^O\|) + S \\ &\leq -\alpha(\|x - x_s\|) + S, \end{aligned} \tag{3.39}$$

with $\alpha(r) = \hat{\alpha} \circ \alpha_e(r)$. □

Lemma 3.7. (ISS bound) Consider that Assumptions 3.1 to 3.5 hold, then there exists a $\mathcal{KL}$-function $\hat{\beta}$ such that the shifted function $V_s(\cdot)$ satisfies

$$V_s^O(x(k), y_t, O(i)) \leq \max\{\hat{\beta}(V_s^O(x(0), y_t, O(i)), k), \hat{\gamma}(S)\} \tag{3.40}$$

with

$$\hat{\gamma}(r) = \hat{\alpha}^{-1} \circ \rho^{-1}(r) \tag{3.41}$$

for all $k \in \mathbb{I}_{\geq 0}$, with $\rho(\cdot)$ being a $\mathcal{K}_\infty$-function such that $(id - \rho)(\cdot)$ is a $\mathcal{K}_\infty$-function, and with $\hat{\alpha}(\cdot)$ being a $\mathcal{K}_\infty$-function such that $\hat{\alpha}(r) \leq \alpha_b \circ \alpha_c^{-1}(r)$, for all $r \geq 0$, and with $(id - \hat{\alpha})(\cdot)$ being a $\mathcal{K}$-function.

Proof.

This proof can be obtained following the steps considered in Jiang & Wang (2001, Lemma 3.5). Thus, rewriting Lemma 3.6 and considering Lemma 3.4, we have

$$V_s^O(x(k+1), y_t, O(i)) - V_s^O(x(k), y_t, O(i)) \leq -\alpha \circ \alpha_c^{-1}(V_s^O(x(k), y_t, O(i))) + S. \tag{3.42}$$

Without loss of generality, for $\hat{\alpha} = \alpha \circ \alpha_c^{-1}$, we assume $(id - \hat{\alpha})(\cdot)$ to be a $\mathcal{K}$-function. Let ρ be any $\mathcal{K}_\infty$-function such that $(id - \rho)(\cdot)$ is a $\mathcal{K}_\infty$-function and consider the set defined by

$$\mathcal{D} = \{x : V_s^O(x(k), y_t, O(i)) \leq b\}, \tag{3.43}$$

where $b = \hat{\alpha}^{-1} \circ \rho^{-1}(S)$.

Claim 3.1. If there is some $k_0 \in \mathbb{Z}_{>0}$ such that $x(k_0) \in \mathcal{D}$, then $x(k) \in \mathcal{D}$ for all $k \geq k_0$.

Proof.

Assume $x(k_0) \in \mathcal{D}$. Then $V_s^O(x(k_0), y_t, O(i)) \leq b$, this is, $\rho \circ \hat{\alpha}(V_s^O(x(k_0), y_t, O(i)) \leq S$. From equation (3.42),

$$V_s^O(x(k_0+1), y_t, O(i)) \leq (id - \hat{\alpha})(V_s^O(x(k_0), y_t, O(i))) + S, \tag{3.44}$$

and since $id - \hat{\alpha}$ is a $\mathcal{K}$-function, we have

$$
\begin{aligned}
V_s^O(x(k_0+1), y_t, O(i)) &\leq (id - \hat{\alpha})(b) + S \\
&= b - \hat{\alpha}(b) + \rho \circ \hat{\alpha}(b) - \rho \circ \hat{\alpha}(b) + S \\
&= -(id - \rho) \circ \hat{\alpha}(b) + b - \rho \circ \hat{\alpha}(b) + S \\
&= -(id - \rho) \circ \hat{\alpha}(b) + b \\
&\leq b.
\end{aligned} \tag{3.45}
$$

By induction, it is possible to show that $V_s^O(x(k_0+j), y_t, O(i)) \leq b$ for all $j \in \mathbb{Z}_{>0}$, that is, $x(k) \in \mathcal{D}$ for all $k \geq k_0$.

□

We now let $j_0 = \min\{k \in \mathbb{Z}_{>0} : x(k) \in \mathcal{D}\} < \infty$. Then, it follows from the above conclusion that $V_s^O(x(k), y_t, O(i)) \leq \hat{\gamma}(S)$ for all $k \geq j_0$, where $\hat{\gamma}(r) = \hat{\alpha}^{-1} \circ \rho^{-1}(r)$. For $k < j_0$, it holds that $\rho \circ \hat{\alpha}(V_s^O(x(k), y_t, O(i))) > S$, and hence

$$
\begin{aligned}
&V_s^O(x(k+1), y_t, O(i)) - V_s^O(x(k), y_t, O(i))) \\
&\qquad \leq -\hat{\alpha}(V_s^O(x(k), y_t, O(i))) + S \\
&\qquad = -\hat{\alpha}(V_s^O(x(k), y_t, O(i))) + S - \rho \circ \hat{\alpha}(V_s^O(x(k), y_t, O(i))) + \rho \circ \hat{\alpha}(V_s^O(x(k), y_t, O(i))) \\
&\qquad = -(id - \rho) \circ \hat{\alpha}(V_s^O(x(k), y_t, O(i))) - \rho \circ \hat{\alpha}(V_s^O(x(k), y_t, O(i))) + S \\
&\qquad \leq -(id - \rho) \circ \hat{\alpha}(V_s^O(x(k), y_t, O(i)))
\end{aligned} \tag{3.46}
$$

By a comparison lemma (Jiang & Wang, 2002), there exists some $\mathcal{KL}$-function $\hat{\beta}$ such that

$$
V_s^O(x(k), y_t, O(i)) \leq \hat{\beta}(V_s^O(x(0), y_t, O(i)), k) \tag{3.47}
$$

for all $0 \leq k < j_0$. Thus,

$$
V_s^O(x(k), y_t, O(i)) \leq \max\{\hat{\beta}(V_s^O(x(0), y_t, O(i)), k), \hat{\gamma}(S)\} \tag{3.48}
$$

for all $k \in \mathbb{Z}_{>0}$.

□

Proof. (**Theorem 3.2**)

From Lemma 3.5 and Lemma 3.7, and knowing that for nonnegative real numbers a and b it holds that $\max\{a, b\} \leq a + b \leq \max\{2a, 2b\}$,

$$
\begin{aligned}
\alpha_b(\|x - x_s\|) &\leq \max\{\hat{\beta}(V_s^O(x(0), y_t, O(i)), k), \hat{\gamma}(S)\} + S \\
&\leq \max\{2\max\{\hat{\beta}(V_s^O(x(0), y_t, O(i)), k), \hat{\gamma}(S)\}, 2S\} \\
&= \max\{2\hat{\beta}(V_s^O(x(0), y_t, O(i)), k), 2\hat{\gamma}(S), 2S\},
\end{aligned} \tag{3.49}
$$

and by the monotonicity of $\alpha_b^{-1}(\cdot)$

$$\begin{aligned}\|x - x_s\| &= \max\{\alpha_b^{-1} \circ 2\hat{\beta}(\alpha_c(\|x(k_0) - x_s\|), k), \alpha_b^{-1} \circ 2\hat{\gamma}(S), \alpha_b^{-1}(2S)\} \\ &\leq \alpha_b^{-1} \circ 2\hat{\beta}(\alpha_c(\|x(k_0) - x_s\|), k)) + \alpha_b^{-1} \circ 2\hat{\gamma}(S) + \alpha_b^{-1}(2S),\end{aligned} \tag{3.50}$$

where $\beta(\cdot)$ and $\gamma(\cdot)$ are the class-$\mathcal{KL}$ and the class-$\mathcal{K}_\infty$ functions, respectively, defined as

$$\begin{aligned}\beta(r_1, s) &= \alpha_b^{-1} \circ 2\hat{\beta}(\alpha_c(r_1, s)) \\ \gamma(r_2) &= \alpha_b^{-1} \circ 2\hat{\gamma}(r_2) + \alpha_b^{-1}(2r_2)\end{aligned} \tag{3.51}$$

Based on Lemmas 3.4 to 3.6, $V_s(x, y_t, O(i))$ is an ISS-Lyapunov function for system (3.1) with bounds $\beta(\cdot)$ and $\gamma(\cdot)$. Then, from Jiang & Wang (2001, Lemma 3.5), the system is ISS, i.e., $\|\phi(k; x(0), \boldsymbol{u}) - x_s\| \leq \beta(\|x(0) - x_s\|, k) + \gamma(S)$ for all $k \in \mathbb{I}_{>0}$, concluding the proof. □

Remark 3.2. (Terminal Equality Constraint) Considering a terminal equality constraint is a practical way to implement the proposed controller. For that, let $(x_a, u_a) \in \lambda Z_s$, $x(N) = x_a$, and $P = O_{n,n}$. Following the same arguments presented before, it can be proved that the results of Theorem 3.2 and Lemma 3.3 still hold under the mild assumption that the N-controllability matrix of the system, $Co_N = [A^{N-1}B \ \cdots \ AB \ B]$, has full rank.

3.4 Controller Properties

In addition to the stability guarantees proved before, some properties of the set-point tracking MPC strategy still hold after the inclusion of the avoidance penalty cost.

3.4.1 Stability under changing references

Theorems 3.1 and 3.2 show that the closed-loop system with the optimal control law $\kappa_N^o(x, y_t, O(i))$ is ISS with respect to the avoidance cost and asymptotic stable for a given target y_t if the avoidance cost tends to zero, i.e., if there are no non-feasible output regions $O(i)$. Besides, since the constraints of the problem $P_N^O(x, y_t, O(i))$ do not depend on y_t, the closed-loop system is feasible for any changing target as long as (3.5) is satisfied. Thus, even in the presence of significant changes in y_t, the controller is still well-posed and recursive feasibility and ISS properties are not lost.

3.4.2 Unreachable references

In the case of unreachable references, either due to the system dynamics and constraints or due to non-feasible output regions $O(i)$, i.e., $y_t \notin Y_r$, $y_t \notin \tilde{Y}$, or $y(k) \notin \tilde{Y}$ for some $k \geq 0$, the proposed controller will steer the system to a reachable steady-output $y_s \in Y_r \subset \tilde{Y}$ such that

$$y_s = \arg\min_{y_a \in Y_r} V_{of}(y_a, y_t) + V_{av}(\boldsymbol{y}, y_a, O(i)). \tag{3.52}$$

The same behavior occurs in the case of local solutions to the optimization problem.

3.4.3 Enlarged domain of attraction

Since the designed terminal set Ω_t in the worst case will be equal to the maximal admissible invariant set of a standard MPC (Mayne et al., 2000), the domain of attraction $X_N(\Omega_t)$ is said to be enlarged. This result is further discussed in Limon et al. (2008).

When a terminal equality constraint condition is under consideration, the terminal set for the standard MPC is composed only by the steady-state x_s related to the desired target y_t. For the proposed controller, on the other hand, the terminal set is the set of all reachable steady-states $\text{Proj}_x(Z_s)$. Thus, by definition, $x_s \in \text{Proj}_x(Z_s)$. Notice that, due to the presence of artificial variables and an offset cost functional, every admissible steady-state is inside the domain of attraction of the proposed controller, i.e., $\text{Proj}_x(Z_s) \subseteq X_N(\Omega_t)$ for all $N \in \mathbb{I}_{>0}$.

3.4.4 Avoidance guarantees

Avoidance can be ensured only if, at each sampling period, the artificial and the predicted output sequence lie outside any non-feasible output regions $O(i)$, i.e., $y_a \in \tilde{Y}$ and $\boldsymbol{y} \in \tilde{Y}$. These constraints, and consequently avoidance, can be enforced exactly through the penalty function (3.11) if $\mu \to \infty$ or if the penalization is considered with $\epsilon = 1$ and μ greater than the biggest corresponding Lagrange multiplier (Luenberger & Ye, 2008; Ferramosca et al., 2011). However, since exact penalization often results in ill-posed optimization problems and $\mu \to \infty$ violates Assumption 3.5, non-exact penalization may be chosen together with a definition of safety regions around the non-feasible regions $O(i)$ to ensure avoidance while keeping the avoidance cost superiorly bounded, e.g., by considering $\sigma O(i)$ with $\sigma > 1$. Furthermore, this cautious approach of considering an enclosure of $O(i)$ can mitigate uncertainties, such as measurement, estimation, modeling, and linearization errors.

3.5 Numerical Examples

This section presents simulation results obtained to corroborate the effectiveness of the proposed MPC strategy to provide set-point tracking control with avoidance features. Two examples are studied. The first one considers a ball-on-plate system with a known non-convex admissible output set. The second example considers a UAV navigating in a cluttered environment with previously unknown obstacles. In both cases, the simulations are performed with MATLAB using the CasADI Toolbox (Andersson et al., 2019) with the IPOPT solver (Wächter & Biegler, 2005). In these examples, all units follows the international system standards.

3.5.1 Ball-on-plate with non-convex plate

Consider the ball-on-plate system described in Appendix A, Section A.1, with a non-convex admissible output set, as proposed in Cotorruelo et al. (2021). Being the system actuated through the desired angular acceleration of the plate, the state and input vectors are, respectively, as $x = [p_1 \; p_2 \; \theta_1 \; \theta_2 \; \dot{p}_1 \; \dot{p}_2 \; \dot{\theta}_1 \; \dot{\theta}_2]'$ and $u = [a_1 \; a_2]'$. Furthermore, the output of the system is the position of the ball $y = [p_1 \; p_2]'$.

The system input is constrained by $\|u\|_\infty \leq 0.2$, and the admissible output space is constrained by the ellipsoids

$$\begin{aligned} Y(1) &= \{y : (y - y_{c_1})' E_1 (y - y_{c_1}) \leq 1\}, \\ Y(2) &= \{y : (y - y_{c_2})' E_2 (y - y_{c_2}) \leq 1\}, \end{aligned} \tag{3.53}$$

with

$$E_1 = \begin{bmatrix} 16 & 0 \\ 0 & 0.5 \end{bmatrix}, \; E_2 = \begin{bmatrix} 5.8551 & 7.3707 \\ 7.3707 & 10.6449 \end{bmatrix}, \; y_{c_1} = y_{c_2} = \begin{bmatrix} 0 \\ 0 \end{bmatrix}.$$

Following the proposed methodology, the admissible output set is $\tilde{Y} = Y(1) \cup Y(2)$. However, for control design purposes, we can consider the output admissible set to be $Y = \{y : \|y\|_\infty \leq 2\}$ with an associate avoidance cost functional to avoid the non-feasible output region $O = Y - \tilde{Y}$. The system is constrained to $\tilde{Y}$ if the disjoint constraint $y \in Y(1) \vee y \in Y(2)$ holds. Thus, a penalty function similar to the one considered in Hermans et al. (2018) is defined, yielding

$$F(y, Y(j)) = \prod_{j=1}^{2} (\max\{0, g_j(y, Y(j))\})^2, \tag{3.54}$$

where $g_1(y, Y(1)) = (y - y_{c_1})' E_1 (y - y_{c_1}) - 1 + \gamma_1$ and $g_2(y, Y(2)) = (y - y_{c_2})' E_2 (y - y_{c_2}) - 1 + \gamma_2$, with $\gamma_1 = \gamma_2 = 0.15$ being a constant to define a safety region around O.

The discrete linear model (A.2) is considered for prediction, which is obtained after linearization around an equilibrium condition and discretization considering a first-order Euler approximation. As for the system dynamics simulation, the non-linear model (A.1) is considered together with the ordinary differential equation solver ODE45 from MATLAB.

The system starts in the initial condition $x(0) = [0 \; -1.2 \; 0 \; 0 \; 0 \; 0 \; 0 \; 0]'$, and it is required to reach the target output $y_t = [-0.85 \; 0.60]'$. The horizon length considered for prediction is $N = 8$, the weighting matrices are $Q = \text{diag}\{2, 2, 1, 1, 10, 10, 50, 50\}$ and $R = \text{diag}\{0.01, 0.01, 0.01, 0.01\}$, which, following Assumption 3.4 and defining $\lambda = 0.9999$, lead to P, K, and Ω_t^a. Furthermore, for the avoidance cost, we consider $\mu = 10^5$, while the offset cost is defined as $V_{of}(y_a, y_t) = \|y_a - y_t\|_\kappa^2$ with $\kappa = \text{diag}\{10^4, 10^4\}$.

Figure 3.1 shows the shape of the non-convex plate defined by the union of the ellipses $Y(1)$ and $Y(2)$. In addition, it depicts the output trajectory performed by the closed-loop system from the initial condition to the desired output (indicated by the black x-shaped marker). Notice that the position of the ball starts following the ellipse $Y(1)$ contour with a safe distance until there is a clear path towards the output target. This behavior can be observed in more detail in Figure 3.2, where the output tracking error is shown. It is worth highlighting, especially on the upper graphic, that the tracking error decay rate reduces up to the point where it becomes almost constant. After the cornering point where the ellipses intersect each other, the decay rate increases again. Unlike any controller designed only for set-point tracking, the avoidance term disturbs the asymptotic convergence to the target when necessary. However, since the closed-loop system is ISS with respect to the avoidance cost, at some point the effect of the avoidance may vanish and the asymptotic convergence to an admissible steady-output point is reached again.

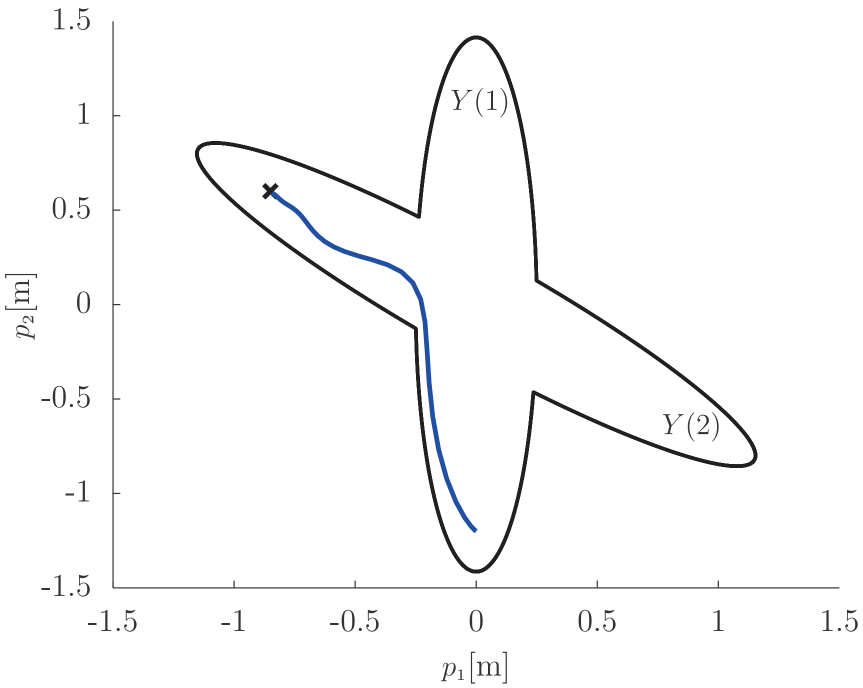

Figure 3.1: Complete trajectory performed by the ball (blue line) over the non-convex plate composed by the union of two ellipses. In the figure, the black cross-mark denotes the desired set-point.

Furthermore, Figure 3.3 shows separately the evolution of the ball position and the plate orientation. Besides showing the convergence to the desired position, this figure also depicts the angles stably converging to the steady condition of null orientation of the plate. Finally, Figure 3.4 depicts the calculated control inputs. It can be observed in the figure that the controller was able to perform set-point tracking while satisfying the constraints imposed on the control action.

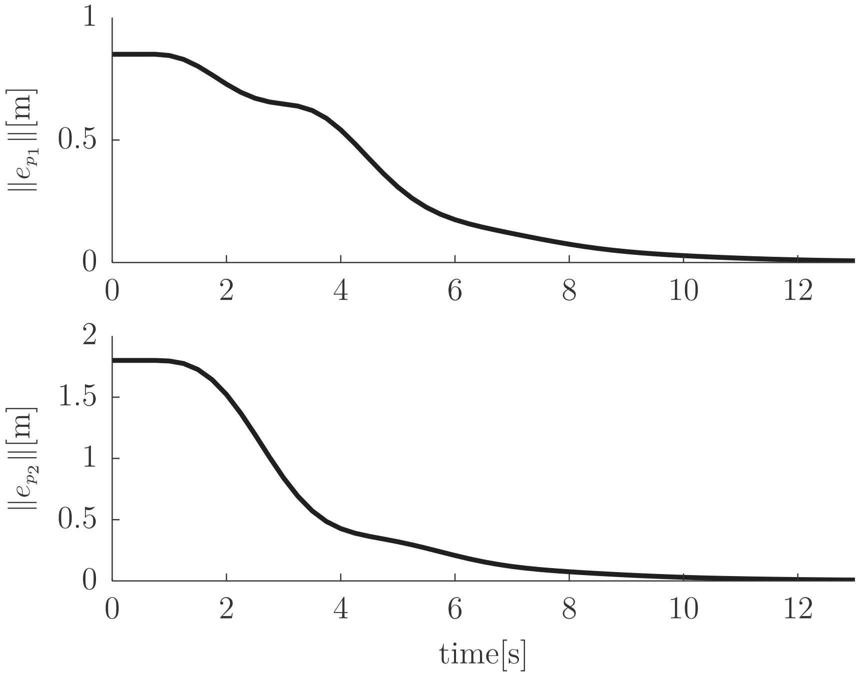

Figure 3.2: Absolute output tracking error with $e_{p_1} = p_1 - p_{1t}$ and $e_{p_2} = p_2 - p_{2t}$. In the figure, it is illustrated the relation between error reduction and avoidance.

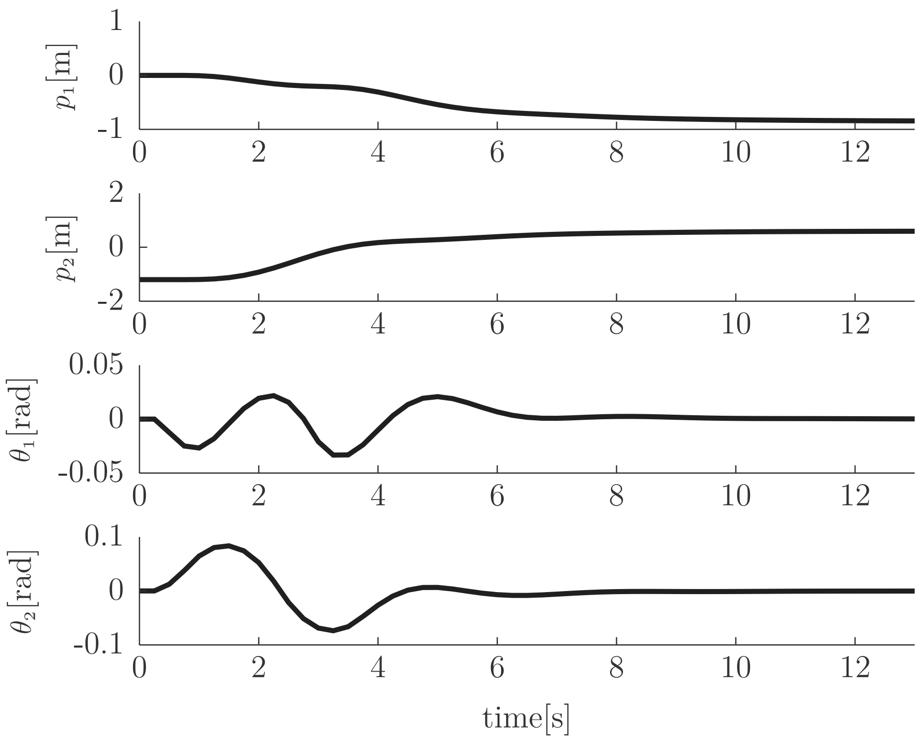

Figure 3.3: Time evolution of the ball position (p_1 and p_2) and the plate angles (θ_1 and θ_2) during the tracking of the provided set-point.

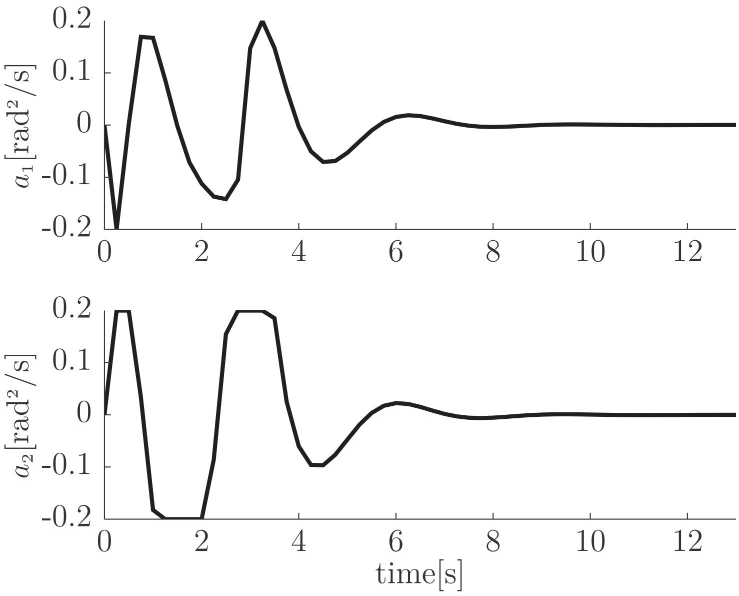

Figure 3.4: Time evolution of the desired angular accelerations (a_1 and a_2), the manipulated variables of the system.

3.5.2 UAV navigation in cluttered environment

Consider the quadrotor UAV system described in Appendix A, Section A.3. The system is actuated through the lift forces, $u = [f_1\ f_2\ f_3\ f_4]'$, with its states composed of position and attitude as well as their time derivatives, $x = \left[x^{\mathcal{I}}\ y^{\mathcal{I}}\ z^{\mathcal{I}}\ \phi\ \theta\ \psi\ \dot{x}^{\mathcal{I}}\ \dot{y}^{\mathcal{I}}\ \dot{z}^{\mathcal{I}}\ \dot{\phi}\ \dot{\theta}\ \dot{\psi}\right]'$. Additionally, the controlled output is chosen as the UAV position and yaw angle, $y = [x^{\mathcal{I}} y^{\mathcal{I}} z^{\mathcal{I}} \psi]'$.

Aiming to better emulate the vehicle dynamics during the simulation, the non-linear dynamic model (A.14) is considered with the parameters provided in Table A.2. Further, the ordinary differential equation solver ODE45 from MATLAB is used for numerical integration with a discretization time-step of 0.01 seconds. However, for control design purposes it is used a discrete linear model, equation (A.17), based on a non-linear model that disregards the coupling between translational and rotational dynamics due to the displacement between the quadrotor's geometric center and its center of mass (see Section A.3).

In order to access the capacity of avoiding non-feasible regions, we consider a $48 \times 30 \times 20$ meters map with nine rectangle-shaped obstacles obstructing the UAV workspace. A 3D LIDAR-like sensor is emulated to detect the obstacles within a spherical range of four meters based on the quadrotor UAV global position and the environment map. However, it is worth noting that, from the control algorithm standpoint, the obstacles are previously unknown and perceived only by the obstacle detection system. Hence, they are only avoided when inside the sensor range. Based on the sensor information, the obstacles are defined in execution time as a two meters radius sphere centered in the closest point measured in the boundary of the obstacle. Therefore, considering $g_j(y) = -(y - y_{c_j})' I_3 (y - y_{c_j}) + 2^2$, the penalty function can be defined as

$$F(y, O(j)) = \sum_{j=1}^{N_O} (\max\{0, g_j(y, O(j))\})^2,$$

with N_0 being the number of detected obstacles.

For this example, we consider the terminal equality constraint version of the controller (see Remark 3.2) with horizon length $N = 50$ and the weighting matrices $Q = \text{diag}\{1, 1, 1, 0.1, 0.1,\ 1, 1, 1, 1, 10, 10, 1\}$ and $R = \text{diag}\{10, 10, 10, 10\}$. As for the offset and avoidance costs, $V_{of}(y_a, y_t) = \|y_a - y_t\|^2_\kappa$ with $\kappa = \text{diag}\{4000, 4000, 30000, 4000\}$ and $\mu = 40000$. Furthermore, the admissible input set is $U = \{(f_1, f_2, f_3, f_4) \in \mathbb{R}^4 : 0 \leq f_1, f_2, f_3, f_4 \leq 12\}$, and the admissible state set is defined accordingly to the map dimensions and the system operational conditions $X = \{[\xi'\ \eta'\ \dot{\xi}'\ \dot{\eta}']' : [-24\ -15\ 0] \leq \xi \leq [24\ 15\ 20]', |\eta| \leq [\pi/2\ \pi/2\ \pi]', |\dot{\xi}| \leq [5\ 5\ 5]', |\dot{\eta}| \leq [\pi/2\ \pi/2\ \pi/2]'\}$. Notice that since the linearization point consider non-null control inputs, the set U must be modified to account for u_{eq} before used in the control problem.

In this simulation scenario, the quadrotor UAV is required to go autonomously from its initial position $[-17\ \ -12\ 0]'$ to the desired one $[18.75\ 8\ 15]'$, depicted in the upper part of Figure 3.5, with $\psi = 0$. If a controller without any avoidance feature was used, the

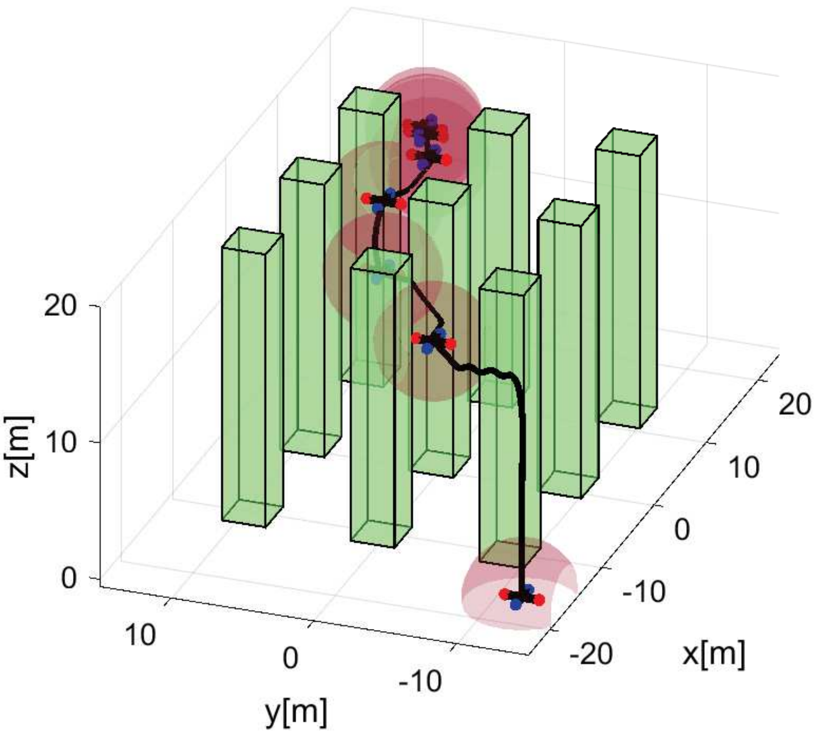

Figure 3.5: Trajectory performed by the UAV (black line) to safely complete a given task while avoiding nine previously unknown obstacles, which are denoted by the green rectangle-shaped objects. In the figure, the UAV is denoted as a black cross with blue and red spheres in its extremities and the light red sphere around the UAV denotes the range in which obstacles can be detected.

most obvious behavior would be to go in a straight line directly to the goal, which would lead to collisions. Therefore, it is expected that the proposed set-point tracking MPC with avoidance features will find an alternative path around the obstacles by means of the artificial variables. In fact, Figure 3.5 shows the vehicle after it reaches the goal and the alternative path performed to reach the desired target. Then, the use of the proposed control strategy provides the system with two interesting features. First, in the presence of obstacles, the controller autonomously finds a path around them by means of the artificial variables. Second, it provides feasible intermediary equilibrium points when the required target is not reachable in N steps by the system due to its dynamics and constraints. It is worthwhile mentioning that the obstacles shape and spatial distribution has direct impact on the ability to obtain a global solution to the optimal control problem. However, the proposed formulation does not limit neither the shape nor the spatial distribution of the regions to be avoided. Furthermore, by perceiving the obstacles within a given range as spheres centered in the closest points measured in the boundaries of each obstacle, from the control algorithm standpoint, the number and position of the perceived obstacles change over-time despite the environment being static.

The avoidance process can also be verified by looking at the absolute position error. In fact, the control algorithm gives up performance to achieve safe navigation, which can be observed in Figure 3.6 where the error stops decreasing at some points even before converging to zero. Moreover, Figure 3.7 presents the time evolution of the quadrotor UAV orientation stably converging to an equilibrium value. This is expected since at the end of the task execution the UAV will be in hovering flight mode due to the equilibrium condition of the artificial variables. Notice that, since the artificial steady-output is defined

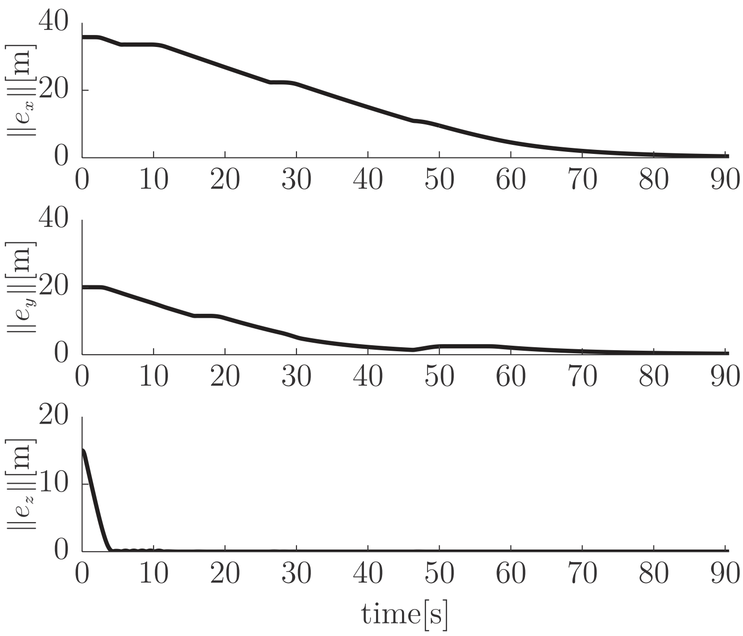

Figure 3.6: Absolute output tracking error illustrating the relation between error reduction and avoidance. In the figure, $e_x = x^{\mathcal{I}} - x_r$, $e_y = y^{\mathcal{I}} - y_r$, and $e_z = z^{\mathcal{I}} - z_r$.

in the output level, there is no need to require a reference for ϕ and θ. In fact, the artificial orientation is obtained from the artificial position by means of the model constraints. Finally, Figure 3.8 shows the control signals applied to the quadrotor UAV. Note that the controller was able to perform the set-point tracking of the desired target output without surpassing the actuators' saturation level.

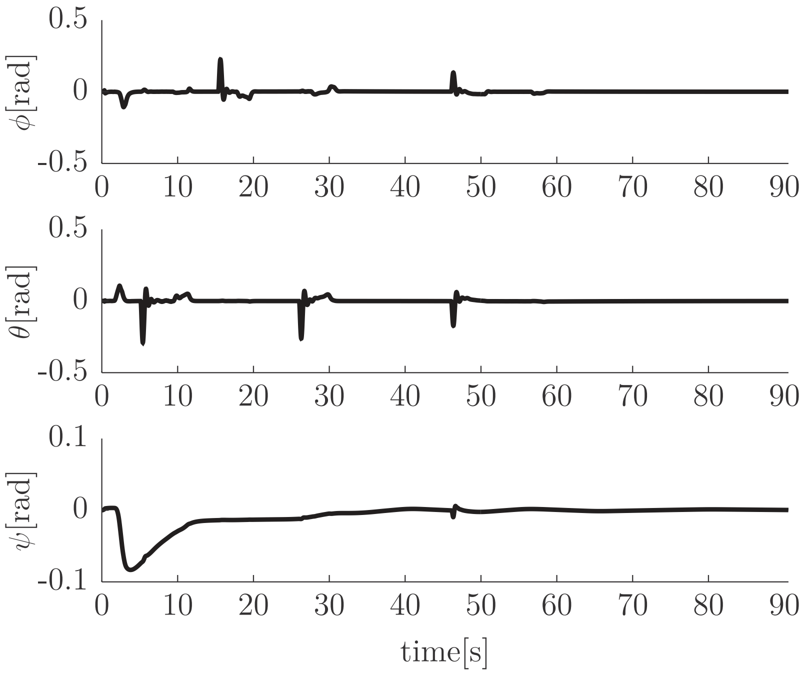

Figure 3.7: Time evolution of the quadrotor UAV orientation (ϕ, θ, and ψ) during the execution of the provided task.

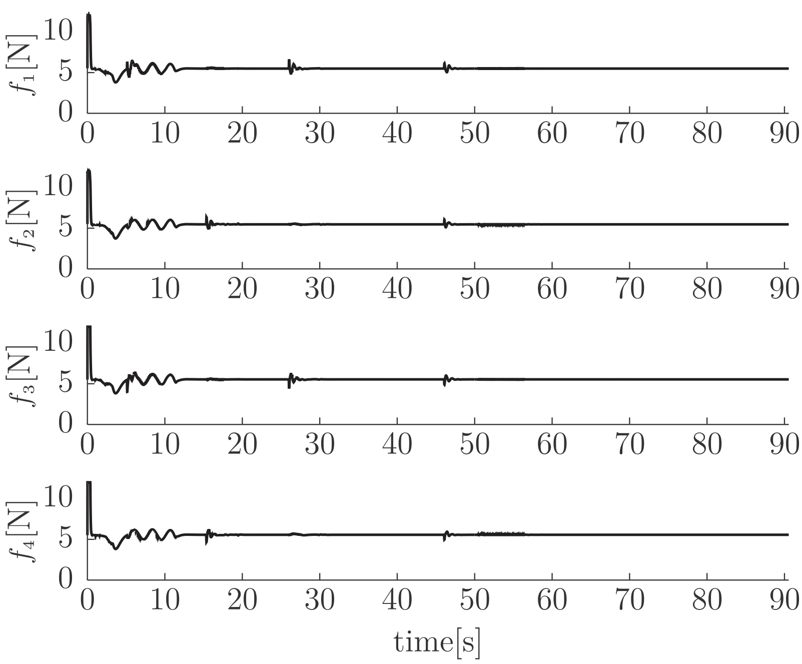

Figure 3.8: Time evolution of the applied lift forces to the quadrotor UAV, with f_i being the lift force of the i-th propeller.

3.6 Final Remarks

In this chapter, it was proposed a linear model predictive control strategy able to perform set-point tracking while avoiding non-feasible regions inside the prior known admissible space. For that, three main ingredients were considered: i) artificial variables to represent artificial steady conditions; ii) offset cost functional playing the role of a steady-state target optimizer; and iii) an avoidance cost functional avoiding the system evolution to lie inside non-feasible regions. It was shown that, under mild conditions, the closed-loop system is ISS with respect to the avoidance cost. Thus, it was possible to demonstrate that the closed-loop system is stable and recursively feasible.

The control strategy proposed in this chapter is not addressing directly problems related to errors caused by measurements, modeling, disturbances, and estimation, among others. Although there is some inherent robustness due to the feedback process and the non-feasible regions could be overestimated to handle the different sources of uncertainties (see Remark 3.1 and Section 3.4.4), ensuring robustness by design is a desired feature. Therefore, in the next chapter, the formulation proposed here is extended by considering the avoidance problem in the presence of unknown but bounded uncertainties.

4

Robust Set-Point Tracking with Avoidance Features

4.1 Introduction

Chapter 3 has shown that the set-point tracking MPC with avoidance features holds the properties of stability under changing references, feasibility under unreachable references, an enlarged domain of attraction, and avoidance guarantees. Nevertheless, in presence of uncertainties such properties may be lost. In this context, the results of Chapter 3 are extended by considering the avoidance problem in the presence of unknown but bounded uncertainties. As in Limon et al. (2010), the problem of feasibility while tracking changing set-points is solved using artificial variables and an offset cost functional. Besides, aiming at robustness, it is considered a semi-feedback formulation together with the notion of tube of trajectories for robust constraint satisfaction, for which a zonotopic set representation is used. Then, the avoidance cost is designed through penalty functions, with the avoidance constraints being enlarged to account for the uncertainties. It is shown that, under mild conditions, the closed-loop system converges to (a neighborhood of) the target if the target is reachable in the obstructed space and the proposed optimal control problem can be solved globally. Otherwise, it is shown that the closed-loop system converges to (a neighborhood of) a reachable steady-output that minimizes a given cost functional. In this chapter, some assumptions and definitions considered in Chapter 3 are restated for the sake of clarity.

4.2 Problem Description

Consider a finite-dimensional uncertain linear discrete-time system of the form

$$\begin{aligned} x(k+1) &= Ax(k) + Bu(k) + w(k), \\ y(k) &= Cx(k) + Du(k), \end{aligned} \tag{4.1}$$

with $x(k) \in \mathbb{R}^n$, $u(k) \in \mathbb{R}^m$, $y(k) \in \mathbb{R}^p$, and $w(k) \in \mathbb{R}^n$ being, respectively, the state, input, output, and process disturbance vectors. The solution of (4.1) for the initial state x, a sequence of control inputs $\boldsymbol{u}$, and a sequence of disturbances $\boldsymbol{w}$, is denoted as $x(j) = \phi(j; x, \boldsymbol{u}, \boldsymbol{w})$, $j \in \mathbb{I}_{\geq 0}$, where $x = \phi(0; x, \boldsymbol{u}, \boldsymbol{w})$.

Assumption 4.1. The dynamical system (4.1) is controllable, observable, and the states are available at each sampling time.

The evolution of the uncertain system (4.1) must be such that the constraint

$$(x(k), u(k)) \in Z \tag{4.2}$$

holds for all $k \geq 0$, defining the sets of admissible states and inputs as $X = \mathrm{Proj}_x(Z)$ and $U = \mathrm{Proj}_u(Z)$, respectively. In addition, there exists an invertible linear map $f : Z \mapsto Y$ defining the set of admissible output Y.

Assumption 4.2. The set $Z \subset \mathbb{R}^{n+m}$ is a compact convex polyhedron containing the origin in its interior.

Assumption 4.3. The process disturbance vector w is unknown but bounded by a compact convex polyhedron, $W \subset \mathbb{R}^n$, containing the origin in its interior.

If a finite number N_o of (possibly) previously unknown non-feasible output regions $O(i)$, strictly contained in Y, are considered, the resultant admissible output set might become a non-convex compact set defined by

$$\tilde{Y} = Y - \bigcup_{i=1}^{N_o} O(i). \tag{4.3}$$

Thus, assuming that the inverse map $f^{-1} : \tilde{Y} \mapsto \tilde{Z}$ exists, the evolution of the system must be constrained by

$$(x(k), u(k)) \in \tilde{Z}, \tag{4.4}$$

for all $k \geq 0$, where $\tilde{Z}$ may be a non-convex set.

Assumption 4.4. Any output non-feasible set $O(i)$ is available at each sampling time either by previous knowledge on the sets or by measurement and estimation. Also, they are considered constant throughout the prediction horizon.

Problem 4.1. Design a control law $\kappa_N^o(x(k), y_t, O(i))$ to track a given target output, y_t, ensuring that the system (4.1) fulfills the constraints (4.4) despite the uncertainties. Furthermore, by considering that a global solution to the problem can be obtained, if the target is reachable in the obstructed space, $\tilde{Y}$, the system output must converge to a bounded set in the neighborhood of the target y_t. Otherwise, the system output must converge to a bounded set in the neighborhood of a reachable steady-output y_s that minimizes a given performance index.

4.3 Tube-Based Robust Approach

Aiming at robustness, the proposed controller for set-point tracking with avoidance features is based on a semi-feedback formulation together with the notion of tube of trajectories for robust constraint satisfaction (Chisci et al., 2001; Langson et al., 2004; Limon et al., 2009). In this formulation, the control input is calculated using nominal predictions and constraint tightening procedures.

Let the nominal model be obtained from (4.1) disregarding the additive uncertainties, that is

$$\begin{aligned} \bar{x}(k+1) &= A\bar{x}(k) + B\bar{u}(k), \\ \bar{y}(k) &= C\bar{x}(k) + D\bar{u}(k), \end{aligned} \tag{4.5}$$

with $\bar{x}(k) \in \mathbb{R}^n$, $\bar{u}(k) \in \mathbb{R}^m$, and $\bar{y}(k) \in \mathbb{R}^p$ being, respectively, the state, input, and output nominal vectors.

For a given control sequence, $\bar{\boldsymbol{u}}$, obtained based on the nominal model (4.5), the nominal prediction might differ from the system evolution due to the uncertainties. Thus, the following control law can be defined to counteract the effect of the disturbances:

$$u(k) = \bar{u}(k) + K(x(k) - \bar{x}(k)). \tag{4.6}$$

Considering (4.1), (4.5), and (4.6), the prediction error dynamics can be described as

$$e(k+1) = A_K e(k) + w(k), \tag{4.7}$$

with $e(k) = x(k) - \bar{x}(k)$ and $A_K = (A + BK)$.

Assumption 4.5. Let $K \in \mathbb{R}^{m \times n}$ be a stabilizing control gain such that the matrix $A_K = A + BK$ is Schur.

Following the concept of tube of trajectories, if Assumption 4.5 holds, the evolution of $e(k)$ is bounded and the evolution of the system states, $x(k)$, lies in the neighborhood of the predicted states, $\bar{x}(k)$. To further exploit this concept, we can assume without loss of generality that the prediction error belongs to an invariant Γ that is an external approximation of the minimum robust positively invariant set (see Definition 2.21).

Considering $e(k) \in \Gamma$, by definition of Γ, $e(k+j) \in \Gamma$, $\forall j \in \mathbb{I}_{>0}$. Consequently, all the evolution of the uncertain system controlled by (4.6) is such that $x(k+j) \in \{\bar{x}(k+j)\} \oplus \Gamma$. Therefore, to ensure that constraint (4.2) holds for any realization of the disturbances, the following tightened constraint may be enforced for the nominal states and inputs as

$$(\bar{x}(k), \bar{u}(k)) \in \bar{Z}, \tag{4.8}$$

where $\bar{Z} = Z \ominus (\Gamma \times K\Gamma)$. Besides, to ensure that $\bar{Z}$ is non-empty for a given j, it must hold that $\Gamma \subset X$ and $K\Gamma \subset U$, for which the feedback gain K plays an important role. The design of K determines the dynamics of the closed-loop system in presence of disturbances, and it can be used to obtain less conservative robust positively invariant sets (Limon et al., 2010).

Notice that Γ can be used to redefine the admissible output set (4.3) since $y(k) \notin O(i), \forall i \in \mathbb{I}_{>0}$, is equivalent to $\bar{y}(k) \notin \bar{O}(i), \forall i \in \mathbb{I}_{>0}$, with $\bar{O}(i) = O(i) \oplus \Gamma$. Therefore, accounting for all realization of the uncertainties, we have

$$\tilde{\bar{Y}} = \bar{Y} - \bigcup_{i=1}^{N_o} \bar{O}(i), \tag{4.9}$$

which, assuming that the inverse map $f^{-1} : \tilde{\bar{Y}} \mapsto \tilde{\bar{Z}}$ exists, constrains the evolution of the nominal system to

$$(\bar{x}(k), \bar{u}(k)) \in \tilde{\bar{Z}}. \tag{4.10}$$

The reachability analysis can be used to compute the minimal robust positively invariant set and, consequently, to obtain the tubes for any bounded uncertainties (see Definition 2.26 and Proposition 2.3). For that, considering the prediction error model (4.7) and the initialization condition $\mathcal{R}_k = \{0\}$, which comes directly from Assumption 4.1, the sequence of reachable sets can be obtained recursively as

$$\mathcal{R}_{k+j+1} = A_K \mathcal{R}_{k+j} \oplus W, \quad \forall j \in \mathbb{I}_{0:N-1}. \tag{4.11}$$

The set $\mathcal{R}_j \to \mathcal{R}_\infty$ in the Hausdorff metric as $j \to \infty$, with $\mathcal{R}_\infty$ being the minimal robust positively invariant for system (4.1) pre-stabilized with the feedback gain K. Conversely, $\mathcal{R}_j$ is not a robust invariant for a finite j.

Any suitable procedure able to estimate the range of a function can be used to obtain a sequence of reachable sets (see Limon et al. (2009) and references therein). Amongst them, the use of zonotopes as an outer bound of the exact function range gives a computationally tractable procedure (see Definitions 2.13 and 2.14, and Proposition 2.1). For further results, refer to Le et al. (2013) and references therein.

Remark 4.1. Since the computation of the robust positively invariant set Γ may be cumbersome, simple implementations for constraint tightening, although more conservative, can be obtained assuming $e(k) = 0$ instead of $e(k) \in \Gamma$. Under such condition, the N-th reachable set $\mathcal{R}_N$ can be used for constraint tightening as $e(k+j) \in \mathcal{R}_N$ holds for all $j \in \mathbb{I}_{1:N}$, leading to

$$(\bar{x}(k+j), \bar{u}(k+j)) \in \bar{Z}_N, \tag{4.12}$$

with $\bar{Z}_N = Z \ominus (\mathcal{R}_N \times K\mathcal{R}_N)$. However, a less conservative approach can be taken based on a sequence of reachable sets, for which $e(k+j) \in \mathcal{R}_j$ holds for all $j \in \mathbb{I}_{1:N}$ if $e(k) = 0$. Therefore, the tightened constraints can be rewritten as

$$(\bar{x}(k+j), \bar{u}(k+j)) \in \bar{Z}_N(j), \tag{4.13}$$

with $\bar{Z}_N(j) = Z \ominus (\mathcal{R}_j \times K\mathcal{R}_j)$, resulting in a funnel containing the uncertain system trajectories.

4.4 Nominal Steady Conditions

Consider the nominal system without the presence of non-feasible output regions $O(i)$, aiming at asymptotic stabilization, a target output y_t must be a nominal steady-output associated with a nominal admissible equilibrium point $(\bar{x}_s, \bar{u}_s)$ (Limon et al., 2008). Therefore, any target output must satisfy

$$\begin{bmatrix} A - I_n & B \\ C & D \end{bmatrix} \begin{bmatrix} \bar{x}_s \\ \bar{u}_s \end{bmatrix} = \begin{bmatrix} O_{n,1} \\ y_t \end{bmatrix}, \tag{4.14}$$

with $(\bar{x}_s, \bar{u}_s) \in \bar{Z}$.

For any given target output y_t, there exists an associated equilibrium point $(\bar{x}_s, \bar{u}_s)$ if and only if (Rawlings & Mayne, 2009)

$$\text{rank}\left(\begin{bmatrix} (A - I_n) & B \\ C & D \end{bmatrix} \right) = n + p. \tag{4.15}$$

Assuming that condition (4.15) is satisfied, it is possible to define the set of joint steady-states and inputs, $\bar{Z}_s$, and the set of reachable outputs, $\bar{Y}_r$, respectively, as

$$\bar{Z}_s = \{(\bar{x}_s, \bar{u}_s) : \bar{x}_s = A\bar{x}_s + B\bar{u}_s, (\bar{x}_s, \bar{u}_s) \in \bar{Z}\}, \tag{4.16}$$

$$\bar{Y}_r = \{y_t : y_t = C\bar{x}_s + D\bar{u}_s, (\bar{x}_s, \bar{u}_s) \in \lambda\bar{Z}_s\}, \tag{4.17}$$

with $\lambda \in (0, 1)$ being a constant defined to avoid loss of controllability related to active constraints (Rao & Rawlings, 1999). Notice, however, that considering $\lambda\bar{Z}_s$ does not imply a reduction of the reachable outputs since taking λ arbitrarily close to 1 makes $\bar{Z}_s$ arbitrarily close $\lambda\bar{Z}_s$ in the Hausdorff sense.

Based on (4.17), a target output is said to be reachable if $y_t \in \bar{Y}_r$. Furthermore, it is said to be reachable in the obstructed space if $y_t \in \bar{Y}_r$ and there exists a nominal output sequence $\bar{\boldsymbol{y}}$ with length N connecting the initial output to the target with $\bar{y}(i) \in \tilde{\bar{Y}}, \forall i \in \mathbb{I}_{0:N-1}$.

4.5 Control Design

The controller proposed in this section is designed to provide set-point tracking in presence of bounded disturbances while ensuring input-to-state stability in the Lyapunov sense for any reachable target in the obstructed space. Besides, the evolution of the output must lie outside any non-feasible output region $O(i)$.

Following the robust approach described in Section 4.3, the control law (4.6) is considered to counteract the effect of the disturbances in the closed-loop system. For that, $\bar{u}(k)$ is obtained through a constrained optimal control problem designed for the nominal system (4.5) subject to the tightened constraints (4.8). In this context, avoidance features can be obtained enforcing the constraint $\bar{y}(k+j) \in \tilde{\bar{Y}}$, $\forall j \in \mathbb{I}_{0:n-1}$, implying that constraint (4.10) holds. On the other hand, robust set-point tracking MPC with avoidance features can be obtained extending the formulation proposed in Limon et al. (2010) to account for the avoidance constraints. Therefore, we consider the central idea of including artificial variables into the optimal control problem together with an offset cost functional playing the role of a steady-state target optimizer. Besides, avoidance constraints are added into the optimal control problem.

Let $\bar{y}_a$ be an artificial steady-output, which is an extra decision variable in the optimal control problem to avoid loss of feasibility. Moreover, let $(\bar{x}_a, \bar{u}_a)$ be an artificial equilibrium point associated with $\bar{y}_a$. Following the results of Limon et al. (2010), the cost functional is composed of two terms: i) a dynamic term, which is a combination of a stage cost with respect to the artificial steady-state and input $(\bar{x}_a, \bar{u}_a)$ and a terminal cost; and ii) a stationary term, which is the offset cost functional penalizing the deviation of the artificial steady-output $\bar{y}_a$ from the target output y_t. This cost functional is defined as

$$V_N(x, y_t; \bar{\boldsymbol{u}}, \bar{x}_a, \bar{u}_a) = \sum_{j=0}^{N-1} \|\bar{x}(j) - \bar{x}_a\|_Q^2 + \|\bar{u}(j) - \bar{u}_a\|_R^2 + \|\bar{x}(N) - \bar{x}_a\|_P^2 + V_{of}(\bar{y}_a, y_t), \qquad (4.18)$$

with $N \in \mathbb{I}_{>0}$ being the horizon length and $V_{of}(\cdot)$ being an offset cost functional.

Assumption 4.6. The following assumptions, standard to tracking MPC formulations, are considered (Limon et al., 2008):

1. Let $R \in \mathbb{R}^{m\times m}$ be a positive definite matrix and $Q \in \mathbb{R}^{n\times n}$ a positive semidefinite matrix such that the pair $(Q^{1/2}, A)$ is observable.

2. Let $\bar{K} \in \mathbb{R}^{m\times n}$ be a stabilizing control gain such that the matrix $A_{\bar{K}} = A + B\bar{K}$ is Schur.

3. Let $P \in \mathbb{R}^{n\times n}$ be a positive definite matrix, solution of $P = A'_{\bar{K}} P A_{\bar{K}} + Q + \bar{K}' R \bar{K}$.

4. Let $\Omega^a_{t,\bar{K}} \subseteq \mathbb{R}^{n+n+m}$ be an admissible polyhedral invariant set for tracking associated with system (4.5) subject to (4.8), under the local control law $\bar{u} = \bar{K}(\bar{x} - \bar{x}_a) + \bar{u}_a$. That is, the following constraints hold for all $(\bar{x}, \bar{x}_a, \bar{u}_a) \in \Omega^a_{t,\bar{K}}$:

$$(\bar{x}, \bar{K}(\bar{x} - \bar{x}_a) + \bar{u}_a) \in \bar{Z},$$
$$(\bar{x}_a, \bar{u}_a) \in \lambda \bar{Z}_s,$$
$$(A\bar{x} + B(\bar{K}(\bar{x} - \bar{x}_a) + \bar{u}_a), \bar{x}_a, \bar{u}_a) \in \Omega^a_{t,\bar{K}}.$$

5. Let the offset cost $V_{of}(\cdot) : \mathbb{R}^{2p} \mapsto \mathbb{R}_{\geq 0}$ be a continuous, convex, and positive definite function with $V_{of}(0,0) = 0$ for $k = 0$, such that

$$\arg \min_{\bar{y}_a \in \bar{Y}_r} V_{of}(\bar{y}_a, y_t)$$

is unique for any y_t.

The proposed controller is based on the solution at each sampling time of an optimal control problem $P^O_N(x, y_t, O(i))$ having as decision variables $(\bar{\boldsymbol{u}}, \bar{x}_a, \bar{u}_a)$, which is given by

$$\begin{aligned} V^O_N(x, y_t, O(i)) = \min_{\bar{\boldsymbol{u}}, \bar{x}_a, \bar{u}_a} & V_N(x, y_t; \bar{\boldsymbol{u}}, \bar{x}_a, \bar{u}_a) \\ \text{s.t. } & \bar{x}(0) \in \{x\} \oplus (-\Gamma), && (4.19a) \\ & \bar{x}(j+1) = A\bar{x}(j) + B\bar{u}(j), && (4.19b) \\ & \bar{y}(j) = C\bar{x}(j) + D\bar{u}(j), && (4.19c) \\ & (\bar{x}(j), \bar{u}(j)) \in \tilde{\bar{Z}}, \; j \in \mathbb{I}_{0:N-1}, && (4.19d) \\ & \bar{y}_a = C\bar{x}_a + D\bar{u}_a, && (4.19e) \\ & \bar{y}_a \in \tilde{\bar{Y}}, && (4.19f) \\ & (\bar{x}(N), \bar{x}_a, \bar{u}_a) \in \Omega^a_{t,\bar{K}}, && (4.19g) \end{aligned}$$

with constraint (4.19a) enforcing that $e(0) \in \Gamma$ and with constraints (4.19b)-(4.19d) subjecting the predicted trajectory to the system dynamics and constraints. Furthermore, constraints (4.19e) and (4.19g), respectively, define the artificial steady-output related to an artificial equilibrium and enforce the terminal state to be in a region where the nominal system can be stabilized by a local control law $\bar{u} = \bar{K}(\bar{x} - \bar{x}_a) + \bar{u}_a$. Notice that constraint (4.19d) enforces the predicted nominal states and the associated nominal input to lie in a space that can be mapped into the tightened non-obstructed output space $\tilde{\bar{Y}}$. Besides, constraint (4.19f) ensures that the artificial output is out of any non-feasible output region $O(i)$. Together, constraints (4.19d) and (4.19f) bring obstacle avoidance features to the problem.

Since $\tilde{\bar{Z}}$ and $\tilde{\bar{Y}}$ are (possibly) non-convex sets priory unknown, enforcing constraints (4.19d) and (4.19f) directly may be impractical from the optimization problem point-of-view. Also, there is no guarantee that the inverse map $f^{-1} : \tilde{\bar{Y}} \mapsto \tilde{\bar{Z}}$ exists. Furthermore, the properties present in the robust set-point tracking MPC formulation proposed in Limon et al. (2009) may be lost, such as, recursive feasibility, stability, and robust constraint satisfaction. A possible solution to work around these issues can be obtained considering a strictly convex equivalent optimization problem that constrains the closed-loop system to the known convex tightened admissible set $\bar{Z}$ by enforcing (4.13) while handling the non-feasible regions $O(i)$ through penalties functions.

Consider the cost functional (4.18) modified to add penalty functions for avoidance as

$$\tilde{V}_N(x, y_t, O(i); \bar{\boldsymbol{u}}, \bar{x}_a, \bar{u}_a) = V_N(x, y_t; \bar{\boldsymbol{u}}, \bar{x}_a, \bar{u}_a) + \sum_{i=1}^{N_o} \Big[\mu F(\bar{y}_a, \bar{O}(i)) + \sum_{j=0}^{N} \mu F(\bar{y}(j), \bar{O}(i))\Big], \quad (4.20)$$

where μ is a positive constant, $\bar{O}(i)$ is the expanded non-feasible region, and $F(\bar{y}, \bar{O}(i))$ is a continuous function such that $F(\bar{y}, \bar{O}(i)) \geq 0$ if $\bar{y} \notin \tilde{\bar{Y}}$ and $F(\bar{y}, \bar{O}(i)) = 0$ otherwise. Representing the tightened admissible output space as $\tilde{\bar{Y}} = \{\bar{y} : g_m(\bar{y}, \bar{O}(i)) \leq 0, m \in \mathbb{I}_{1:q}, \forall i\}$, a general class of penalty functions can be defined as

$$F(\bar{y}, \bar{O}(i)) = \sum_{m=1}^{q} (\max\{0, g_m(\bar{y}, \bar{O}(i))\})^{\epsilon}, \quad (4.21)$$

for some $\epsilon > 0$. As $\mu \to \infty$, the solution of the penalty problem converges to the solution of the original problem. Besides, if $\epsilon = 1$, exact penalization can be obtained if μ is chosen to be greater than the biggest corresponding Lagrange multiplier (Luenberger & Ye, 2008; Ferramosca et al., 2011).

Therefore, an optimal control problem denoted by $\tilde{P}_N^O(x, y_t, O(i))$, equivalent to (4.19), can be defined having as parameters $(x, y_t, O(i))$ and as decision variables $(\bar{\boldsymbol{u}}, \bar{x}_a, \bar{u}_a)$.

$$\tilde{V}_N^O(x, y_t, O(i)) = \min_{\bar{\boldsymbol{u}}, \bar{x}_a, \bar{u}_a} \tilde{V}_N(x, y_t, O(i); \bar{\boldsymbol{u}}, \bar{x}_a, \bar{u}_a)$$

$$\text{s.t. } \bar{x}(0) \in \{x\} \oplus (-\Gamma), \quad (4.22a)$$

$$\bar{x}(j+1) = A\bar{x}(j) + B\bar{u}(j), \quad (4.22b)$$

$$(\bar{x}(j), \bar{u}(j)) \in \bar{Z}, \ j \in \mathbb{I}_{0:N-1}, \quad (4.22c)$$

$$\bar{y}(j) = C\bar{x}(j) + D\bar{u}(j), \quad (4.22d)$$

$$\bar{y}_a = C\bar{x}_a + D\bar{u}_a, \quad (4.22e)$$

$$(\bar{x}(N), \bar{x}_a, \bar{u}_a) \in \Omega^a_{t,\bar{K}}. \quad (4.22f)$$

Notice that the constraints of the equivalent problem $\tilde{P}_N^O(x, y_t, O(i))$ depend neither on y_t nor $O(i)$, making it feasible for any changing set-point and non-feasible output region $O(i)$.

Considering the receding policy of MPC controllers and the fact that the optimization problem (4.22) is solved at each sampling time based on the current knowledge of the optimization parameters, the optimal control law is given by

$$\kappa_N^O(x(k), y_t, O(i)) = \bar{u}^O(0; x, y_t, O(i)) + K(x(k) - \bar{x}(k)). \tag{4.23}$$

Besides, defining $\Omega_{t,\bar{K}} = \text{Proj}_x(\Omega^a_{t,\bar{K}})$, the feasible region $X_N(\Omega_{t,\bar{K}})$ is defined as the set of states that can be steered to $\Omega_{t,\bar{K}}$ in N steps. Notice that $X_N(\Omega_{t,\bar{K}})$ is by definition the domain of attraction for the proposed controller.

Without avoidance features, Assumptions 4.1 to 4.3 and 4.6 are sufficient conditions for asymptotic stability and robust constraint satisfaction (Limon et al., 2010). In order to show that the controller proposed in this chapter holds the properties of stability and robust constraint satisfaction, we must derive the ISS property with respect to the uncertainties and the avoidance cost defined by the penalty functions. For that, the following assumption is required.

Assumption 4.7. Let the continuous function $V_{av}(\cdot) : \mathbb{R}^p \mapsto \mathbb{R}_{\geq 0}$ be given by $V_{av}(\cdot) = \sum_{i=1}^{N_o} [\mu F(\bar{y}_a, \bar{O}(i)) + \sum_{j=0}^{N} \mu F(\bar{y}(j), \bar{O}(i))]$. Moreover, let the bound of the avoidance function be defined as $S = \sup(V_{av}(\cdot))$, such that V_{av} tends to S if $\bar{y}_a \notin \tilde{\bar{Y}}$ or $\bar{y}(j) \notin \tilde{\bar{Y}}$ for any $j \in \mathbb{I}_{0:N}$, with $V_{av}(\cdot) = 0$ whenever $\bar{y}_a \in \tilde{\bar{Y}}$ and $\bar{y}(j) \in \tilde{\bar{Y}}$ for all $j \in \mathbb{I}_{0:N}$.

Lemma 4.1. (Adapted from Chapter 3, Lemma 3.1) Consider that Assumptions 4.1 to 4.7 hold for the system (4.1) constrained by (4.2). For a given target y_t, initial state $x \in X_N(\Omega_{t,\bar{K}})$, and bound S, the optimal solution to $\tilde{P}_N^O(x, y_t, O(i))$ is such that $\bar{x}^O = \bar{x}_a^O$, $\bar{u}^O = \bar{u}_a^O$, and $\bar{y}^O = \bar{y}_a^O$. Let $\bar{y}_s$ be the argument that minimizes the function $V_{of}(\cdot) + V_{av}(\cdot)$, which is associated with the joint steady-states and inputs $(\bar{x}_s, \bar{u}_s)$. Then, $\bar{x}_a^O = \bar{x}_s$, $\bar{u}_a^O = \bar{u}_s$, and $\bar{y}_a^O = \bar{y}_s$.

Lemma 4.2. (Ferramosca et al., 2012, Lemma 1) Let us define the following two state sequences $\bar{\boldsymbol{x}}$ and $\tilde{\boldsymbol{x}}$ as

$$\begin{aligned} \bar{\boldsymbol{x}} &= (\bar{x}^O(0), \bar{x}^O(1), \cdots, \bar{x}^O(N), \bar{x}(N+1)), \\ \tilde{\boldsymbol{x}} &= (\bar{x}^O(1), \cdots, \bar{x}^O(N), \bar{x}(N+1), \bar{x}(N+2)). \end{aligned} \tag{4.24}$$

Then, for all $j \in \mathbb{I}_{1:N+1}$ we have

$$\tilde{\boldsymbol{x}}(j) - \bar{\boldsymbol{x}}(j+1) = A_K^{j-1} w. \tag{4.25}$$

Lemma 4.3. (Adapted from Chapter 3, Lemma 3.4) Consider that Assumptions 4.1 to 4.7 hold, then the shifted value function $V_s(\cdot)$ satisfies

$$V_s(x, y_t, O(i)) \leq \alpha_c(\|x - \bar{x}_s\|), \tag{4.26}$$

with $\alpha_c(\cdot)$ being a $\mathcal{K}_\infty$-function.

Lemma 4.4. (Adapted from Chapter 3, Lemma 3.5) Consider that Assumptions 4.1 to 4.7 hold, then the shifted value function $V_s(\cdot)$ satisfies

$$V_s(x, y_t, O(i)) \geq \alpha_b(\|x - \bar{x}_s\|) - S \tag{4.27}$$

with $\alpha_b(\cdot)$ being a $\mathcal{K}_\infty$-function.

Lemma 4.5. (Decreasing property) Consider that Assumptions 4.1 to 4.7 hold, then the shifted function $V_s(\cdot)$ satisfies

$$V_s^O(x(k+1), y_t, O(i)) - V_s^O(x(k), y_t, O(i)) \leq -\alpha(\|x - \bar{x}_s\|) + S + \sigma(\|w\|), \tag{4.28}$$

with $\alpha(\cdot)$ being a $\mathcal{K}_\infty$-function and $\sigma(\cdot)$ being a $\mathcal{K}$-function.

Proof.

Define the optimal control sequence, the auxiliary feasible input sequence, the feasible nominal state sequence, and the auxiliary feasible state sequence, and the auxiliary feasible output sequence, respectively, as

$$\begin{aligned}
\bar{\boldsymbol{u}} &= (\bar{u}^O(0), \bar{u}^O(1), \cdots, \bar{u}^O(N-1)), \\
\tilde{\boldsymbol{u}} &= (\bar{u}^O(1), \cdots, \bar{u}^O(N-1)), \bar{K}(\bar{x}^O(N) - \bar{x}_a^O) + \bar{u}_a^O), \\
\bar{\boldsymbol{x}} &= (\bar{x}^O(0), \bar{x}^O(1), \cdots, \bar{x}^O(N), \bar{x}(N+1)), \\
\tilde{\boldsymbol{x}} &= (x^O(1), \cdots, x^O(N), x(N+1)), \\
\tilde{\boldsymbol{y}} &= (\bar{y}^O(1), \cdots, \bar{y}^O(N), \bar{y}(N+1)).
\end{aligned} \tag{4.29}$$

Further, let $\tilde{x}_a = \bar{x}_a^O$, $\tilde{u}_a = \bar{u}_a^O$, and $\tilde{y}_a = \bar{y}_a^O$ be, respectively, auxiliary feasible artificial state, input, and output, with the triplet $(\tilde{x}_a, \tilde{u}_a, \tilde{y}_a)$ being the feasible solution to the one-step ahead optimization problem.

Aiming to compare $V_s(x(k+1), y_t, O(i); \tilde{\boldsymbol{u}}, \tilde{x}_a, \tilde{u}_a)$ and $V_s^O(x(k), y_t, O(i))$ at time $k+1$ when $w \neq O_{n,1}$, we define the successor state as $x(k+1) = \bar{x}(k+1) + w$, with $\bar{x}(k+1) = A\bar{x}(k) + B\bar{u}^O(0)$. Then, we have

$$\begin{aligned}
V_s(x(k+1), y_t,&O(i); \tilde{\boldsymbol{u}}, \tilde{x}_a, \tilde{u}_a) - V_s^O(x(k), y_t, O(i)) \\
&= V_s(x(k+1), y_t, O(i); \tilde{\boldsymbol{u}}, \tilde{x}_a, \tilde{u}_a) - V_s(\bar{x}(k+1), y_t, O(i); \tilde{\boldsymbol{u}}, \tilde{x}_a, \tilde{u}_a) + \\
&\quad V_s(\bar{x}(k+1), y_t, O(i); \tilde{\boldsymbol{u}}, \tilde{x}_a, \tilde{u}_a) - V_s^O(x(k), y_t, O(i)) \\
&= \Delta V_s^w + \Delta V_s^n,
\end{aligned} \tag{4.30}$$

with

$$\Delta V_s^w = V_s(x(k+1), y_t, O(i); \tilde{\boldsymbol{u}}, \tilde{x}_a, \tilde{u}_a) - V_s(\bar{x}(k+1), y_t, O(i); \tilde{\boldsymbol{u}}, \tilde{x}_a, \tilde{u}_a), \tag{4.31}$$

$$\Delta V_s^n = V_s(\bar{x}(k+1), y_t, O(i); \tilde{\boldsymbol{u}}, \tilde{x}_a, \tilde{u}_a) - V_s^O(x(k), y_t, O(i)). \tag{4.32}$$

Following the results of Lemma 3.6, it can be shown that

$$\Delta V_s^n \leq -\alpha(\|x - \bar{x}_s\|) + S. \tag{4.33}$$

Now, expanding ΔV_s^w, we have

$$\begin{aligned}
\Delta V_s^w = & \sum_{j=0}^{N-1} (\|\tilde{x}(j) - \tilde{x}_a\|_Q^2 + \|\tilde{u}(j) - \tilde{u}_a\|_R^2) + \|\tilde{x}(N) - \tilde{x}_a\|_P^2 + V_{of}(\tilde{y}_a, y_t) + V_{av}(\tilde{\boldsymbol{y}}, \tilde{y}_a, O(i)) \\
& - S - \sum_{j=0}^{N-1} (\|\bar{x}(j+1) - \tilde{x}_a\|_Q^2 + \|\bar{u}(j+1) - \tilde{u}_a\|_R^2) - \|\bar{x}(N+1) - \tilde{x}_a\|_P^2 - V_{of}(\tilde{y}_a, y_t) \\
& - V_{av}(\tilde{\boldsymbol{y}}, \tilde{y}_a, O(i)) + S \\
= & \sum_{j=0}^{N-1} (\|\tilde{x}(j) - \tilde{x}_a\|_Q^2 + \|\tilde{u}(j) - \tilde{u}_a\|_R^2 - \|\bar{x}(j+1) - \tilde{x}_a\|_Q^2 - \|\bar{u}(j+1) - \tilde{u}_a\|_R^2) + \\
& \|\tilde{x}(N) - \tilde{x}_a\|_P^2 - \|\bar{x}(N+1) - \tilde{x}_a\|_P^2.
\end{aligned} \tag{4.34}$$

Based on Lemma 4.2, we have $\tilde{x}(N) = \bar{x}(N+1) + A_K^N w$. Thus, the following bound can be obtained

$$\begin{aligned}
\|\tilde{x}(N) - \tilde{x}_a\|_P^2 - \|\bar{x}(N+1) - \tilde{x}_a\|_P^2 &\leq \sigma_P(\|\tilde{x}(N) - \bar{x}(N+1)\|) \\
&\leq \sigma_P(\|A_K^N\| \; \|w\|) \\
&\leq \sigma_P(\|w\|),
\end{aligned} \tag{4.35}$$

where $\sigma_P(\cdot)$ is a $\mathcal{K}$-function, and the first inequality is based on the fact that a squared norm weighted by a positive definite matrix is uniformly continuous. Moreover, considering similar arguments, i.e., Lemma 4.2 and uniform continuity of a quadratic function restricted to a bounded set, the following bound can be obtained:

$$\begin{aligned}
\sum_{j=0}^{N-1} (\|\tilde{x}(j) - \tilde{x}_a\|_Q^2 - \|\bar{x}(j+1) - \tilde{x}_a\|_Q^2) &\leq \sigma_Q\left(\sum_{j=0}^{N-1} \|\tilde{x}(j) - \bar{x}(j+1)\|\right) \\
&\leq \sigma_Q\left(\|w\| \sum_{j=0}^{N-1} \|A_K^j\|\right) \\
&\leq \sigma_Q\left(\|w\| \left(\frac{1 - \|A_K\|^N}{1 - \|A_K\|}\right)\right) \\
&\leq \sigma_Q\left(\|w\|\right),
\end{aligned} \tag{4.36}$$

where $\sigma_Q(\cdot)$ is a $\mathcal{K}$-function. Thus, for ΔV_s^w, we have

$$\Delta V_s^w \leq \sigma_P(\|w\|) + \sigma_Q\left(\|w\|\right) \leq \sigma(\|w\|). \tag{4.37}$$

Considering the bounds (4.33) and (4.37), we have

$$V_s(x(k+1), y_t, O(i); \tilde{\boldsymbol{u}}, \tilde{x}_a, \tilde{u}_a) - V_s^O(x(k), y_t, O(i)) \leq -\alpha(\|x - \bar{x}_s\|) + S + \sigma(\|w\|). \tag{4.38}$$

Furthermore, based on the optimality principle,

$$\begin{aligned} V_s^O(x(k+1), y_t, O(i)) - V_s^O(x(k), y_t, O(i)) &\leq V_s(x(k+1), y_t, O(i); \tilde{\boldsymbol{u}}, \tilde{x}_a, \tilde{u}_a) - V_s^O(x(k), y_t, O(i)) \\ &\leq -\alpha(\|x - \bar{x}_s\|) + S + \sigma(\|w\|), \end{aligned} \tag{4.39}$$

which concludes the proof.

□

Lemma 4.6. (ISS bound) Consider that Assumptions 4.1 to 4.7 hold, then the closed-loop system with the optimal control law $\kappa_N^o(x, y_t, O(i))$ is ISS with respect to the avoidance cost $V_{av}(\cdot)$ and the bounded disturbance w, i.e., there is a $\mathcal{KL}$-function $\tilde{\beta}(\cdot)$ and $\mathcal{K}$-functions $\tilde{\gamma}(\cdot)$ and $\tilde{\sigma}(\cdot)$ such that for any feasible initial state $x(0) \in X_N(\Omega_{t,\bar{K}})$, steady-state $\bar{x}_s \in \text{Proj}_x(\bar{Z}_s)$, and bound S, the solution $\phi(k; x(0), \boldsymbol{u})$ exists and satisfies

$$\|\phi(k; x(0), \boldsymbol{u}) - \bar{x}_s\| \leq \tilde{\beta}(\|x(0) - \bar{x}_s\|, k) + \tilde{\gamma}(S) + \tilde{\sigma}(\|w\|), \tag{4.40}$$

for all $k \in \mathbb{I}_{>0}$.

Proof.

Rewriting Lemma 4.5 considering Lemma 4.3, we have

$$V_s^O(x(k+1), y_t, O(i)) - V_s^O(x(k), y_t, O(i)) \leq -\alpha \circ \alpha_c^{-1}(V_s^O(x(k), y_t, O(i))) + S + \sigma(\|w\|). \tag{4.41}$$

Without loss of generality, for $\hat{\alpha} = \alpha \circ \alpha_c^{-1}$, we assume $(id - \hat{\alpha})(\cdot)$ to be a $\mathcal{K}$-function (Jiang & Wang, 2001).

Following the steps considered to prove Theorem 3.2, which is based on Jiang & Wang (2001) and Alessandretti et al. (2017), it is straightforward to show that there exists some $\mathcal{KL}$-function $\hat{\beta}$ such that

$$V_s^O(x(k), y_t, O(i)) \leq \max\{\hat{\beta}(V_s^O(x(0), y_t, O(i)), k), \hat{\gamma}(S), \hat{\sigma}(\|w\|)\}, \tag{4.42}$$

being $\hat{\gamma}(r) = \hat{\alpha}^{-1} \circ \rho^{-1}(r)$ and $\hat{\sigma}(r) = \hat{\gamma} \circ \sigma(r)$ for all $k \in \mathbb{I}_{>0}$, with $\rho(\cdot)$ being a $\mathcal{K}_\infty$-function such that $(id - \rho)(\cdot)$ is a $\mathcal{K}_\infty$-function, and with $\hat{\alpha}(\cdot)$ being a $\mathcal{K}_\infty$-function such that $\hat{\alpha}(r) \leq \alpha_b \circ \alpha_c^{-1}(r)$, for all $r \geq 0$.

From Lemma 4.4, equation (4.42), and knowing that for nonnegative real numbers a

and b it holds that $\max\{a,b\} \leq a+b \leq \max\{2a,2b\}$,

$$\begin{aligned}\alpha_b(\|x-\bar{x}_s\|) &\leq \max\{\hat{\beta}(V_s^O(x(0),y_t,O(i)),k),\hat{\gamma}(S),\hat{\sigma}(\|w\|)\}+S\\ &\leq \max\{2\max\{\hat{\beta}(V_s^O(x(0),y_t,O(i)),k),\hat{\gamma}(S),\hat{\sigma}(\|w\|)\},2S\}\\ &= \max\{2\hat{\beta}(V_s^O(x(0),y_t,O(i)),k),2\hat{\gamma}(S),2\hat{\sigma}(\|w\|)\},2S\}, \end{aligned} \tag{4.43}$$

and by the monotonicity of $\alpha_b^{-1}(\cdot)$

$$\begin{aligned}\|x-\bar{x}_s\| &\leq \alpha_b^{-1}\circ 2\hat{\beta}(\alpha_c(\|x(k_0)-\bar{x}_s\|),k)) + \alpha_b^{-1}\circ 2\hat{\gamma}(S) + \alpha_b^{-1}\circ 2\hat{\sigma}(\|w\|) + \alpha_b^{-1}(2S),\\ &= \tilde{\beta}(\|x(0)-\bar{x}_s\|,k) + \tilde{\gamma}(S) + \tilde{\sigma}(\|w\|),\end{aligned} \tag{4.44}$$

where $\tilde{\beta}(\cdot)$, $\tilde{\gamma}(\cdot)$, and $\tilde{\sigma}(\cdot)$ are, respectively, defined as

$$\begin{aligned}\tilde{\beta}(r_1,s) &= \alpha_b^{-1}\circ 2\hat{\beta}(\alpha_c(r_1,s)),\\ \tilde{\gamma}(r_2) &= \alpha_b^{-1}\circ 2\hat{\gamma}(r_2) + \alpha_b^{-1}(2r_2),\\ \tilde{\sigma}(r_3) &= \alpha_b^{-1}\circ 2\hat{\sigma}(\|r_3\|).\end{aligned} \tag{4.45}$$

Based on Lemmas 4.3 to 4.5, $V_s(x,y_t,O(i))$ is an ISS-Lyapunov function for system (4.1) with bounds $\tilde{\beta}(\cdot)$, $\tilde{\gamma}(\cdot)$ and, $\tilde{\sigma}(\cdot)$. Then, from Jiang & Wang (2001, Lemma 3.5), the system is ISS, i.e., $\|\phi(k;x(0),\boldsymbol{u})-\bar{x}_s\| \leq \tilde{\beta}(\|x(0)-\bar{x}_s\|,k)+\tilde{\gamma}(S)+\tilde{\sigma}(\|w\|)$ for all $k\in\mathbb{I}_{>0}$, which concludes the proof.

□

Theorem 4.1. Consider that the Assumptions 4.1 to 4.7 hold for system (4.1) constrained by (4.4). For a given target y_t and for any feasible initial state $x\in X_N(\Omega_{t,\bar{K}})$, the closed-loop system with the optimal control law $\kappa_N^O(x(k),y_t,O(i))$ is input-to-state stable with respect to the disturbance input w, robustly fulfills the constraints throughout the time, and besides,

(i) if $y_t\in\bar{Y}_r$, then the closed-loop system converges to a set $\{y_t\}\oplus(C+DK)\Gamma$;

(ii) if $y_t\notin\bar{Y}_r$, then the closed-loop system converges to the neighborhood of a reachable steady-output $\{\bar{y}_s\}\oplus(C+DK)\Gamma$ such that

$$\bar{y}_s = \arg\min_{\bar{y}_a\in\bar{Y}_r} V_{of}(\bar{y}_a,y_t) + V_{av}(\bar{\boldsymbol{y}},\bar{y}_a,O(i)). \tag{4.46}$$

Proof.

- Recursive feasibility

  Recursive feasibility for the closed-loop system with the optimal control law $\kappa_N^o(x(k),y_t,O(i))$, which implies in robust constraint satisfaction, can be easily demonstrated following the results of (Limon et al., 2010, Theorem 1) and Lemma 3.3.

- Input-to-state stability

  To derive the proof, only the second statement must be proved, since if $y_t \in \bar{Y}_r$, then

$$y_t = \arg\min_{\bar{y}_a \in \bar{Y}_r} V_{of}\left(\bar{y}_a, y_t\right). \tag{4.47}$$

  Thus, consider the shifted value function defined by

$$V_s(x, y_t, O(i)) = \tilde{V}_N(x, y_t, O(i)) - S, \tag{4.48}$$

  as a Lyapunov candidate for the problem $\tilde{P}_N^O(x, y_t, O(i))$. Then, for a given steady-state $\bar{x}_s \in \bar{Z}_s$ associated to $\bar{y}_s$, there exist $\mathcal{K}_\infty$-functions $\alpha(\cdot)$, $\alpha_c(\cdot)$, $\alpha_b(\cdot)$, and a $\mathcal{K}$-function $\sigma(\cdot)$ such that

  1. $V_s(x, y_t, O(i)) \leq \alpha_c(\|x - \bar{x}_s\|)$, see Lemma 4.3.
  2. $V_s(x, y_t, O(i)) \geq \alpha_b(\|x - \bar{x}_s\|) - S$, see Lemma 4.4.
  3. $V_s^O(x(k+1), y_t, O(i)) - V_s^O(x(k), y_t, O(i)) \leq -\alpha(\|x - \bar{x}_s\|) + S + \sigma(\|w\|)$, see Lemma 4.5.

  Therefore, it can be proved (see Lemma 4.6) that under mild conditions, the closed-loop system is ISS with respect to the uncertainties and the avoidance cost, i.e., there is a $\mathcal{KL}$-function $\tilde{\beta}(\cdot)$ and $\mathcal{K}$-functions $\tilde{\gamma}(\cdot)$ and $\tilde{\sigma}(\cdot)$ such that

$$\|\phi(k; x(0), \boldsymbol{u}) - \bar{x}_s\| \leq \tilde{\beta}(\|x(0) - \bar{x}_s\|, k) + \tilde{\gamma}(S) + \tilde{\sigma}(\|w\|), \tag{4.49}$$

  for all $k \in \mathbb{I}_{\geq 0}$.

  Resorting to ISS arguments (Limon et al., 2009), when $k \to \infty$, we have $\bar{x}^O(k) = \bar{x}_a^O$ and $\bar{u}^O(k) = \bar{u}_a^O$, which implies $\bar{y}^O(k) = \bar{y}_a^O$. Then, based on Lemma 4.1, we have $\bar{x}^O(k) = \bar{x}_s$ and $\bar{u}^O(k) = \bar{u}_s$, and so, the states are steered to the set $\{\bar{x}_s\} \oplus \Gamma$ while the applied control input tends to $\{\bar{u}_s\} \oplus K\Gamma$. Therefore, the system output converges to $C(\{\bar{x}_s\} \oplus \Gamma) \oplus D(\{\bar{u}_s\} \oplus K\Gamma) = \{\bar{y}_s\} \oplus (C + DK)\Gamma$, which concludes the proof.

□

Remark 4.2. (Local Convergence) When the output target is reachable in the obstructed space but the optimal control problem $\tilde{P}_N^O(x, y_t, O(i))$ cannot be solved globally, the proposed controller only steer the system to a neighborhood of a reachable steady-output $\{\bar{y}_s\} \oplus (C + DK)\Gamma$ that locally minimizes $\tilde{V}_N(x, y_t, O(i); \bar{\boldsymbol{u}}, \bar{x}_a, \bar{u}_a)$.

Remark 4.3. (Asymptotic Stability) In presence of non-feasible output regions, the avoidance cost acts as disturbance and only ISS can be ensured. Therefore, the closed-loop system converges to a bounded set around a feasible steady-state. In this context, asymptotic stability, as demonstrated in Limon et al. (2010), either to a set $\{y_t\} \oplus (C + DK)\Gamma$ or $\{y_s\} \oplus (C + DK)\Gamma$, is only recovered when the avoidance cost goes to zero.

Remark 4.4. (Properties) It is easy to see that the inclusion of avoidance features does not prevent the proposed controller to have some of the properties presented in the robust tracking MPC framework proposed in Limon et al. (2010), such as i) stability under changing references; ii) feasibility under unreachable references; and iii) enlarged domain of attraction. Besides, the proposed controller has a fourth property of avoidance guarantees for all realizations of the uncertainties if exact penalization is under consideration.

Remark 4.5. (Funnel approach) The constraint tightening procedure can be made considering a funnel, as explained in Remark 4.1, instead of a tube. In this case, it can be shown that the results of Theorem 4.1 still hold for the problem $\tilde{P}_N^O(x, y_t, O(i))$ with constraint (4.22c) replaced by constraint (4.13), and with a robust constraint invariant $\Gamma = \mathcal{R}_\infty$. However, the recursive feasibility proof is slightly different and the results Ferramosca et al. (2012, Lemma 4) together with Lemma 3.3 should be considered instead.

The computation of an invariant set for tracking might be cumbersome for high order systems. However, in such cases, design schemes based on a relaxed terminal equality constraint or on a weighted terminal cost can be considered (Limon et al., 2018).

Remark 4.6. (Relaxed Terminal Equality Constraint) Let $(\bar{x}_a, \bar{u}_a) \in \bar{Z}_s$, $\bar{x}(N) = \bar{x}_a$, and $P = O_{n,n}$ in the optimal control problem (4.22). It can be proved that the results of Theorem 4.1 still hold under the mild assumption that the N-controllability matrix of the system, $Co_N = [A^{N-1}B \ \cdots \ AB \ B]$, has full rank, allowing the system to reach a maximum robust positive invariant set in the neighborhood of an equilibrium.

Remark 4.7. (Weighted Terminal Cost) Let $(\bar{x}_a, \bar{u}_a) \in \bar{Z}_s$, $\bar{x}(N) \in \bar{X}$, and $P_\gamma = \gamma P$ in the optimal control problem (4.22), with P_γ being the new terminal cost penalization with $\gamma \geq 1$. If γ is chosen following the conditions specified in Limon et al. (2018), it can be proved that the results of Theorem 4.1 still hold.

4.6 Numerical Examples

This section presents numerical results obtained with the proposed MPC strategy to illustrate its features. In the first example, we consider a double integrator system having one non-feasible region in its output space. With this example, we aim to clarify the concepts and behaviors of the proposed controller. In the second example, we consider a physical problem that can benefit from the avoidance features of the proposed controller. For that, we look at a quadrotor UAV system navigating in an environment with previously unknown obstacles.

It is worthwhile mentioning that the proposed framework can be applied without previous knowledge of the non-feasible regions, that is, their number, shape, and even their existence, may change over time. The only requirement made concerns the ability to represent them as polyhedra. Although this assumption brings conservatism in the accuracy of the region representation, it is not limiting because a polyhedron enclosing the actual region can always be used. Besides, when avoidance is required, a certain level of conservatism is not undesirable. For the second example, this representation problem is related to obstacle detection, which is beyond the scope of this work. Therefore, for the sake of exemplifying the proposed controller, we assume the existence of a detection algorithm that can provide online information about the obstacles represented as polyhedra.

The simulations are performed with MATLAB® using the CasADI Toolbox (Andersson et al., 2019) with the IPOPT solver (Wächter & Biegler, 2005) to solve the optimization problems together with the 2021 version of the CORA toolbox to perform the set operations with zonotopes (Althoff, 2015). In these examples, all units follow the international system standards.

4.6.1 Double integrator

Consider a double integrator system of the form

$$\begin{aligned} \dot{x} &= \begin{bmatrix} 0 & 1 \\ 0 & 0 \end{bmatrix} x + \begin{bmatrix} 1 & 0.5 \\ 0 & 1 \end{bmatrix} u + w, \\ y &= x, \end{aligned} \tag{4.50}$$

with $x = [x_1 \;\, x_2]' \in X$, $u = [u_1 \;\, u_2]' \in U$, and $w \in W$. On one hand, the states and inputs constraint sets are defined in the half-space representation (see Definition 2.11), respectively, by $X = \{x \in \mathbb{R}^2 : |x| \leq [10 \;\, 4]'\}$ and $U = \{u \in \mathbb{R}^2 : |u| \leq [2 \;\, 2]'\}$. On the other hand, the disturbance set and the non-feasible region are defined in the zonotopic form as (see Definition 2.13)

$$W = \left\{ \begin{bmatrix} 0.2 & 0 \\ 0 & 0.2 \end{bmatrix}, \begin{bmatrix} 0 \\ 0 \end{bmatrix} \right\} \text{ and } O = \left\{ \begin{bmatrix} 4 & 0 \\ 0 & 1.5 \end{bmatrix}, \begin{bmatrix} 4 \\ -1.5 \end{bmatrix} \right\}.$$

This choice of set representation simplify the reachability and invariance analysis, exploiting the fact that zonotopes are closed under the Minkowski sum and linear transformation (Definition 2.14). As for the constraint tightening procedures, Proposition 2.1 can be used since X and U are in the half-space representation. Furthermore, to limit the Minkowski sum effect in the order of the resulting zonotope, the order reduction algorithm proposed in Combastel (2003) is considered to set an order threshold at 4.

For implementation, the continuous dynamical system is discretized using the forward Euler method with sampling time $T_s = 0.3$. The stabilizing control gain for the mismatch error dynamics, K, is obtained solving the Riccati equation associated to a linear quadratic regulator (LQR) with weighting matrices $Q_K = I_2$ and $R_K = 0.1 I_2$. In terms of the nominal

MPC law, the horizon length is $N = 5$ and the states and inputs weighting matrices are $Q = I_2$ and $R = 50I_2$, which, following Assumption 4.6 and defining $\lambda = 0.9999$, lead to P, $\bar{K}$, and $\Omega^a_{t,\bar{K}}$. As for the offset and avoidance costs, $V_{of}(\bar{y}_a, y_t) = \|\bar{y}_a - y_t\|^2_\kappa$ with $\kappa = 10I_2$ and $\mu = 1000$. As a general tuning rule, Q should be at least one order of magnitude smaller than κ, and κ should be at least one order of magnitude smaller than μ, while R can be chosen taking into account the control effort.

Figure 4.1 illustrates the evolution of the system from an initial condition $x(0) = [6\ 3]'$ to the target $y_t = [-4\ 0]'$ using both a nominal controller and a controller for region avoidance. In both cases, disturbances are not being considered yet. To justify the non-feasible region choice, the system phase portrait is drawn, showing that the region prevents the closed-loop system to follow its natural evolution. Therefore, the avoidance controller must be able to force the system into a direction that is suboptimal from the standpoint of the set-point tracking problem, but optimal when considering the set-point tracking with avoidance features. The non-feasible region considered is defined as $O = \{x \in \mathbb{R}^2 : [0\ -3]' \leq x \leq [8\ 0]'\}$.

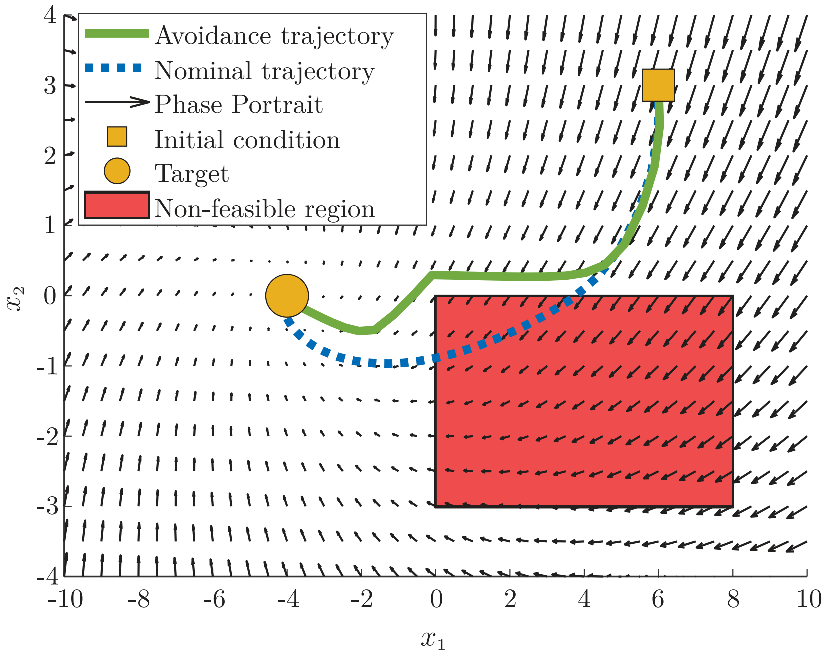

Figure 4.1: The figure displays the nominal (dashed blue) and avoidance (solid green) trajectories for a disturbance-free case. Arrows depict the double integrator phase portrait, the red set represents the non-feasible region, the circle yellow marker identifies the target, and the square yellow marker indicates the initial condition.

Figure 4.2 shows the responses of the closed-loop system controlled with the framework proposed in this work. Considering the same initial condition, 50 simulations were performed for different disturbance realizations and with each one of them being limited to 40 iterations. The process disturbances are assumed to be zero mean 2-dimensional random variables with Gaussian distribution having covariance matrix $0.1^2 I_2$ and truncated at $\|w\| \leq 0.2$.

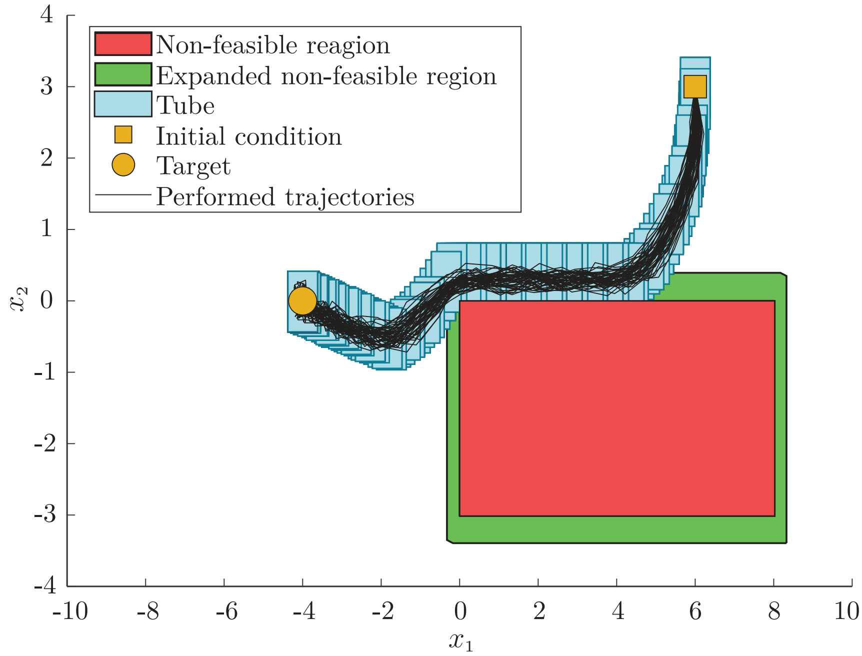

Figure 4.2: The figure illustrates the evolution of the disturbed system for different disturbance realizations. The red set represents the non-feasible region, while the green set denotes the enlarged non-feasible region. The light blue sets depict the tubes containing the evolution of the disturbed system.

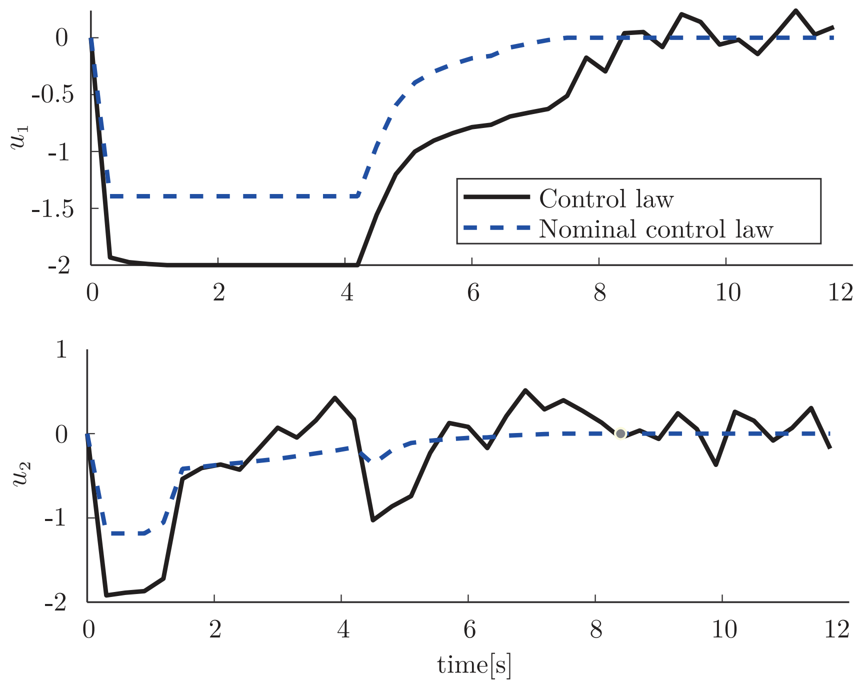

Figure 4.3: The figure displays the time evolution of the control inputs for a single simulation. The dashed blue line represents the nominal control law, while the solid black line depicts the dual feedback control law that incorporates a feedback term to reduce the prediction error (see equation (4.23)).

As it can be observed on Figure 4.2, the non-feasible region was expanded considering the minimal robust control invariant set, Γ, obtained using recursion (4.11). The sets defined around the system trajectory compose the tubes, in which, in this example, Γ was used in all steps in the form described in Section 3. The penalties for avoidance are considered with respect to the expanded non-feasible region such that the nominal trajectory, which defines the center of the tubes, lies outside this new region throughout the time. We can conclude based on the obtained results that the tubes together with the proportional law for mismatch error reduction have limited the disturbance effects. Furthermore, the expansion of the non-feasible region prevented the evolution of the system from intersecting the actual non-feasible region. Finally, Figure 4.3 shows the control signals for one of the simulations performed. The nominal control law is the one obtained solving the optimal control problem (4.22), while the control law applied to the system, (4.23), is modified taking into account the reduction of the mismatch error.

4.6.2 Quadrotor UAV

The dynamics of the quadrotor UAV are obtained from the Euler-Lagrange formulation with the physical parameters presented in Appendix A, Section A.3. The generalized coordinates are composed by the position $\xi = [x^{\mathcal{I}}\ y^{\mathcal{I}}\ z^{\mathcal{I}}]'$ and its attitude $\eta = [\phi\ \theta\ \psi]'$, yielding $q = [\xi'\ \eta']'$. Consequently, the state and output vectors can be defined respectively as $x = [q\ \dot{q}]'$ and $y = \xi$, which unlike in Chapter 3 does not include ψ to simplify the process of enlargement of the non-feasible regions. The quadrotor UAV is assumed to be actuated directly on its lift forces. Thus, the system inputs are $u = [f_1\ f_2\ f_3\ f_4]'$, with f_i being the thrust force generated by the i-th rotor.

For the quadrotor, the implementation of the proposed controller encounters computational difficulties related to the calculations of the tracking invariant set and the robust control invariant set. Therefore, for the nominal MPC controller, we considered the formulation with weighted terminal cost (Remark 4.7), avoiding the need to compute $\Omega^a_{t,\bar{K}}$. Also, assuming $e(k) = 0$, we can define funnels for constraint tightening using the N-step reachability analysis (see Remark 4.1, equation (4.13)).

A linear model for control purposes can be obtained through the linearization of the Euler-Lagrange model (A.14) around an equilibrium condition disregarding the coupling between translational and rotational dynamics due to the displacement between the quadrotor's geometric center and its center of mass (see Appendix A). Additionally, the model is discretized using the forward Euler method, which results in the prediction model (A.17). Similarly to the quadrotor numerical example of Chapter 3, to better emulate the vehicle dynamics during the simulation, the non-linear dynamic model (A.14) is considered with the parameters provided in Table A.2. Further, the ordinary differential equation solver ODE45 from MATLAB is used for numerical integration with a discretization time-step of 0.01 seconds.

The states and inputs constraint sets are defined in the half-space representation, respectively, as $X = \{[\xi' \ \eta' \ \dot{\xi}' \ \dot{\eta}']' : [-20 \ \ -20 \ 0] \leq \xi \leq [20 \ 20 \ 20]', |\eta| \leq [\pi/2 \ \pi/2 \ \pi]', |\dot{\xi}| \leq [5 \ 5 \ 5]', |\dot{\eta}| \leq [\pi/2 \ \pi/2 \ \pi/2]'\}$ and $U = \{(f_1, f_2, f_3, f_4) \in \mathbb{R}^4 : 0 \leq f_1, f_2, f_3, f_4 \leq 12\}$, with all variables in SI units. Notice that since the linearization point consider non-null control inputs, the set U must be modified to account for u_{eq} before used in the control problem. Furthermore, the disturbance set is defined as

$$W = \left\{ \begin{bmatrix} 0.5I_3 & O_{3,3} & O_{3,3} & O_{3,3} \\ O_{3,3} & 0.2I_3 & O_{3,3} & O_{3,3} \\ O_{3,3} & O_{3,3} & 0.1I_3 & O_{3,3} \\ O_{3,3} & O_{3,3} & O_{3,3} & 0.05I_3 \end{bmatrix}, O_{12,1} \right\}.$$

As for the non-feasible output regions, we consider three previously unknown obstacles expanded with the N-th reachable set, as shown in Figure 4.4.

Similarly to the previous example, the stabilizing control gain for the mismatch error dynamics, K, is obtained solving the Riccati equation associated to an LQR controller with weighting matrices $Q_K = \text{diag}\{0.01, 0.01, 0.01, 0.1, 0.1, 1, 1, 1, 1, 10, 10, 1\}$ and $R_K = I_4$. In terms of the nominal MPC law, the horizon length is $N = 5$ and the states and inputs weighting matrices are $Q = \text{diag}\{1, 1, 1, 0.1, 0.1, 1, 1, 1, 0.1, 0.1, 0.1, 1\}$ and $R = 200I_4$. Moreover, P is obtained following Assumption 4.6.3 with terminal weight $\gamma = 250$ (Remark 4.7). As for the offset and avoidance costs, $V_{of}(\bar{y}_a, y_t) = \|\bar{y}_a - y_t\|_\kappa^2$ with $\kappa = \text{diag}\{4000, 4000, 20000\}$ and $\mu = 100000$.

The system starts in the initial condition $x(0) = [-13 \ 6 \ 5 \ O_{9,1}]'$, and it is required to reach the target output $y_t = [15 \ 0 \ 17]'$. In terms of disturbances, we consider positive and negative steps in all states with their values being obtained considering a pseudo-random binary signal with 11 bits, with each new value held for 1000 time samples.

Figure 4.4 shows the evolution of the system from its initial condition towards the target. Notice that the avoidance features of the proposed control framework helps the quadrotor UAV to find a path between the first two obstacles and, afterwards, a path over the last obstacle. Even in the presence of disturbances in all states, the expansion of obstacles based on the Mikowski sum, $O(i) \oplus \mathcal{R}_N$, allowed navigation without the occurrence of collision with real obstacles $O(i)$. This feature was only possible due to the combination of the offset cost with penalties for avoidance.

In Figures 4.5 to 4.8, the time evolution of all states is presented along with the applied disturbance profile. It is worth highlighting that the effect of the perturbation directly impacts the evolution of the state, being this effect clearer in the states related to ψ (Figure 4.6) and angular velocities (Figure 4.8). Another reason of change in the states time evolution is the avoidance maneuvers, which appear clearly in the position (Figure 4.5) and attitude (Figure 4.6).

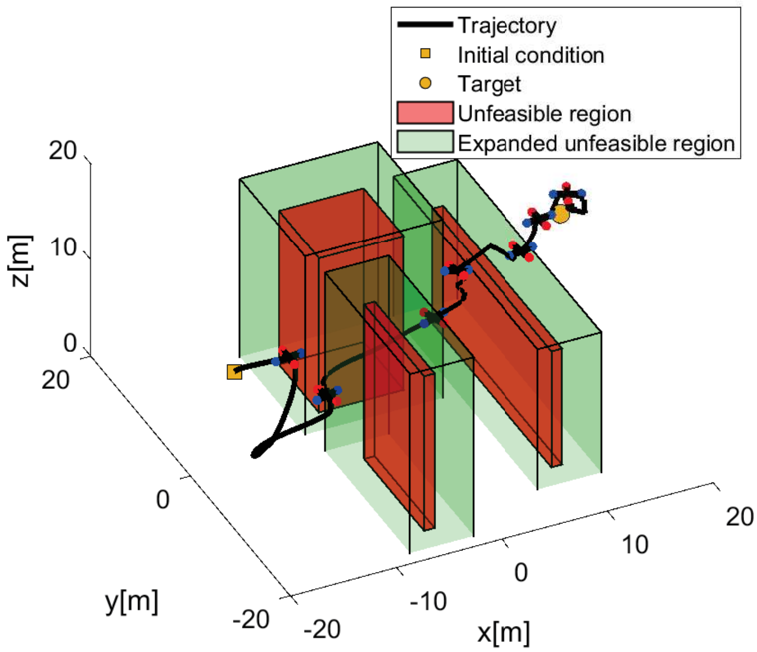

Figure 4.4: Complete trajectory followed by the UAV as it safely navigates from the initial condition (bottom-left) to the target (upper-right), while avoiding three obstacles. The red sets in the figure represent the obstacles, while the green sets depict the enlarged non-feasible regions.

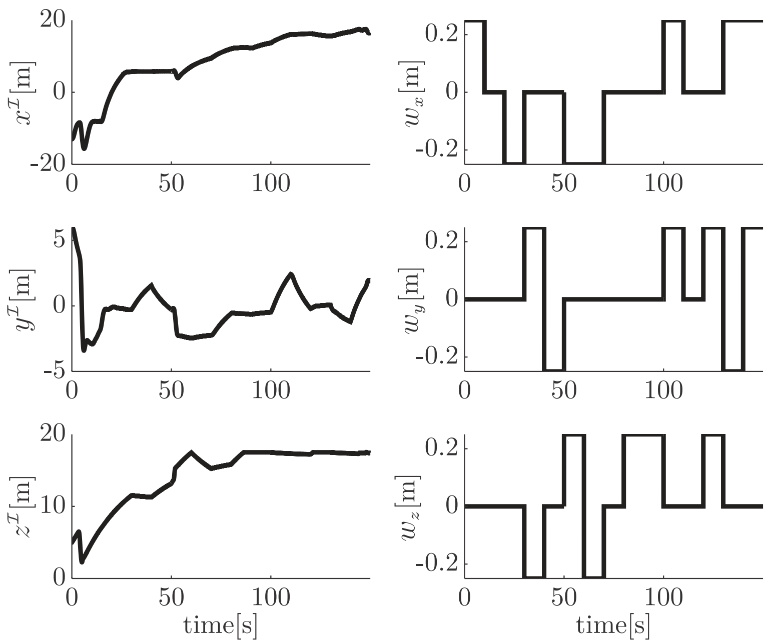

Figure 4.5: Time evolution of the quadrotor UAV position ($x^{\mathcal{I}}$, $y^{\mathcal{I}}$, and $z^{\mathcal{I}}$) alongside the considered disturbance profile during the execution of the provided task.

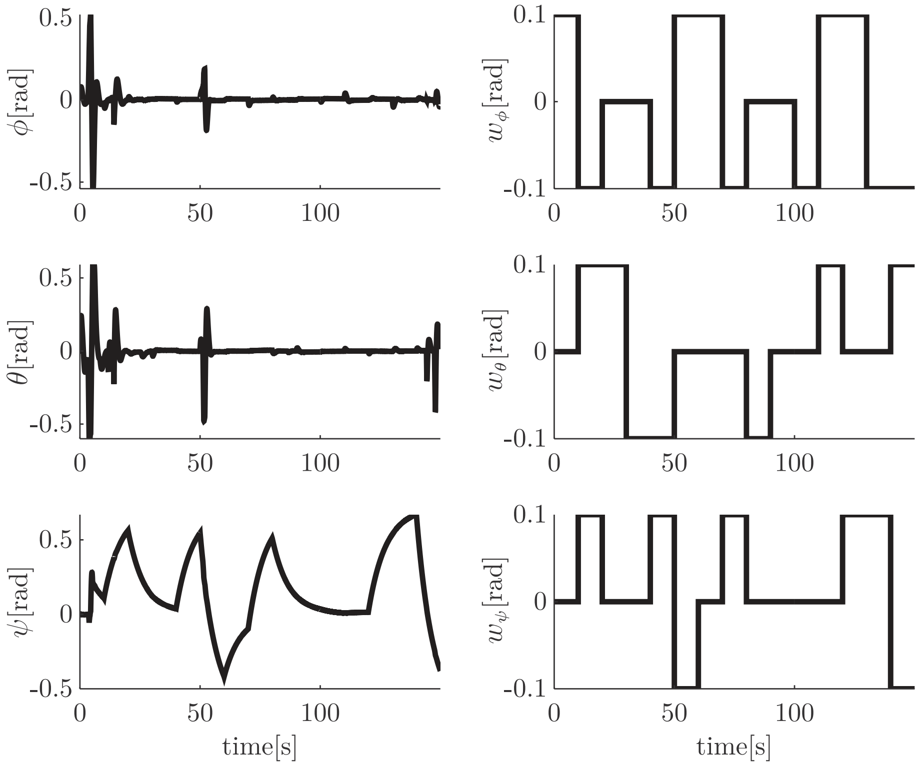

Figure 4.6: Time evolution of the quadrotor UAV attitude (ϕ, θ, and ψ) alongside the considered disturbance profile during the execution of the provided task.

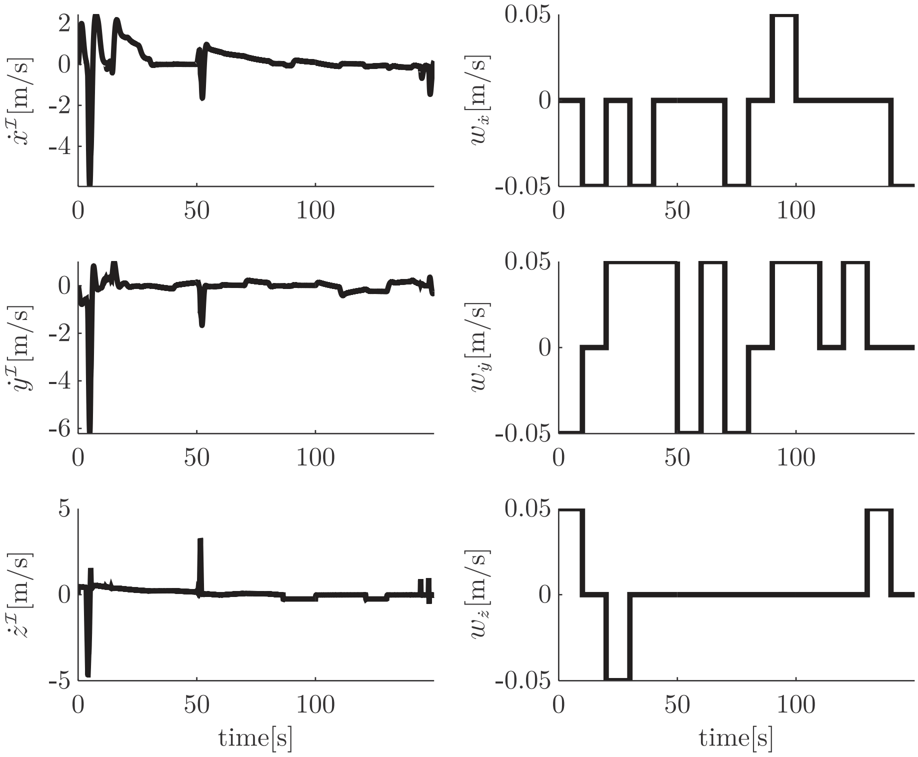

Figure 4.7: Time evolution of the quadrotor UAV linear velocity ($\dot{x}^{\mathcal{I}}$, $\dot{y}^{\mathcal{I}}$, and $\dot{z}^{\mathcal{I}}$) alongside with the considered disturbance profile during the execution of the provided task.

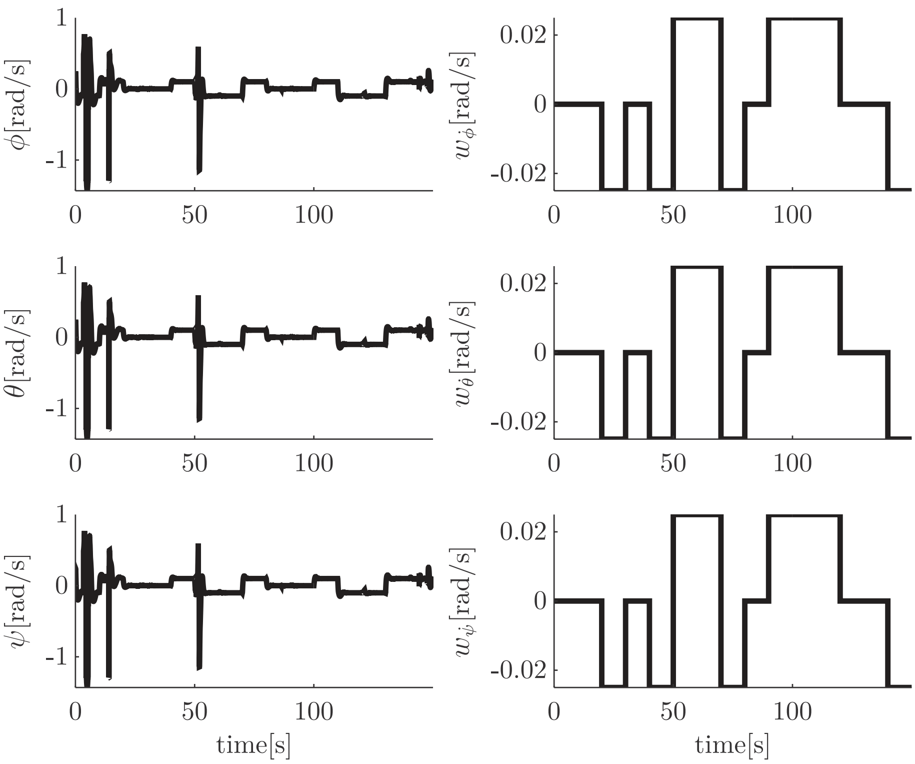

Figure 4.8: Time evolution of the quadrotor UAV angular velocity ($\dot{\phi}$, $\dot{\theta}$, and $\dot{\psi}$) alongside with the considered disturbance profile during the execution of the provided task.

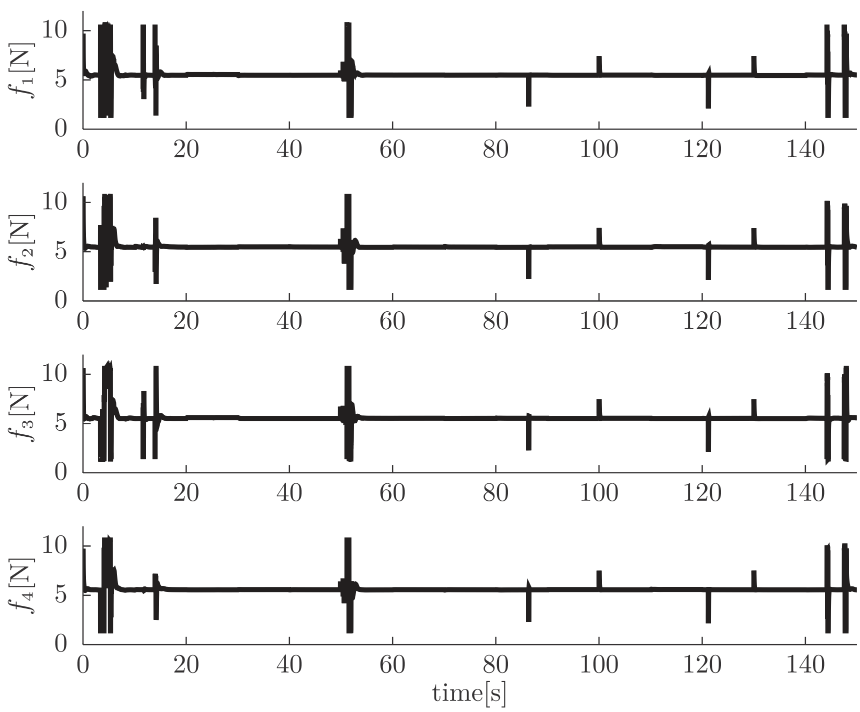

Figure 4.9: Time evolution of the applied lift forces to the quadrotor UAV, with f_i being the lift force of the i-th propeller.

Finally, Figure 4.9 shows the control signals applied to the the system. These show that the proposed controller was able to perform the set-point tracking of the desired target output while avoiding obstacles without violating the actuators' saturation level. Unlike the previous example, since here we assume that $e(k) = 0$, the control law applied to the system is equal to the nominal one obtained after solving the optimal control problem. In fact, the robustness appears in this example through the constraint tightening procedures.

4.7 Final Remarks

In this chapter, we addressed the problem of robustness for a linear predictive controller performing set-point tracking with avoidance features. The uncertain system was assumed to be subjected to unknown but bounded uncertainties and to be constrained inside a non-convex output space obstructed by a previously unknown number of non-feasible regions. For that, we considered artificial variables together with an offset cost functional playing the role of a steady-state target optimizer. Additionally, the problem of avoidance was approached throughout penalty functions, allowing the optimal control problem to be solved in a known convex output space. As for the robustness problem, a set-based approach was considered using zonotopic set representation to efficiently perform the constraint tightening operations and the reachability analysis.

It was shown that, under mild conditions, the closed-loop system converges to a neighborhood of the target if the target is reachable in the obstructed space and the proposed optimal control problem can be solved globally. Otherwise, it was shown that the closed-loop system converges to a neighborhood of a reachable steady-output that minimizes the proposed cost functional. Besides, the proposed controller holds the properties of input-to-state stability and feasibility under changing references, an enlarged domain of attraction, and avoidance guarantees.

The control strategies proposed until now were developed for systems described by linear dynamics, which, for real-world applications, limits the properties and performance guarantees to a region in which the linearized system is valid. For that reason, in the next chapter, we will explore the problem of avoidance for non-linear systems.

5

Non-linear Set-Point Tracking with Avoidance Features

5.1 Introduction

This chapter extends the results of Chapter 3 by proposing single-layer non-linear model predictive control schemes to solve the set-point tracking control problem while providing the closed-loop system with avoidance features. Ultimately, the set-point tracking MPC proposed in Ferramosca (2011), later analyzed in Limon et al. (2018), is extended to address the avoidance problem of a previously unknown number of non-feasible regions in the presence of changing set-points. For that, the penalty method of non-linear programming is taken into account to enforce avoidance constraints without losing stability and feasibility guarantees. Following the results of Alessandretti et al. (2017), it is shown that the closed-loop system is recursively feasible and input-to-state stable under the mild assumption that the avoidance cost is uniformly bounded over time. Furthermore, since for non-linear systems the computation of invariant sets might be cumbersome, simplified design schemes based on a relaxed terminal equality constraint and on a weighted terminal cost are explored. Similar formulations appeared in Chapters 3 and 4, however, here they are explored in more detail.

5.2 Problem Description

Consider a finite-dimensional non-linear time-invariant dynamical system of the form

$$\begin{aligned} x(k+1) &= f(x(k), u(k)), \\ y(k) &= h(x(k), u(k)), \end{aligned} \tag{5.1}$$

with $x(k) \in \mathbb{R}^n$, $u(k) \in \mathbb{R}^m$, and $y(k) \in \mathbb{R}^p$ being, respectively, the state, input, and output vectors.

Assumption 5.1. The state vector is available at each sampling time, and the state-transition, $f(\cdot)$, and the state-output, $h(\cdot)$, maps are continuously differentiable at any equilibrium point. Moreover, based on continuity arguments, $f(\cdot)$ is bounded for bounded states with $f(O_{n,1}, O_{m,1}) = O_{n,1}$.

The evolution of the system states and inputs are constrained as

$$(x(k), u(k)) \in Z,\ \forall k \in \mathbb{I}_{\geq 0}, \tag{5.2}$$

with the sets of admissible states and inputs being, respectively, $X = \text{Proj}_x(Z)$ and $U = \text{Proj}_u(Z)$.

Assumption 5.2. The constraint set $Z \subset \mathbb{R}^{n+m}$ is a compact convex polyhedron containing the origin.

Any suitable target y_t for system (5.1) is associated with an equilibrium point (x_s, u_s), which is described by

$$\begin{aligned} x_s &= f(x_s, u_s), \\ y_t &= h(x_s, u_s), \end{aligned} \tag{5.3}$$

with x_s and u_s being, respectively, the steady-states and inputs. Thus, the set of joint steady-states and inputs, Z_s, and the set of reachable set-points, Y_r, can be defined as

$$\begin{aligned} Z_s &= \{(x_s, u_s) : x_s = f(x_s, u_s), (x_s, u_s) \in \lambda Z\}, \\ Y_r &= \{y_t : y_t = h(x_s, u_s), (x_s, u_s) \in Z\}, \end{aligned} \tag{5.4}$$

with $\lambda \in (0, 1)$ being a constant defined to avoid loss of controllability related to having equilibrium points at active constraints (Rao & Rawlings, 1999). This definition does not imply a reduction of the reachable targets since λ can be chosen arbitrarily close to 1 making Z arbitrarily close to λZ in the Hausdorff sense.

Assumption 5.3. The steady-output y_s uniquely defines the equilibrium (x_s, u_s), and there exists a locally Lipschitz continuous function $g_x : \mathbb{R}^p \mapsto \mathbb{R}^n$ and a continuous function $g_u : \mathbb{R}^p \mapsto \mathbb{R}^m$ such that $x_s = g_x(y_s)$ and $u_s = g_u(y_s)$.

Similar to the previous chapters, let O denotes the space obstructed by a finite number N_o of previously unknown non-feasible regions, with $O(i)$ being the i-th non-feasible region. Therefore, the admissible output set can be defined as

$$\tilde{Y} = Y - \bigcup_{i=1}^{N_o} O(i), \tag{5.5}$$

with Y being the set of admissible outputs obtained from (5.2) considering the output-state map $h(\cdot)$. Further, to account for the obstacles, the constraint (5.2) can be modified based on (5.5), yielding

$$(x(k), u(k)) \in \tilde{Z}, \ \forall k \in \mathbb{I}_{\geq 0}, \tag{5.6}$$

with $\tilde{Z} = g_x(\tilde{Y}) \times g_u(\tilde{Y})$.

It is worthwhile mentioning that no prior knowledge of the number of non-feasible regions, their shapes, and their spatial distribution is required. However, for control purposes, some online knowledge of such non-feasible regions is assumed.

Assumption 5.4. Any output non-feasible set $O(i)$ is available at each sampling time by measurement and estimation or, if available, by previous knowledge on the sets. Also, they are considered constant throughout the prediction horizon.

Problem 5.1. Consider a system described by (5.1) subject to the constraints (5.2). The problem is to design a control law to make the error between the system output and the target be arbitrarily small as time evolves while ensuring that the evolution of the system output lies outside any non-feasible output region $O(i)$. Also, by considering that a global solution to the problem can be obtained, if the target is feasible and reachable in the obstructed space ($y_t \in Y_r \cap \tilde{Y}$), and there is no non-feasible output region in the neighborhood of the target, the tracking error must tend to zero asymptotically

$$\lim_{k \to \infty} \|y(k) - y_t\| = 0.$$

Otherwise, the system output must converge asymptotically to a bounded set around a reachable steady-output $y_s \in Y_r \subset \tilde{Y}$ that minimizes a given performance index.

5.3 Control Design

The non-linear controller proposed in this section is designed to ensure ISS in the Lyapunov sense for any reachable target in the obstructed space while avoiding any non-feasible output region $O(i)$. For that, let $y_a \in Y_r$ be an artificial steady-output, which is an extra decision variable in the optimal control problem to avoid loss of feasibility. Moreover, let $(x_a, u_a) \in Z_s$ be an artificial equilibrium point associated with y_a.

In terms of avoidance, since $\tilde{Z}$ is possibly a non-convex set priory unknown, enforcing constraint (5.6) directly may be impractical from the optimization problem point-of-view. Furthermore, if regions are removed from the admissible space, the assurances of stability and recursive feasibility that are present in tracking MPC formulations will no longer exist. As in the previous chapters, these problems can be avoided if the non-feasible regions are considered without limiting the optimization problem search-space, which can be made in non-linear programming through the penalty method (Luenberger & Ye, 2008). For that, let the non-obstructed admissible output space be described by the intersection of a set of q non-linear inequalities g_j as

$$\tilde{Y} = \{y : g_j(y, O(i)) \leq 0, j \in \mathbb{I}_{1:q}, \forall i \in \mathbb{I}_{1:N_o}\}, \tag{5.7}$$

which, as in (5.5), it is possibly a non-convex set. Then, the penalty function can be defined as

$$F(y, O(i)) = \sum_{j=1}^{q} (\max\{0, g_j(y, O(i))\})^{\epsilon}, \tag{5.8}$$

for some $\epsilon > 0$ such that $F(y, O(i)) \geq 0$ if $y \notin \tilde{Y}$, for all $i \in \mathbb{I}_{1:N_o}$, and $F(y, O(i)) = 0$ otherwise.

Following the presented penalty method, the proposed controller is based on the solution at each sampling time of an optimal control problem having as parameters $(x, y_t, O(i))$ and as decision variables $(\boldsymbol{u}, x_a, u_a)$. In this formulation, the cost functional is composed of three terms: i) a dynamic term, which is a combination of a stage cost with respect to the artificial steady-state and input (x_a, u_a) and a terminal cost; ii) a stationary term, which is the offset cost functional penalizing the deviation of the artificial steady-output y_a to the target output y_t; and iii) a combination of stationary and dynamic terms, which is the avoidance cost functional for the artificial steady-output y_a and the system predicted output sequence $\boldsymbol{y}$. This cost functional is defined as

$$\begin{aligned} V_{N_c,N_p}(x, y_t, O(i); \boldsymbol{u}, x_a, u_a) = &\sum_{j=0}^{N_c-1} \ell(x(j) - x_a, u(j) - u_a) + \sum_{j=N_c}^{N_p-1} \ell(x(j) - x_a, \kappa_f(x(j), y_a) - u_a) + \\ &V_f(x(N_p) - x_a) + V_{of}(y_a - y_t) + \\ &\sum_{i=1}^{N_o} \Big[\mu F(y_a, O(i)) + \sum_{j=0}^{N_p} \mu F(y(j), O(i))\Big], \end{aligned} \tag{5.9}$$

with $\ell(\cdot)$, $\kappa_f(\cdot)$, $V_f(\cdot)$, and $V_{of}(\cdot)$ being, respectively, the stage cost, the terminal control law, the terminal cost, and the offset cost. Additionally, μ is a positive constant and $N_p \in \mathbb{I}_{>0}$ and $N_c \in \mathbb{I}_{>0}$, with $N_p \geq N_c$, are, respectively, the prediction and control horizons.

Assumption 5.5. The following assumptions are sufficient conditions to ensure asymptotic stability for the closed-loop system without non-feasible regions $O(i)$ (Limon et al., 2018):

1. Let α_ℓ be a $\mathcal{K}_\infty$-function such that $\ell(x - x_a, u - u_a) \geq \alpha_\ell(\|x - x_a\|)$ for all $(x, u) \in \mathbb{R}^{n+m}$ and $(x_a, u_a) \in Z_s$;

2. Let $\kappa_f(x, y_a)$ be a continuous control law defined over the set Ω_t^a, such that (x_a, u_a) is an asymptotically stable equilibrium point for the closed-loop system (5.1) controlled by $\kappa_f(x, y_a)$;

3. Let $\Omega_t^a \subseteq \mathbb{R}^{n+n+m}$ be an invariant set for tracking for the closed-loop system (5.1) controlled by $\kappa_f(x, y_a)$ such that for all $(x, x_a, u_a) \in \Omega_t^a$ we have that $(x, \kappa_f(x, y_a)) \in Z$, $(x_a, u_a) \in Z_s$, and $f(x, \kappa_f(x, y_a)) \in \Omega_t$, with $\Omega_t = \mathrm{Proj}_x(\Omega_t^a)$;

4. Let $V_f(x - x_a)$ be a control Lyapunov function for the closed-loop system (5.1) controlled by $\kappa_f(x, y_a)$ such that for all $(x, x_a, u_a) \in \Omega_t^a$ there exist constants $b > 0$ and $\sigma > 1$ which verify
$$V_f(x - x_a) \leq b\|x - x_a\|^\sigma \tag{5.10}$$
and
$$V_f(f(x, \kappa_f(x, y_a)) - x_a) - V_f(x - x_a) \leq -\ell(x - x_a, \kappa_f(x, y_a) - u_a); \tag{5.11}$$

5. Let $V_{of}\left(y_a - y_t\right) : \mathbb{R}^{2p} \mapsto \mathbb{R}_{\geq 0}$ be a continuous, convex, and positive definite function with $V_{of}(O_{p,1}, O_{p,1}) = 0$, such that the minimizer
$$y_a^O = \arg \min_{y_a \in Y_r} V_{of}(y_a - y_t) \tag{5.12}$$
is unique for any y_t. Moreover, there exists a $\mathcal{K}_\infty$-function α_o such that
$$V_{of}(y_a - y_t) - V_{of}(y_a^O - y_t) \geq \alpha_o(\|y_a - y_a^O\|). \tag{5.13}$$

By definition, the domain of attraction for the proposed controller is the N-steps controllable set to Ω_t, denoted as $X_{N_c,N_p}(\Omega_t)$. Moreover, to provide the controller with avoidance features and to later derive the ISS property with respect to the avoidance cost, consider the following assumption.

Assumption 5.6. Let the continuous function $V_{av}\left(\boldsymbol{y}, y_a, O(i)\right) : \mathbb{R}^p \mapsto \mathbb{R}_{\geq 0}$ be given by
$$V_{av}\left(\boldsymbol{y}, y_a, O(i)\right) = \sum_{i=1}^{N_O} \Big[\mu F(y_a, O(i)) + \sum_{j=0}^{N_P} \mu F(y(j), O(i))\Big]. \tag{5.14}$$
Moreover, let $S \in \mathbb{R}_{\geq 0}$ be an upper bound of the avoidance penalty function, i.e.,
$$S = \sup V_{av}\left(\boldsymbol{y}, y_a, O(i)\right)). \tag{5.15}$$

The MPC controller with avoidance features is derived from the solution of the optimization problem $P_{N_c,N_p}(x, y_t, O(i))$ having as parameters $(x, y_t, O(i))$ and as decision variables $(\boldsymbol{u}, x_a, u_a)$, which is given by

$$
\begin{aligned}
V^O_{N_c,N_p}(x, y_t, O(i)) = \min_{\boldsymbol{u},x_a,u_a} & V_{N_c,N_p}(x, y_t, O(i); \boldsymbol{u}, x_a, u_a) \\
\text{s.t. } & x(0) = x, && (5.16a)\\
& x(j+1) = f(x(j), u(j)), j \in \mathbb{I}_{0:N_c-1}, && (5.16b)\\
& (x(j), u(j)) \in Z, j \in \mathbb{I}_{0:N_c-1}, && (5.16c)\\
& x(j+1) = f(x(j), \kappa_f(x, y_a)), j \in \mathbb{I}_{N_c:N_p-1}, && (5.16d)\\
& (x(j), \kappa_f(x, y_a)) \in Z, j \in \mathbb{I}_{N_c:N_p-1}, && (5.16e)\\
& y_a = h(x_a, u_a), && (5.16f)\\
& (x(N), x_a, u_a) \in \Omega^a_t, && (5.16g)
\end{aligned}
$$

with the predicted trajectory subject to the system dynamics and constraints (5.16a)-(5.16e), and with constraints (5.16f) and (5.16g), respectively, defining the artificial steady-output related to an artificial equilibrium and enforcing the terminal state to be in a region where the system can be stabilized by the terminal control law $\kappa_f(x, y_a)$.

The optimization problem $P_{N_c,N_p}(x, y_t, O(i))$ can be solved at each sampling time following the receding horizon policy of MPC controllers, which results in the following optimal control law

$$\kappa^O_{N_c,N_p}(x, y_t, O(i)) = u^O(0; x, y_t, O(i)). \tag{5.17}$$

Theorem 5.1. (Asymptotic nominal stability (Limon et al., 2018, Theorem 1)) Consider that Assumptions 5.1 to 5.3, and 5.5 hold for the system (5.1) constrained by (5.2) without the presence of non-feasible output regions $O(i)$. For a given target y_t and for any feasible initial state $x \in X_{N_c,N_p}(\Omega_t)$, the closed-loop system with the control law $\kappa^O_{N_c,N_p}(x, y_t, O(i))$ is stable, fulfills the constraints throughout the time and, besides

(i) If $y_t \in Y_r$, then the closed-loop system asymptotically converges to y_t.

(ii) If $y_t \notin Y_r$, then the closed-loop system asymptotically converges to a reachable steady-output that minimizes

$$\arg \min_{y_a \in Y_r} V_{of}(y_a - y_t).$$

Lemma 5.1. (Steady condition convergence) Consider that Assumptions 5.1 to 5.5 hold for the system (5.1) constrained by (5.2). For any feasible initial state $x \in X_{N_c,N_p}(\Omega_t)$, target y_t, and bound S, let the optimal solution to $P^O_{N_c,N_p}(x, y_t, O(i))$ be such that $x = x^O_a$, $u = u^O_a$, and $y = y^O_a$. Moreover, let (x_s, u_s, y_s) be the optimal triplet satisfying (5.3), such that function $V_{of}(y_a - y_t) + V_{av}(\boldsymbol{y}, y_a, O(i))$ is minimized. Then, $x = x_s$, $u = u_s$, and $y = y_s$.

Proof.

Consider that (x_a^O, u_a^O, y_a^O) is the optimal solution to $P^O_{N_c,N_p}(x, y_t, O(i))$. Then

$$V_{N_c,N_p}(x, y_t, O(i)) = V_{of}(y_a^O - y_t) + V_{av}(\boldsymbol{y}, y_a^O, O(i)). \tag{5.18}$$

This Lemma can be proved by contradiction following the steps considered to prove Lemma 3.1 in Chapter 3, however, here convexity and Lipschitz continuity arguments must be used. For that, assume now that the stationary point is not optimal, i.e., $(x_a^O, u_a^O) \neq (x_s, u_s)$. Let us define

$$(\tilde{x}_a, \tilde{u}_a) = \gamma(x_a^O, u_a^O) + (1-\gamma)(x_s, u_s) \tag{5.19}$$

with $\gamma \in [0, 1]$. Since both (x_s, u_s) and (x_a^O, u_a^O) are in Z_s, and this set is convex, then a convex combination of these points, $(\tilde{x}_a, \tilde{u}_a)$, is also in Z_s.

Considering Assumptions 5.5 and 5.6, it is possible to obtain a convex cost functional that superiorly bounds the non-convex cost $V_{of}(y_a - y_t) + V_{av}(\boldsymbol{y}, y_a, O(i))$. Then, we can define

$$V_B(y_a - y_t) = V_{of}(y_a - y_t) + S, \tag{5.20}$$

for any bound S, such that

$$V_B(\tilde{y}_a - y_t) \leq V_B(y_a^O - y_t) \tag{5.21}$$

for every γ. In other words, since the system is not at the optimal point (x_s, u_s), it is more convenient to move towards $(\tilde{x}_a, \tilde{u}_a)$ than to remain in (x_a^O, u_a^O).

Let $\tilde{\boldsymbol{u}}$ be a feasible control sequence that drives the system from (x_a^O, u_a^O) to $(\tilde{x}_a, \tilde{u}_a)$. This sequence is such that, the j-th element is given by $\tilde{u}(j) = \kappa_f(\tilde{x}(j), \tilde{y}_a)$ and $\tilde{x}(j+1) = f(\tilde{x}(j), \tilde{u}(j))$, with $\tilde{x}(0) = x_a^O$. Additionally, from the Lipschitz continuity of the function $g_x(\cdot)$ (see Assumption 5.3), we have that $\|x_a^O - \tilde{x}_a\| \leq L_g \|y_a^O - \tilde{y}_a\|$, with $L_g > 0$ being the Lipschitz constant. Then, the cost to drive the system to $(\tilde{x}_a, \tilde{u}_a)$ in N_p steps is

$$\begin{aligned}
V_{N_c,N_p}(x_a^O, y_t, O(i)) = &\sum_{j=0}^{N_p-1} \ell(\tilde{x}(j) - \tilde{x}_a, \kappa_f(\tilde{x}(j), \tilde{y}_a) - \tilde{u}_a) + V_f(\tilde{x}(N_p) - \tilde{x}_a) + \\
&V_{of}(\tilde{y}_a - y_t) + V_{av}(\tilde{\boldsymbol{y}}, \tilde{y}_a, O(i)) \\
\leq &\sum_{j=0}^{N_p-1} \ell(\tilde{x}(j) - \tilde{x}_a, \kappa_f(\tilde{x}(j), \tilde{y}_a) - \tilde{u}_a) + V_f(\tilde{x}(N_p) - \tilde{x}_a) + V_{of}(\tilde{y}_a - y_t) + S \\
\leq &V_f(x_a^O - \tilde{x}_a) + V_{of}(\tilde{y}_a - y_t) + S \\
\leq &b\|x_a^O - \tilde{x}_a\|^\sigma + V_{of}(\tilde{y}_a - y_t) + S \\
\leq &b(L_g\|y_a^O - \tilde{y}_a\|)^\sigma + V_{of}(\tilde{y}_a - y_t) + S \\
= &L_g^\sigma b(1-\gamma)^\sigma \|x_a^O - x_s\|^\sigma + V_{of}(\tilde{y}_a - y_t) + S.
\end{aligned} \tag{5.22}$$

Now, define $W(\gamma) = L_g^\sigma b(1-\gamma)^\sigma \|x_a^O - x_s\|^\sigma + V_B(\tilde{y}_a - y_t)$ and notice that for $\gamma = 1$, $W(1) = V_B(y_a^O - y_t)$. Taking the partial derivative of this function with respect to γ and evaluating it for $\gamma = 1$, we obtain

$$\left.\frac{\partial W}{\partial \gamma}\right|_{\gamma=1} = g^{O'}(y_a^O - y_t), \tag{5.23}$$

with $g^{O'}(y_a^O - y_t) \in \partial V_B(y_a^O - y_t)$, where $\partial V_B(y_a^O - y_t)$ is defined as the subdifferential of $V_B(y_a^O - y_t)$.

From convexity and from (5.21),

$$\left.\frac{\partial W}{\partial \gamma}\right|_{\gamma=1} = g^{O'}(y_a^O - y_t) \geq V_B(y_a^O - y_t) - V_B(\tilde{y}_a - y_t) > 0. \tag{5.24}$$

This means that there exists a value of $\gamma \in [0,1)$ such that $V_B(\tilde{y}_a - y_t)$ is smaller than the value of the cost $V_B(\tilde{y}_a - y_t)$ for $\gamma = 1$, which is $V_B(y_a^O - y_t)$. This contradicts the optimality of the solution of $P^O_{N_p,N_c}(x, y_t, O(i))$. Then, it has to be $(x_a^O, u_a^O) = (x_s, u_s)$, with (x_s, u_s) being the minimizer of $V_{of}(y_a - y_t) + V_{av}(\boldsymbol{y}, y_a, O(i))$, which concludes the proof. □

Lemma 5.2. (Artificial error boundedness) Consider that Assumptions 5.1 to 5.5 hold. Let x_s be the optimal steady state associated to the optimal target y_s, such that function $V_{N_c,N_p}(x, y_t, O(i))$ is minimized. For all $x \in X_{N_c,N_p}(\Omega_t)$ and $x_a^O \in \text{Proj}_x(Z_s)$, define the function $e(x) = x - x_a^O$. Then, there exists a $\mathcal{K}$-function $\alpha_e(\cdot)$ such that

$$\|e(x)\| \geq \alpha_e(\|x - x_s\|). \tag{5.25}$$

Proof.

The same proof of Lemma 3.2 in Chapter 3 applies if we consider Lemma 5.1 instead of Lemma 3.1.

□

Lemma 5.3. (Recursive feasibility) Consider that Assumptions 5.1 to 5.5 hold, then the closed-loop system with the optimal control law $\kappa^O_{N_c,N_p}(x, y_t, O(i))$ is recursively feasible for any feasible state $x \in X_{N_c,N_p}(\Omega_t)$.

Proof.

For a feasible state $x \in X_{N_c,N_p}(\Omega_t)$ at time k, the optimal cost is $V^O_{N_p,N_c}(x, y_t, O(i))$, with $(\boldsymbol{u}^O, x_a^O, u_a^O)$ being the optimal solution of $P^O_{N_p,N_c}(x, y_t, O(i))$. The obtained optimal control sequence $\boldsymbol{u}^O = (u^O(0), \cdots, u^O(N_c-1), k_f(x(N_c), y_a^O), \cdots, k_f(x(N_p-1), y_a^O))$ is associated with the optimal predicted state sequence $\boldsymbol{x}^O = (x^O(0), x^O(1), \cdots, x^O(N_p-1), x^O(N_p))$ with $x^O(N_p) \in \Omega_t$. Defining an auxiliary feasible input sequence, an auxiliary feasible artificial state, and an auxiliary feasible artificial input, respectively,

$$
\begin{aligned}
\tilde{\boldsymbol{u}} &= (u^O(1), \cdots, u^O(N_c-1), k_f(x(N_c), y_a^O), \cdots, k_f(x(N_p), y_a^O)),\\
\tilde{x}_a &= x_a^O,\\
\tilde{u}_a &= u_a^O,
\end{aligned}
\tag{5.26}
$$

the state sequence associated to $(\tilde{\boldsymbol{u}}, \tilde{x}_a, \tilde{u}_a)$ starting from $x(k+1) = f(x(k), u^O(0))$ is

$$
\tilde{\boldsymbol{x}} = (x^O(1), \cdots, x^O(N_p), f(x^O(N_p), k_f(x(N_p), y_a^O))),
\tag{5.27}
$$

with $x(N_p+1) = f(x^O(N_p), k_f(x(N_p), y_a^O))$.

Since $(x^O(N_p), x_a^O, u_a^O) \in \Omega_t^a$, the terminal control action $k_f(x(N_p), y_a^O)$ is admissible and the terminal state $x(N_p+1)$ is feasible due to the positive invariance of Ω_t^a, i.e., $(x(N_p+1), \tilde{x}_a, \tilde{u}_a) \in \Omega_t^a$. Therefore, $x(k+1) \in X_{N_c,N_p}(\Omega_t)$, proving that the closed-loop system is recursively feasible. □

Consider the shifted value function defined by

$$
V_s(x, y_t, O(i)) = V_{N_p,N_c}(x, y_t, O(i)) - S,
\tag{5.28}
$$

as a Lyapunov candidate for the problem $P^O_{N_c,N_p}(x, y_t, O(i))$.

Lemma 5.4. (Upper bound) Consider that Assumptions 5.1 to 5.5 hold, then the shifted value function $V_s(\cdot)$ satisfies

$$
V_s(x, y_t, O(i)) \leq \alpha_c(\|x - x_s\|),
\tag{5.29}
$$

with $\alpha_c(\cdot)$ being a $\mathcal{K}_\infty$-function.

Proof.

From the shifted value function definition and based on the suboptimality of the feasible law $\tilde{u}$, i.e., $\tilde{u}(j) \in U \ \forall j \geq 0$, it holds that

$$
\begin{aligned}
&\sum_{j=0}^{N_c-1} \ell(x^O(j) - x_a^O, u^O(j) - u_a^O) + \sum_{j=N_c}^{N_p-1} \ell(x^O(j) - x_a^O, \kappa_f(x^O(j), y_a^O) - u_a^O) +\\
&V_f(x^O(N_p) - x_a^O) + V_{of}(y_a^O - y_t) + V_{av}(\boldsymbol{y}^O, y_a^O, O(i)) - S\\
\leq &\sum_{j=0}^{N_c-1} \ell(x(j) - x_a, \tilde{u}(j) - u_a) + \sum_{j=N_c}^{N_p-1} \ell(x(j) - x_a, \kappa_f(x(j), y_a) - u_a) +\\
&V_f(x(N_p) - x_a) + V_{of}(y_a - y_t) + V_{av}(\boldsymbol{y}, y_a, O(i)) - S
\end{aligned}
\tag{5.30}
$$

Since $V_{av}(\boldsymbol{y}, y_a, O(i)) - S \leq 0$ based on the boundedness of the avoidance function, we have

$$
\begin{aligned}
&\sum_{j=0}^{N_c-1} \ell(x(j)-x_a, \tilde{u}(j)-u_a) + \sum_{j=N_c}^{N_p-1} \ell(x(j)-x_a, \kappa_f(x(j),y_a)-u_a) + \\
&V_f(x(N_p)-x_a) + V_{of}(y_a-y_t) + V_{av}(\boldsymbol{y}, y_a, O(i)) - S \\
\leq &\sum_{j=0}^{N_c-1} \ell(x(j)-x_a, \tilde{u}(j)-u_a) + \sum_{j=N_c}^{N_p-1} \ell(x(j)-x_a, \kappa_f(x(j),y_a)-u_a) + \\
&V_f(x(N_p)-x_a) + V_{of}(y_a-y_t) \\
= &J(x).
\end{aligned} \tag{5.31}
$$

Since $J(x)$ is a locally bounded positive definite continuous function with $J(x_s) = 0$ (Lemma 5.1), then there exists a $\mathcal{K}_\infty$-function $\alpha_c(\cdot)$ such that $J(x) \leq \alpha_c(\|x - x_s\|)$, for all $x \in X_{N_c,N_p}(\Omega_t)$ (Rawlings & Mayne, 2009). □

Lemma 5.5. (Lower bound) Consider that Assumptions 5.1 to 5.5 hold, then the shifted value function $V_s(\cdot)$ satisfies

$$
V_s(x, y_t, O(i)) \geq \alpha_b(\|x - x_s\|) - S \tag{5.32}
$$

with $\alpha_b(\cdot)$ being a $\mathcal{K}_\infty$-function.

Proof.

From Assumptions 5.5.1 end 5.5.4, there is a $\mathcal{K}_\infty$-function $\alpha(\|x - x_a\|)$ such that

$$
\ell(x - x_a, u - u_a) + V_f(x - x_a) \geq \alpha(\|x - x_a\|). \tag{5.33}
$$

Following the definition of the shifted value function (5.28), we have

$$
\begin{aligned}
&\sum_{j=0}^{N_c-1} \ell(x(j)-x_a, u(j)-u_a) + \sum_{j=N_c}^{N_p-1} \ell(x(j)-x_a, \kappa_f(x(j),y_a)-u_a) + \\
&V_f(x(N_p)-x_a) + V_{of}(y_a-y_t) + V_{av}(\boldsymbol{y}, y_a, O(i)) - S \\
\geq &\sum_{i=0}^{N_p-1} \alpha(\|x - x_a\|) + V_{of}(y_a-y_t) + V_{av}(\boldsymbol{y}, y_a, O(i)) - S \\
\geq &\sum_{i=0}^{N_p-1} \alpha(\|x - x_a\|) - S.
\end{aligned} \tag{5.34}
$$

Thus, based on Lemma 5.2 and on the optimality principle, we have

$$
\sum_{i=0}^{N_p-1} \alpha(\|x - x_a\|) - S \geq \hat{\alpha}_b(\|x - x_a^O\|) - S \geq \alpha_b(\|x - x_s\|) - S, \tag{5.35}
$$

with $\alpha_b(r) = \hat{\alpha}_b \circ \alpha_e(r)$. □

Lemma 5.6. (Decreasing property) Consider that Assumptions 5.1 to 5.5 hold, then the shifted function $V_s(\cdot)$ satisfies

$$V_s^O(x(k+1), y_t, O(i)) - V_s^O(x(k), y_t, O(i)) \leq -\alpha(\|x - x_s\|) + S. \tag{5.36}$$

Proof.

Similar to the proof of Lemma 3.6 in Chapter 3, let the optimal control sequence, the auxiliary feasible input sequence, the optimal output sequence, the auxiliary feasible output sequence, the auxiliary feasible artificial state, the auxiliary feasible artificial output, and the auxiliary feasible artificial input be given, respectively, by

$$\begin{aligned}
\boldsymbol{u}^O &= (u^O(0), \cdots, u^O(N_c-1), k_f(x(N_c), y_a^O), \cdots, k_f(x(N_p-1), y_a^O)),\\
\tilde{\boldsymbol{u}} &= (u^O(1), \cdots, u^O(N_c-1), k_f(x(N_c), y_a^O), \cdots, k_f(x(N_p), y_a^O)),\\
\boldsymbol{y}^O &= (y^O(0), y^O(1), \cdots, y^O(N_p)),\\
\tilde{\boldsymbol{y}} &= (y^O(1), \cdots, y^O(N_p), y(N_p+1)),\\
\tilde{x}_a &= x_a^O,\\
\tilde{u}_a &= u_a^O,\\
\tilde{y}_a &= y_a^O,
\end{aligned} \tag{5.37}$$

with the triplet $(\tilde{x}_a, \tilde{u}_a, \tilde{y}_a)$ being the feasible solution to the one-step ahead optimization problem. Besides, $x(k+1) = f(x(k), u^O(0))$ is the successor state.

Comparing, at $k+1$, $V_s(x(k+1), y_t, O(i); \tilde{\boldsymbol{u}}, \tilde{x}_a, \tilde{u}_a)$ and $V_s^O(x(k), y_t, O(i))$, we have

$$\begin{aligned}
V_s(x(k+1), y_t, &O(i);\ \tilde{\boldsymbol{u}}, \tilde{x}_a, \tilde{u}_a) - V_s^O(x(k), y_t, O(i)) =\\
&\ell(x^O(N_p) - \tilde{x}_a, K_f(x^O(N_p), \tilde{y}_a) - \tilde{u}_a) + V_f(x(N_p+1) - \tilde{x}_a) +\\
&V_{of}(\tilde{y}_a - y_t) + V_{av}(\tilde{\boldsymbol{y}}, \tilde{y}_a, O(i)) - S - \ell(x(0)^O - x_a^O, u^O(0) - u_a^O) -\\
&V_f(x^O(N_p) - x_a^O) - V_{of}(y_a^O - y_t) - V_{av}(\boldsymbol{y}^O, y_a^O, O(i)) + S,
\end{aligned} \tag{5.38}$$

which, considering Assumptions 5.5.4 and 5.5.5, becomes

$$\begin{aligned}
V_s(x(k+1), y_t, &O(i);\ \tilde{\boldsymbol{u}}, \tilde{x}_a, \tilde{u}_a) - V_s^O(x(k), y_t, O(i))\\
&\leq V_{av}(\tilde{\boldsymbol{y}}, \tilde{y}_a, O(i)) - V_{av}(\boldsymbol{y}^O, y_a^O, O(i)) - \ell(x(0)^O - x_a^O, u^O(0) - u_a^O).
\end{aligned} \tag{5.39}$$

Based on the boundedness of the avoidance function, $V_{av}(\tilde{\boldsymbol{y}}, \tilde{y}_a, O(i)) - V_{av}(\boldsymbol{y}^O, y_a^O, O(i)) \leq S$, on the optimality principle, $V_s^O(x(k+1), y_t, O(i)) \leq V_s(x(k+1), y_t, O(i); \tilde{\boldsymbol{u}}, \tilde{x}_a, \tilde{u}_a)$, and on Lemma 5.2, there exists a $\mathcal{K}_\infty$-function $\alpha(\|x - x_s\|)$ such that

$$V_s^O(x(k+1), y_t, O(i)) - V_s^O(x(k), y_t, O(i)) \leq -\hat{\alpha}(\|x - x_a^O\|) + S \leq -\alpha(\|x - x_s\|) + S, \tag{5.40}$$

with $\alpha(r) = \hat{\alpha} \circ \alpha_e(r)$. □

Lemma 5.7. (ISS bound) Consider that Assumptions 5.1 to 5.5 hold, then there exists a $\mathcal{KL}$-function $\hat{\beta}$ such that the shifted function $V_s(\cdot)$ satisfies

$$V_s^O(x(k), y_t, O(i)) \leq \max\{\hat{\beta}(V_s^O(x(0), y_t, O(i)), k), \hat{\gamma}(S)\} \tag{5.41}$$

with

$$\hat{\gamma}(r) = \hat{\alpha}^{-1} \circ \rho^{-1}(r) \tag{5.42}$$

for all $k \in \mathbb{I}_{\geq 0}$, with $\rho(\cdot)$ being a $\mathcal{K}_\infty$-function such that $(id - \rho)(\cdot)$ is a $\mathcal{K}_\infty$-function, and with $\hat{\alpha}(\cdot)$ being a $\mathcal{K}_\infty$-function such that $\hat{\alpha}(r) \leq \alpha_b \circ \alpha_c^{-1}(r)$, for all $r \geq 0$, and with $(id - \hat{\alpha})(\cdot)$ being a $\mathcal{K}$-function.

Proof.

Considering Lemmas 5.4 and 5.6, this proof follows directly from the proof of Lemma 3.7 in Chapter 3. □

Theorem 5.2. (ISS-based avoidance) Consider that Assumptions 5.1 to 5.5 hold, then the closed-loop system with the optimal control law $\kappa_{N_c,N_p}^O(x, y_t, O(i))$ is ISS with respect to the avoidance cost $V_{av}(\boldsymbol{y}, y_a, O(i))$, i.e., there exist a $\mathcal{KL}$-function $\beta(\cdot)$ and a $\mathcal{K}$-function $\gamma(\cdot)$ such that for any feasible initial state $x(0) \in X_{N_c,N_p}(\Omega_t)$, steady-state $x_s \in \text{Proj}_x(Z_s)$, and bound S, the solution $\phi(k; x(0), \boldsymbol{u})$ exists and satisfies

$$\|\phi(k; x(0), \boldsymbol{u}) - x_s\| \leq \beta(\|x(0) - x_s\|, k) + \gamma(S), \tag{5.43}$$

for all $k \in \mathbb{I}_{>0}$.

Proof.

This proof follows directly from the proof of Theorem 3.2 in Chapter 3, being easy to show that based on Lemmas 5.4 to 5.7, $V_s(x, y_t, O(i))$ is an ISS-Lyapunov function for system (5.1) with bounds $\beta(\cdot)$ and $\gamma(\cdot)$. □

5.3.1 Relaxed terminal equality constraint

A simple stabilizing design for set-point tracking is obtained considering $N_c = N_p = N$ and that the terminal state reaches $x(N) = x_a$, with $x_a = g_x(y_a)$ and $y_a \in Y_r$. Therefore, the invariant set for tracking in this formulation comes down to $\Omega_t^{a,N} = \{(x, x_a, u_a) : x = x_a, (x_a, u_a) \in Z_s\}$, which defines the domain of attraction $X_N(\Omega_t^N)$ with $\Omega_t^N = \text{Proj}_x(\Omega_t^{a,N})$. Additionally, the penalty method described previously can be used to represent in the value function the avoidance constraints.

In this formulation, the cost functional is composed of three terms: i) a dynamic term, which is the stage cost with respect to the artificial steady-state and input (x_a, u_a); ii) a stationary term, which is the offset cost functional penalizing the deviation of the artificial steady-output y_a to the target output y_t; and iii) a combination of stationary and dynamic terms, which is the avoidance cost functional penalizing the artificial steady-output y_a and the system predicted output sequence $\boldsymbol{y}$. This cost functional is defined as

$$\begin{aligned} V_N(x, y_t, O(i); \boldsymbol{u}, x_a, u_a) = &\sum_{j=0}^{N-1} \ell(x(j) - x_a, u(j) - u_a) + V_{of}(y_a - y_t) + \\ &\sum_{i=1}^{N_o} \Big[\mu F(y_a, O(i)) + \sum_{j=0}^{N_p} \mu F(y(j), O(i)) \Big], \end{aligned} \tag{5.44}$$

which does not require any terminal cost functional due to the constraint $x(N) = x_a$.

Therefore, the proposed controller for set-point tracking with avoidance features is based on the solution at each sampling time of an optimal control problem $P_N(x, y_t, O(i))$ having as parameters $(x, y_t, O(i))$ and as decision variables $(\boldsymbol{u}, x_a, u_a)$, which is given by

$$V_N^O(x, y_t, O(i)) = \min_{\boldsymbol{u}, x_a, u_a} V_N(x, y_t, O(i); \boldsymbol{u}, x_a, u_a)$$

$$\text{s.t. } x(0) = x, \tag{5.45a}$$

$$x(j+1) = f(x(j), u(j)), \quad j \in \mathbb{I}_{0:N-1}, \tag{5.45b}$$

$$(x(j), u(j)) \in Z, \quad j \in \mathbb{I}_{0:N-1}, \tag{5.45c}$$

$$x_a = f(x_a, u_a), \tag{5.45d}$$

$$y_a = h(x_a, u_a), \tag{5.45e}$$

$$y_a \in Y_r, \tag{5.45f}$$

$$x(N) = x_a. \tag{5.45g}$$

Solving the optimization problem $P_N(x, y_t, O(i))$ at each sampling time, following the receding policy of MPC controllers, the following optimal control law can be obtained:

$$\kappa_N^O(x, y_t, O(i)) = u^O(0; x, y_t, O(i)). \tag{5.46}$$

As usual in MPC with terminal equality constraint, a controllability assumption is required to the problem $P_N(x, y_t, O(i))$ be feasible for a given prediction horizon N. Thus, the controllability condition presented in Limon et al. (2018, Assumption 4) can be stated.

Assumption 5.7. The model function $f(x, u)$ is differentiable at any equilibrium point $(x_a, u_a) \in Z_s$ associated to a steady-output $y_a \in Y_r$, and the linearized model given by the Jacobians $A(x_a, u_a)$ and $B(x_a, u_a)$ is controllable. Furthermore, there exist constants $\epsilon_1 > 0$, $\epsilon_2 > 0$, $b > 0$, and $\sigma > 1$ such that, $\forall j \in \mathbb{I}_{0:N-1}$, the condition

$$\sum_{j=0}^{N-1} \ell(x(j) - x_a, u(j) - u_a) \leq b \|x - x_a\|^\sigma \tag{5.47}$$

holds for any feasible solution $(\boldsymbol{u}, x_a, u_a)$ such that $\|x - x_a\| \leq \epsilon_1$ and $\|u(j) - u_a\| \leq \epsilon_2$.

5.3.2 Weighted terminal cost

Despite its simplicity, the previous formulation has a drawback, as enforcing an equilibrium constraint at the end of the prediction horizon requires that the one-step difference of the states be null after N steps. Thus, the terminal constraint creates a relation between the horizon length and the convergence rate of the closed-loop system, which ends up creating a trade-off between the controller's convergence rate and its computational burden. This problem can be solved considering a set-point tracking MPC scheme without terminal constraint by adding a terminal cost weighting factor γ into the cost functional.

Assumption 5.8.

1. Let $\Omega_t^{a,\gamma}$ be an invariant set for tracking for some $\alpha > 0$ such that

$$\Omega_t^{a,\gamma} = \{(x, x_a, u_a) : V_f(x - x_a) \leq \alpha, (x_a, u_a) \in Z_s\}. \tag{5.48}$$

2. Let $\kappa_f^\gamma(x, y_a)$ be a continuous control law defined over the set $\Omega_t^{a,\gamma}$, such that (x_a, u_a) is an asymptotically stable equilibrium point for the closed-loop system (5.1) controlled by $\kappa_f^\gamma(x, y_a)$.

Similar to (5.9) and (5.44), consider a cost functional with a weighted terminal cost, yielding

$$\begin{aligned} V_{N_c,N_p}^\gamma(x, y_t, O(i); \boldsymbol{u}, x_a, u_a) = &\sum_{j=0}^{N_c-1} \ell(x(j) - x_a, u(j) - u_a) + \sum_{j=N_c}^{N_p-1} \ell(x(j) - x_a, \kappa_f^\gamma(x(j), y_a) - u_a) + \\ &\gamma V_f(x(N_p) - x_a) + V_{of}(y_a - y_t) + \\ &\sum_{i=1}^{N_o} \Big[\mu F(y_a, O(i)) + \sum_{j=0}^{N_p} \mu F(y(j), O(i))\Big], \end{aligned} \tag{5.49}$$

with $\gamma \geq 1$.

Therefore, an optimal control problem $P_{N_c,N_p}^\gamma(x, y_t, O(i))$ can be defined as

$$V_{N_c,N_p}^{\gamma,O}(x, y_t, O(i)) = \min_{\boldsymbol{u}, x_a, u_a} V_{N_c,N_p}^\gamma(x, y_t, O(i); \boldsymbol{u}, x_a, u_a)$$

$$\text{s.t.} \quad x(0) = x, \tag{5.50a}$$

$$x(j+1) = f(x(j), u(j)), j \in \mathbb{I}_{0:N_c-1}, \tag{5.50b}$$

$$(x(j), u(j)) \in Z, j \in \mathbb{I}_{0:N_c-1}, \tag{5.50c}$$

$$x(j+1) = f(x(j), \kappa_f^\gamma(x(j), y_a)), j \in \mathbb{I}_{N_c:N_p-1}, \tag{5.50d}$$

$$(x(j), \kappa_f^\gamma(x(j), y_a)) \in Z, j \in \mathbb{I}_{N_c:N_p-1}, \tag{5.50e}$$

$$x_a = f(x_a, u_a), \tag{5.50f}$$

$$y_a = h(x_a), \tag{5.50g}$$

$$y_a \in Y_r, \tag{5.50h}$$

which, solving at each sampling time in a receding horizon fashion, results in the following optimal control law for safe navigation of the motion system:

$$\kappa^{\gamma,O}_{N_c,N_p}(x, y_t, O(i)) = u^O(0; x, y_t, O(i)). \tag{5.51}$$

The set of states from which the optimization problem $P^{\gamma}_{N_c,N_p}(x, y_t, O(i))$ is feasible can be defined through the following level set (Limon et al., 2018):

$$X^{\gamma}_{N_c,N_p}(y_t) = \{x : V^{\gamma,O}_{N_c,N_p}(x, y_t, O(i)) - V_{of}(y_a - y_t) \leq N_p d + \gamma\alpha\}, \tag{5.52}$$

with $d \in \mathbb{R}_{\geq 0}$ being defined such that for all $(x, x_a, u_a) \notin \Omega^{a,\gamma}_t$ it holds that $\ell(x-x_a, u-u_a) \geq d$.

It has been shown in Limon et al. (2018) that (5.52) is enlarged as the prediction horizon N_p and/or the weighting factor γ are enlarged. Besides, for $N = N_c$, it holds that $X_N(\Omega^N_t) \subseteq X^{\gamma}_{N_c,N_p}(y_t)$ if γ_0 is such that

$$\gamma_0 = \max\left(\frac{N_c D - N_p d + \hat{V}_o}{\alpha}, 1\right), \tag{5.53}$$

with $D \in \mathbb{R}_{\geq 0}$ being a constant such that $\ell(x - x_a, u - u_a) \leq D$ for all $(x, u) \in Z$ and $(x_a, u_a) \in Z_s$. Furthermore, $\hat{V}_o \in \mathbb{R}_{\geq 0}$ is a constant such that $V_{of}(y_a - y_t) \leq \hat{V}_o$ for all $y_a \in Y_r$ and for all possible y_t.

5.4 Numerical Examples

In this section, the behavior of the proposed non-linear MPC schemes is evaluated considering applications in which motion systems are navigating in cluttered environments with previously unknown obstacles. For that, two case studies considering, respectively, a differential mobile robot and a quadrotor UAV are proposed with the simulations being performed with MATLAB, using the CasADI Toolbox (Andersson et al., 2019) with the IPOPT solver (Wächter & Biegler, 2005). Aiming to avoid the computation of the terminal invariant sets, it is considered the formulations with relaxed terminal equality constraint and with weighted terminal cost. In these examples, all units follows the international system standards.

5.4.1 Control strategies setup

The proposed controllers require a discrete dynamical model for prediction. Therefore, in both case studies, the systems are discretized using the first-order Euler approximation with sampling time T_s. Further, the set-point tracking schemes share some definitions that are kept equal in the simulations for comparison purposes. Particularly, the stage-cost is defined as $\ell(x-x_a, u-u_a) = \|x-x_a\|^2_Q + \|u-u_a\|^2_R$, with Q and R being weighting matrices. The offset cost functional is defined as a quadratic function of the form $V_{of}(y_a - y_t) = \|y_a - y_t\|^2_\kappa$, with κ being a weighting matrix. Finally, the selected terminal cost and terminal control law are, respectively, $V_f(x - x_a) = \|x - x_a\|^2_P$ and $\kappa^\gamma_f(x, y_a) = K(x - x_a) + u_a$, with P and K being obtained by solving the Riccati equation associated to an LQR controller obtained for the linearized dynamics.

The obstacles are defined in execution time either as a sphere or a circle with a radius ρ, which is centered at a point measured in the boundary of the obstacle, y_{c_i}, with the smallest distance to the motion system position, y. The choice between a sphere or a circle depends on the dimension of the output space $Y \subset \mathbb{R}^p$. Therefore, considering $g_l(y, O(i)) = -(y - y_{c_i})' I_p (y - y_{c_i}) + \rho^2$, the penalty function can be defined as

$$F(y, O(i)) = \sum_{i=1}^{N_O} (\max\{0, g_l(y, O(i))\})^2,$$

with N_o being the number of detected obstacles at time instant k.

Since the obstacles are assumed to be previously unknown from the controller standpoint, a detection algorithm is made to perceive the obstacles within a range of τ meters based on the system's global position and the environment map. Therefore, the obstacles can be avoided only when inside the sensor range.

5.4.2 Differential Mobile Robot

Consider the differential mobile robot described in Appendix A, Section A.2. The robot is actuated through forward velocity, v, and the angular velocity, ω. Moreover, the generalized coordinates describing the robot in the workspace is defined combining the robot position, $x^\mathcal{I}$ and $y^\mathcal{I}$, and orientation, θ. Thus, the state, input, and output vectors can be defined, respectively, as $x = [x^\mathcal{I}\ y^\mathcal{I}\ \theta]'$, $u = [v\ \omega]'$, and $y = [x^\mathcal{I}\ y^\mathcal{I}]'$. It is worthwhile mentioning that there is no limitation regarding the controlled output choice; however, it is important to choose it not only to define suitable targets but also to represent the motion system relative to the obstacles. For that reason, we avoid adding the orientation as a controlled output. Besides, since the system is underactuated, it is only possible to control a number of degrees of freedom equal to the number of inputs (assuming they are not redundant).

For the proposed simulation, it is considered a 3.2×2 meters map with nine squared objects representing the previously unknown obstacles. Further, the mobile robot rotation center displacement is $d = 0.1$ and the sampling time considered for discretization is $T_s = 0.01$. For the detection algorithm, the radius of the circle representing the obstacles is $\rho = 0.1$, and the obstacle detection range is $\tau = 0.2$. In the control algorithm, the states and inputs weighting matrices are, respectively, $Q = \mathrm{diag}\{1, 1, 1\}$ and $R = \mathrm{diag}\{1, 0.3\}$. However, it is worth mentioning that the matrices P and K, respectively, for the terminal cost and terminal control law, are obtained by solving the Riccati equation associated with an LQR controller considering $Q_{LQR} = 10^{-4} I_3$ and $R_{LQR} = 10 I_2$ as weighting matrices for the linearized dynamics. Furthermore, the offset cost weighting matrix is chosen as $\kappa = \text{diag}\{1000, 1000\}$, while the penalty cost weight considered is $\mu = 10^6$. For the formulation with relaxed terminal equality constraint the prediction/control horizon is $N = 4$. As for the formulation with weighted terminal cost, the prediction and control horizons are, respectively, $N_p = 6$ and $N_c = 4$. Also, it was chosen a terminal cost weighting factor $\gamma = 200$, and the smallest weight for $X_N(\Omega_t^N) \subseteq X^{\gamma}_{N_c,N_p}(y_t)$ is $\gamma_0 = 1$ (see equation (5.53)). In terms of constraints, the set of admissible inputs and states are given, respectively, by $U = \{\|v\| \leq 1.5, \|\omega\| \leq 10\}$ and $X = \{\|x\| \leq 1.6, \|y\| \leq 1, \|\theta\| \leq \pi\}$. Additionally, the constant λ used in (5.4) to avoid controllability loss is equal to 0.9999.

Figure 5.1 presents the results for the set-point tracking problem in which the robot starts from an initial position $(-1.4, 0.8)$ and must reach the target $(1.25, -0.4)$. In the figure, the robot pose is depicted at different instants of time with the orientation of the robot being inferred from the orientation of the triangle used to represent it. Further, the circle around the robot indicates the detection range of the emulated sensor. Despite the robot workspace being obstructed by previously unknown obstacles, it can be observed that both control strategies were able to provide set-point tracking without collisions.

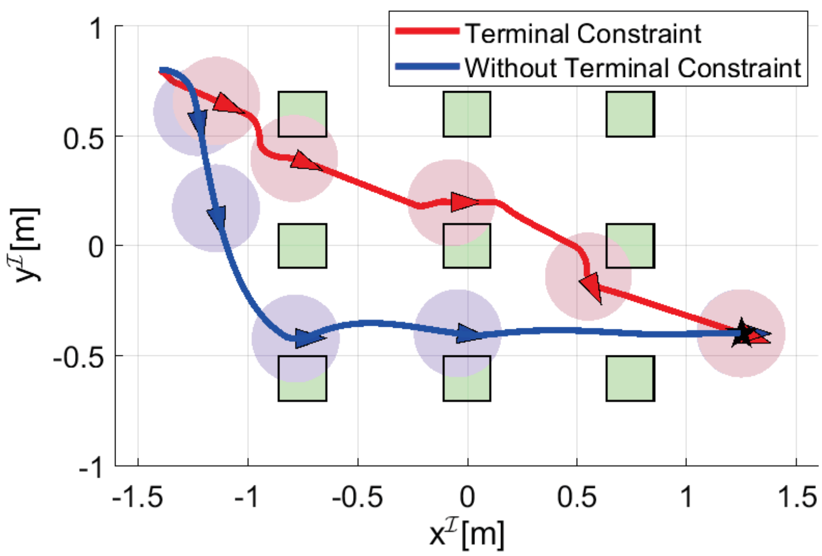

Figure 5.1: The trajectory of the differential mobile robot is shown in the figure for cases with and without terminal constraints. The desired set-point is denoted by a black star marker in the bottom-right, green squares represent obstacles, the triangle shape represents the robot pose, and the circle around the robot depicts the sensor range of detection.

In Figure 5.2, it is possible to see the robot absolute error with respect to the target. Particularly, it is interesting to observe how the multiple objectives defined in the optimal control problems make the error increase at some points of the navigation process, which

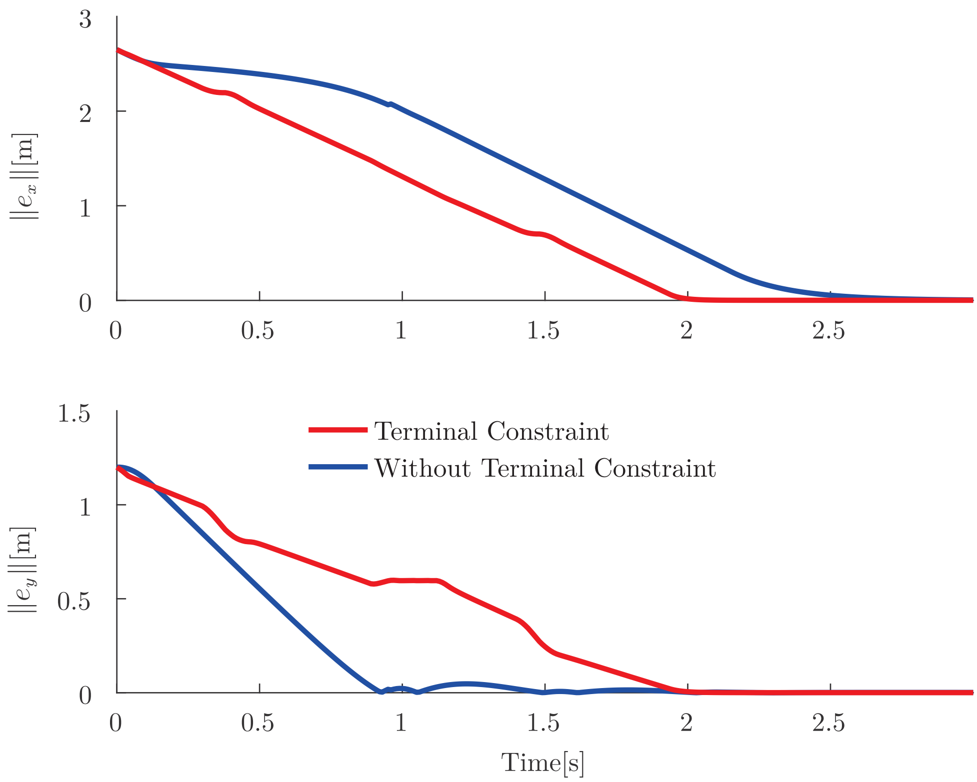

Figure 5.2: Absolute position error with $e_x = x^{\mathcal{I}} - x_t$ and $e_y = y^{\mathcal{I}} - y_t$ for the cases with and without terminal constraint. In the figure, it is illustrated the relation between error reduction and avoidance.

is expected due to the avoidance cost. Further, it can be noted that the control strategies present close performance with a similar convergence time. In fact, since it is considered a first-order dynamic model to describe the differential mobile robot dynamics, both controllers will present similar performance. However, for motion systems described by differential equations with order bigger than one, the control strategy without terminal equality constraint will present faster convergence. Finally, Figures 5.3 and 5.4 show, respectively, the states and inputs for both control strategies, which are kept stable and within the constraints.

As explained throughout this work, the set-point tracking strategies are suitable for applications considering changing set-points because they reduce feasibility issues present in regulatory strategies. These properties can be easily observed by comparing the domain of attraction for both strategies. Particularly, if we consider the formulations with terminal equality constraint, the domains of attraction can be easily computed. Therefore, Figure 5.5 presents the domains of attraction considering the set-point stabilization problem with terminal equality constraint and the set-point tracking problem with terminal equality constraint. As corroborated by the theoretical results, the domain of attraction for the set-point tracking strategy is enlarged, which minimizes feasibility issues when using this framework.

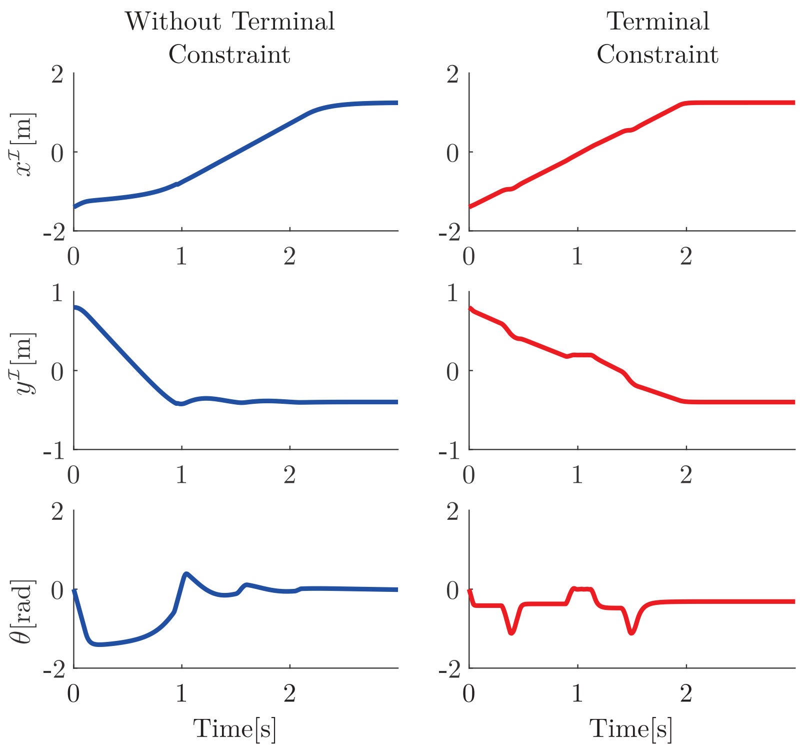

Figure 5.3: Time evolution of the mobile robot states ($x^{\mathcal{I}}$ $y^{\mathcal{I}}$ θ) for the cases with and without terminal constraint during the tracking of the desired target.

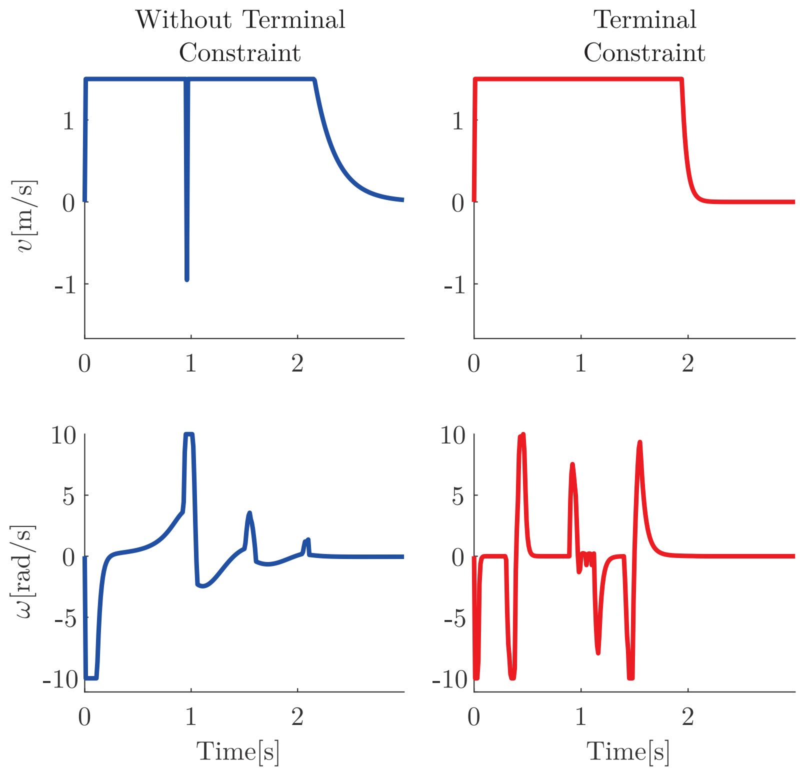

Figure 5.4: Time evolution of the manipulated variables (forward and angular velocities) for the cases with and without terminal constraint.

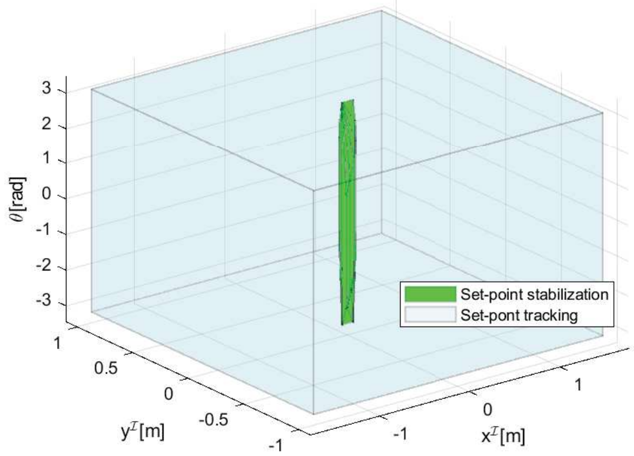

Figure 5.5: Domains of attraction for the set-point tracking and set-point stabilization strategies considering formulations with terminal equality constraints. In the figure, the blue set represents the domain of attraction for the tracking approach, while the green set represents the domain of attraction for the regulatory approach.

5.4.3 Quadrotor UAV

Consider the quadrotor UAV system described in Appendix A, Section A.3. The system is actuated through the lift forces, $u = [f_1\ f_2\ f_3\ f_4]'$, with its states composed of position and attitude as well as their time derivatives, $x = \left[x^{\mathcal{I}}\ y^{\mathcal{I}}\ z^{\mathcal{I}}\ \phi\ \theta\ \psi\ \dot{x}^{\mathcal{I}}\ \dot{y}^{\mathcal{I}}\ \dot{z}^{\mathcal{I}}\ \dot{\phi}\ \dot{\theta}\ \dot{\psi}\right]'$. Similarly to the previous numerical example, the controlled output is chosen to define suitable targets and to represent the motion system relative to the obstacles. Therefore, the controlled output is chosen as the UAV position, $y = [x^{\mathcal{I}} y^{\mathcal{I}} z^{\mathcal{I}}]'$.

Aiming to better emulate the vehicle dynamics during the simulation, the non-linear dynamic model (A.14) is considered with the parameters provided in Table A.2. Further, the ordinary differential equation solver ODE45 from MATLAB is used for numerical integration with a discretization time-step of 0.01 seconds. However, for control design purposes, it is used a non-linear model, equation (A.14), disregarding the coupling between translational and rotational dynamics due to the displacement between the quadrotor's geometric center and its center of mass (see Section A.3).

Similar to the previous case study, it is considered a $48 \times 30 \times 20$ meters map with five rectangle-shaped objects representing the previously unknown obstacles. For the detection algorithm, the radius of the sphere representing the obstacles is $\rho = 2$ and the obstacle detection range is $\tau = 4$. In the control algorithm, the states and inputs weight matrices are, respectively, $Q = \mathrm{diag}\{0.25, 0.25, 0.25, 0.4, 0.4, 0.1, 0.25, 0.25, 0.25, 0.01, 0.01, 0.02\}$ and $R = \mathrm{diag}\{24, 24, 24, 24\}$. Further, the matrices P and K are obtained by solving the Riccati equation associated with an LQR controller considering $Q_{LQR} = Q$ and $R_{LQR} = 0.1R$ as weighting matrices. The offset cost weighting matrix is chosen as $\kappa = \mathrm{diag}\{1500, 1000, 3000\}$, while the penalty cost weight considered is $\mu = 10^4$. For the formulation with relaxed terminal equality constraint the prediction/control horizon is $N = 50$. As for the formulation with weighted terminal cost, the prediction and control horizons are, respectively, $N_p = 20$ and $N_c = 5$. Also, it was chosen a terminal cost weighting factor $\gamma = 200$ and the smallest weight for $X_N(\Omega_t^N) \subseteq X^{\gamma}_{N_c,N_p}(y_t)$ is $\gamma_0 = 26.564$ (see equation (5.53)). In terms of constraints, the set of admissible inputs and states are given, respectively, by $U = \{0 \leq f_1, f_2, f_3, f_4 \leq 12\}$ and $X = \{-[24\ 15\ 0]' \leq \xi \leq [24\ 15\ 20]', \|\dot{\xi}\| \leq [5\ 5\ 5]', \|\dot{\eta}\| \leq [\pi\ \pi\ \pi]', \|\eta\| \leq [\pi/2\ \pi/2\ \pi]'\}$. Additionally, the constant λ used in (5.4) is equal to 0.9999. Finally, the sampling time considered for discretization is $T_s = 0.01$.

In this simulation scenario, the quadrotor UAV is required to go autonomously from its initial position $(-18, -9, 0)$ to the desired one $(18, 7.5, 14)$, in the upper right side of Figure 5.6 as a black dot. The stop criteria considered for the simulations are the Euclidean distance between the target and the UAV being smaller than 0.5 meters, i.e., $\|y - y_t\| \leq 0.5$, or the simulation time reaching 500 seconds.

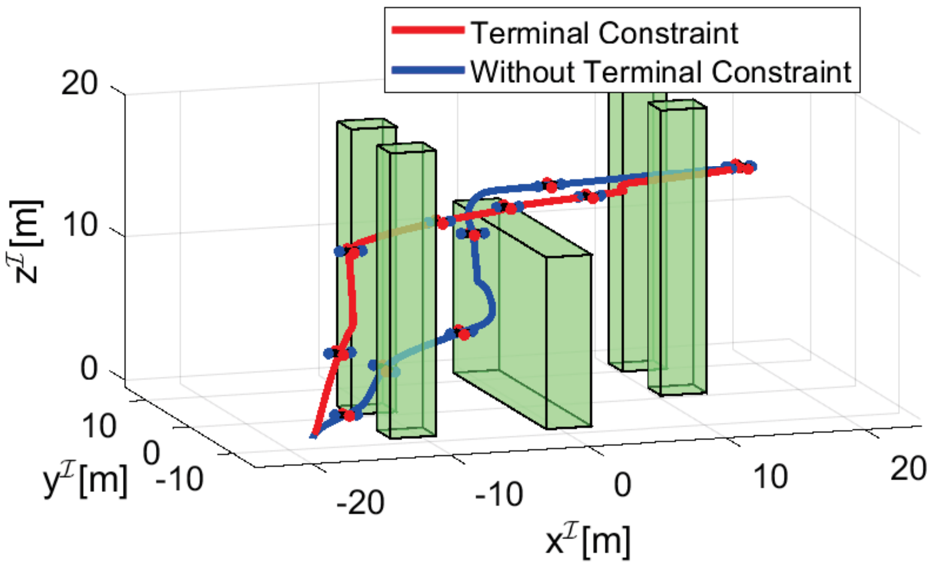

Figure 5.6: Complete trajectory performed by the UAV to safely navigates from the initial condition (bottom-left) to the target (upper-right) while avoiding five obstacles (green sets). In the figure, the UAV is denoted as a black cross with blue and red spheres in its extremities.

In Figure 5.6, it is shown the simulations performed with both set-point tracking control strategies considered. It can be noted that in both cases the quadrotor UAV, without any prior knowledge of the obstacles, finds a path across the obstacles that appear during its navigation in order to avoid the imminent collisions. It is worthwhile noticing that, after reaching the wall-like obstacle, the aerial vehicle climbs it and passes above the obstacle. As expected, the similar behavior can be observed for the strategy with and without terminal constraint since they are both based on artificial variables, offset cost functional, and avoidance constraints as penalties on the value function. In Figures 5.7 and 5.8, the alternative path performed to accomplish the task safely is shown, respectively, in X-Y and X-Z views. Also, in Figures 5.7 and 5.8, the circles around the UAV denotes the sensor range of detection.

The behavior of the proposed control strategies for avoidance can be better understood considering the role played by the offset cost functional and the obstacle avoidance penalty. In this framework, both costs work together as a built-in steady-state target optimizer, which, for the considered application, results in a planning strategy that increases the value function based on the distance to the target and the presence of obstacles. Thus, an optimal artificial target can be obtained by minimizing this cost. Besides, since the proposed strategy works in a single-layer, the controller also minimizes the error between its predicted trajectory and the generated artificial target, accounted in the stage cost. The avoidance process can also be verified by looking at the absolute position error. In fact, the control algorithm gives up performance to achieve safe navigation, which can be observed in Figure 5.9, where the error stops decreasing at some points even before converging asymptotically.

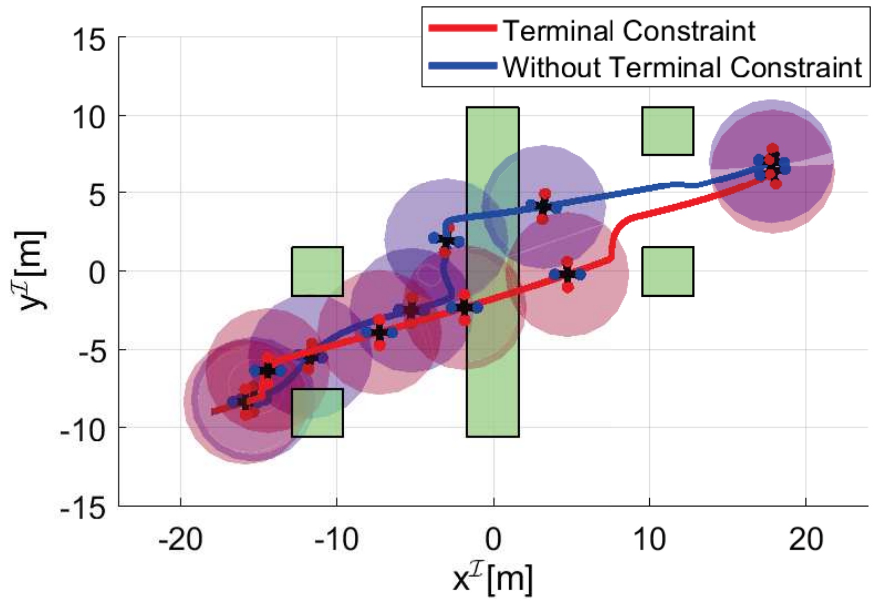

Figure 5.7: X-Y view of the complete trajectory performed by the UAV to safely complete the given task. In the figure, the circles around the UAV denote the sensor range of detection.

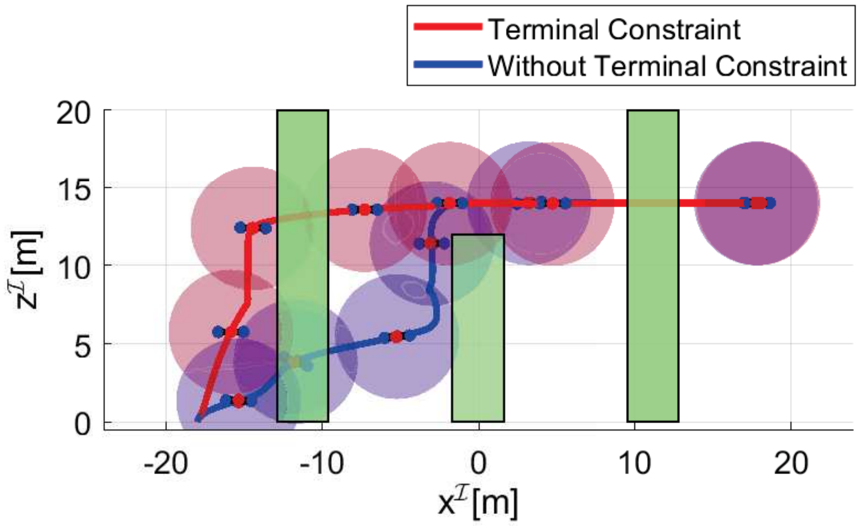

Figure 5.8: X-Z view of the complete trajectory performed by the UAV to safely complete the given task. In the figure, the circles around the UAV denote the sensor range of detection.

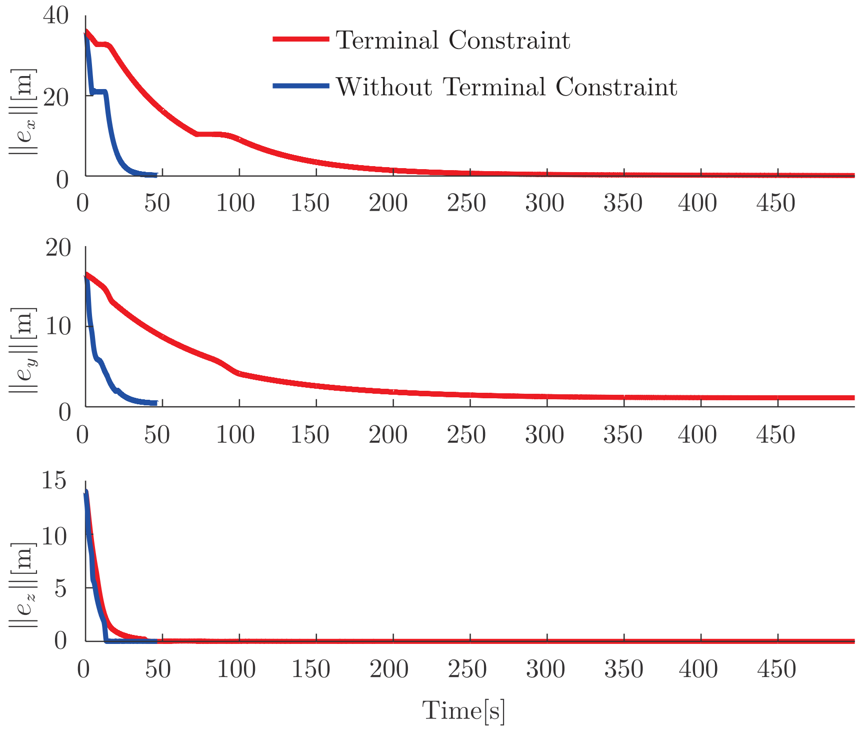

Figure 5.9: Absolute output tracking error illustrating the relation between error reduction and avoidance for the cases with and without terminal constraint. In the figure, $e_x = x^{\mathcal{I}} - x_t$, $e_y = y^{\mathcal{I}} - y_t$, and $e_z = z^{\mathcal{I}} - z_t$.

Notice in Figure 5.9 that the convergence rates for the set-point tracking control strategies considered are significant different. In fact, the stop criteria for the strategy without terminal constraint is based on the distance to the target and occurs around 46 seconds. As for the formulation with terminal constraint, the simulation stops when the system reaches 500 seconds. This behavior can be explained by recalling the problems related to the terminal constraint enforcing an equilibrium condition in N steps for motion systems described by differential equations with order higher than one. Such constraint creates a trade-off between the horizon length and the motion system acceleration capacity, which, ultimately, ties the closed-loop convergence rate to the control strategy computational burden. Table 5.1 presents the translational velocities and accelerations for the quadrotor UAV controlled with both strategies. It can be noted that, despite the higher prediction horizon chosen for the formulation with terminal constraint, the formulation without it achieved higher velocities and accelerations, which explains its fast convergence time. Finally, it is noteworthy that the closed-loop system may present steady-state offset due to external disturbances, unmodeled dynamics, among other reasons. Indeed, in the performed simulations, the use of a non-linear model for control disregarding the coupling between translational and rotational dynamics causes some steady-state offset. In order to work around this issue, offset-free strategies can be used (Morari & Maeder, 2012; Ferramosca et al., 2017).

Table 5.1: Quadrotor UAV translational velocities and accelerations given, respectively, in m/s and m/s².

Variable	**Without Terminal Constraint**	**Terminal Constraint**
$\dot{x}^{\mathcal{I}}$	$[-0.93, 4.98]$	$[-0.04, 0.63]$
$\dot{y}^{\mathcal{I}}$	$[-0.18, 3.51]$	$[-0.16, 0.41]$
$\dot{z}^{\mathcal{I}}$	$[-0.05, 3.31]$	$[0.00, 0.98]$
$\ddot{x}^{\mathcal{I}}$	$[-11.38, 8.30]$	$[-1.60, 1.72]$
$\ddot{y}^{\mathcal{I}}$	$[-2.82, 3.18]$	$[-0.75, 0.50]$
$\ddot{z}^{\mathcal{I}}$	$[-7.90, 7.40]$	$[-0.11, 2.26]$

Figure 5.10 presents the time evolution of the quadrotor UAV orientation stably converging to an equilibrium value, which is expected since at the end of the task execution the UAV will be in hovering flight mode due to the equilibrium condition of the artificial variables. Notice that, since the artificial reference is defined in the output-level, there is no need to require a reference for orientation. In fact, the artificial orientation for the stabilizing stage cost is obtained from the artificial position by means of the model constraints. Further, Figure 5.11 shows that the control signals applied to the quadrotor UAV for both considered control strategies are within the constraints.

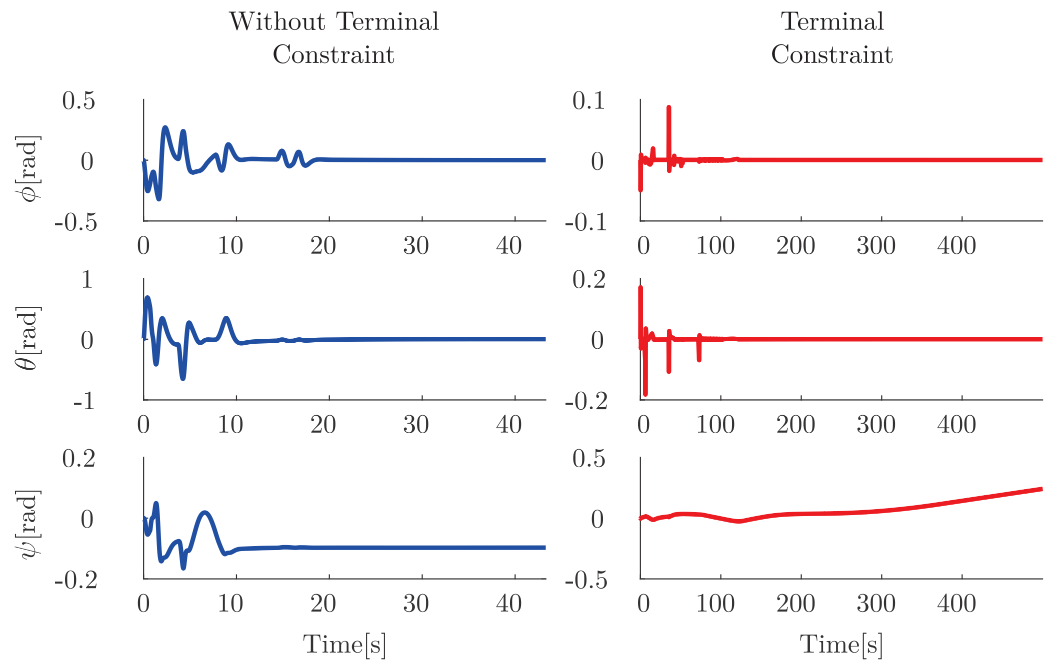

Figure 5.10: Time evolution of the quadrotor UAV orientation (ϕ, θ, and ψ) for the cases with and without terminal constraint.

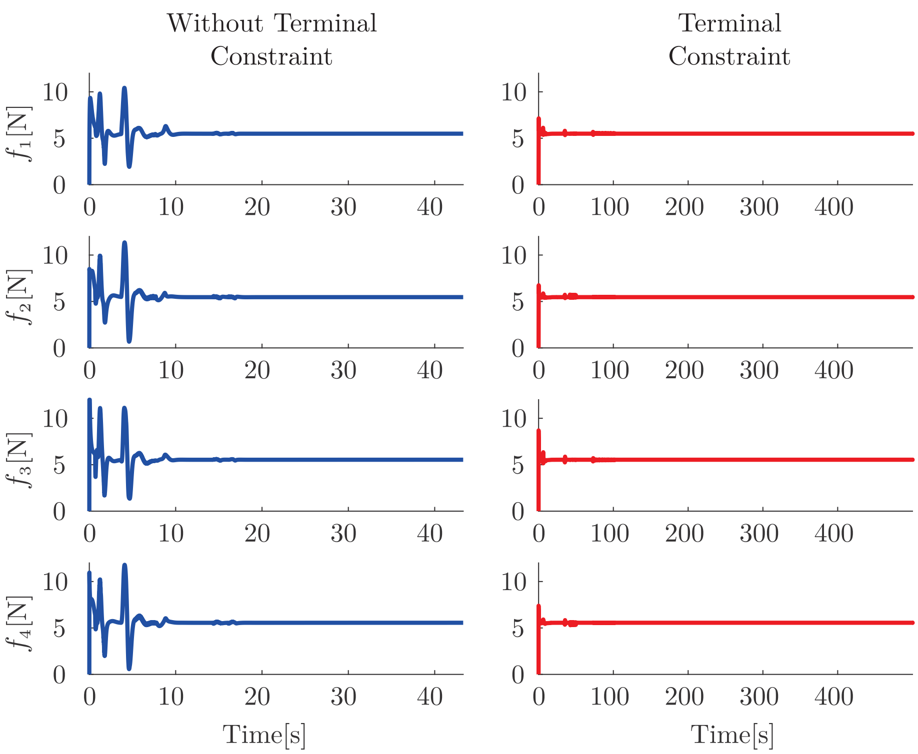

Figure 5.11: Applied lift forces to the quadrotor UAV for the cases with and without terminal constraint. In the figure, f_i denotes the lift force of the i-th propeller.

Based on the results of Limon et al. (2018), it is possible to state that the proposed strategies for set-point tracking have enlarged domain of attractions with respect to the strategies designed for regulation. Therefore, since motion systems are subjected to changing targets during autonomous navigation, the set-point tracking formulations are more suitable to solve the problem. Further, from the computed $\gamma_0 = 26.564$ and the chosen $\gamma = 200$, it is possible to state that the domain of attraction for the formulation without terminal constraint contains the domain of attraction for the case with terminal equality constraint considering $N = N_c = 5$. Since for the simulations we considered $N = 50$ to mitigate the convergence rate issue, the domain of attraction considering the terminal equality constraint strategy could be larger than the one without it. However, the framework without terminal constraint provides the additional parameter γ that enlarges the domain of attraction when increased. Therefore, in the formulation without the terminal constraint, it is possible to obtain smaller optimization problems with satisfactory domain of attraction.

In order to corroborate this argument, Table 5.2 shows for each formulation the number of decision variables and constraints of the optimization problem considering a multiple-shooting approach to solve the problem (Bock & Plitt, 1984). Notice that the problem for the formulation without terminal constraint has around three times fewer decision variables and constraints, and its cost functional has fewer terms. These facts make the optimization problem for the case without terminal constraints easier to solve.

Table 5.2: Dimension of the optimization problems in terms of decision variables and constraints.

Optimization Problem	**Without Terminal Constraint**	**Terminal Constraint**
Variables	288	828
Constraints	840	2292

When compared to set-point stabilization schemes, the optimization problems for set-point tracking have similar sizes. The difference between both approaches will be the use of artificial variables as decision variables and the constraints related to them. Therefore, in set-point stabilization formulations, we have optimization problems with fewer decision variables and fewer constraints. As for the cost functional, the differences are the presence of an offset cost functional and a penalty avoidance term for the artificial variables, which do not change the optimization problem class since a non-linear programming problem still needs to be solved. Although the formulation designed for set-point stabilization has a smaller computation burden, we can fairly assume that this difference is not significant, mostly for applications requiring long prediction horizons. So, with the set-point tracking formulations, we can reduce feasibility issues while solving optimization problems of about the same size as the ones for the set-point stabilization formulations.

5.5 Final Remarks

In this chapter, non-linear model predictive control schemes with avoidance features were proposed. For that, the non-linear model predictive framework for set-point tracking was extended by adding avoidance constraints as a penalty to the problem. Aiming to work around the necessity of computing terminal invariant sets, two simplified schemes were proposed and analyzed. It was shown that, under mild conditions, the closed-loop system is ISS with respect to the avoidance cost, which allows showing that the closed-loop system is stable and recursively feasible.

In the next chapter, final remarks are made on the results obtained in this thesis. Additionally, ideas for the continuity of this research are proposed.

6
Conclusion

There is a clear movement towards MPC to benefit from its flexibility and the advances regarding the guarantee of stability and robustness, and the incorporation of secondary objectives to those of traditional dynamic control. Particularly, the flexibility to impose constraints and to design the objective function brought new possibilities for applications requiring multiple objectives. In this context, there has been an increasing number of solutions within the MPC framework aiming to exploit the optimization problem design through its objective function and constraints. Among these solutions, the problem of avoidance stood out as a challenging problem because it involves non-convexities caused by holes inside the admissible space.

Most of the works considering MPC for avoidance leave some fundamentals aside, mainly focusing on the application. For instance, when constraints are directly added to the optimal control problem, the resulting MPC algorithm presents feasibility issues. Also, in the case of regulatory formulations for applications that require tracking or changing targets, no stability guarantee can be provided. Finally, those works modifying the cost functional to add avoidance do not analyze the impact of losing the decreasing properties of the value function. In this context, the main motivation of this thesis was to formalize concepts and provide a solid theoretical background for a control problem that is becoming more prevalent in the literature.

The main argument throughout this thesis is related to how one could work around non-convexity issues by proposing equivalent convex problems. Here, we have considered avoidance through penalty functions, which allowed us to work with convex admissible constraint sets at the cost of having non-convex value functions that do not hold any decreasing property. Additionally, the proposed solutions considered the idea of artificial variables to achieve enlarged domains of attraction and to avoid loss of recursive feasibility in the presence of changing targets or even when non-feasible targets are considered. The main result obtained in this thesis shows that such formulations are stable and recursively feasible under the mild assumption that the penalty designed for avoidance is bounded over time. For that, we considered the ISS framework by looking at the avoidance penalty as a disturbance in the value function. In such context, we could prove that the MPC frameworks for avoidance proposed are input-to-state stable and can recover asymptotic stability when the regions to be avoided are not present.

In Chapter 3, the ideas considered to add avoidance within the MPC framework are first introduced. We designed a linear control strategy for set-point tracking that extends the results of Limon et al. (2008) to the avoidance case, showing that the closed-loop system is recursively feasible under changing set-points, and that the presence of non-feasible regions does not affect this property. We demonstrated the ISS property of the closed-loop system by establishing a shifted value function based on the penalized MPC cost for avoidance as an ISS-Lyapunov function. Thus, the proposed control scheme remains stable even in the presence of non-feasible regions within a known admissible space, and it recovers the asymptotic stability property when the non-feasible regions are removed. Moreover, the closed-loop system exhibits an enlarged domain of attraction compared to approaches based on regulatory formulations. It also performs well in handling unreachable references, which is a crucial feature in avoidance scenarios. Finally, a potential drawback of using penalties for avoidance is the loss of avoidance guarantees. However, our findings show that avoidance guarantees can be preserved by employing exact penalization. Two numerical examples were proposed to analyze the behavior of the proposed control strategy. First, a ball-on-plate system with a non-convex plate is considered to show how a problem with non-convex admissible sets could be handled within the proposed formulation. Second, it is considered the autonomous navigation problem of a quadrotor UAV in a cluttered environment with previously unknown obstacles.

In Chapter 4, our main focus was to answer the question of how the set-point tracking MPC with avoidance features performs in the presence of unknown but bounded uncertainties. Building upon the ideas of Limon et al. (2010), we adopted a semi-feedback formulation and utilized the notion of tube of trajectories for robust constraint satisfaction. Additionally, to account for the impact of uncertainties in the avoidance problem, we based the considered penalties on enlarged non-feasible regions. Since the control approach we considered is set-based, we used zonotopic set representation to efficiently perform constraint tightening, enlargement operations, and reachability analysis. Our findings showed that, under mild conditions, the closed-loop system converges to a neighborhood of the target if the target is reachable in the obstructed space. Otherwise, it converges to a neighborhood of a reachable steady-output that minimizes a given cost functional. Moreover, the proposed controller exhibits properties of ISS, recursive feasibility under changing set-points and an unknown number of non-feasible regions to be avoided, an enlarged domain of attraction, and avoidance guarantees. To further analyze the behavior of the proposed control strategy, we conducted numerical examples involving a double integrator with its state space obstructed by one non-feasible region, and a quadrotor UAV navigating in an environment obstructed by a prior unknown number of obstacles.

In Chapter 5, we addressed the avoidance problem for non-linear systems within the MPC framework. Particularly, we extended the non-linear set-point tracking MPC proposed in Ferramosca (2011), later analyzed in Limon et al. (2018), to the avoidance case considering a previously unknown number of non-feasible regions. Similar to the previous formulations, we demonstrated that non-linear systems in closed-loop with the proposed strategies are recursively feasible and satisfy the ISS property, under the mild assumption of uniformly bounded avoidance cost over time. To avoid the need for computing terminal invariant sets, we analyzed simplified design schemes based on relaxed terminal equality constraints and weighted terminal costs. The chapter concludes with the presentation of two case studies involving a differential mobile robot and a quadrotor UAV navigating in environments obstructed by an unknown number of obstacles.

6.1 Continuity Proposals

This research raised five main interesting topics that should be pursued in future works.

- Avoidance within the stochastic MPC framework:

  Systems are subject to different sources of uncertainties, which are usually random and better described as stochastic variables with a known probability distribution. However, when dealing with the problem of robustness of a control strategy, the classic solution is to assume that the uncertainties affecting the system are deterministic and lies inside a given compact set. This assumption makes the control system conservative since it relies on worst-case approaches. A possible way to work around the problem is to consider the stochastic nature of the uncertainties and their statistical properties into the control problem. Besides, one of the key features of this framework is the inclusion of chance constraints, enabling a systematic trade-off between control performance and state constraint violations in a probabilistic sense.

- Invariance analysis for non-linear systems:

  In order to compute positive invariants for non-linear systems with a large number of states, efficient approaches for performing non-linear reachability analysis need to be investigated using proper set representations.

- Computationally efficient solutions:

  Aiming at real-world examples, investigating computationally efficient solutions is paramount. For instance, explicit formulations could be considered for avoidance, although it is still an open problem how a multi-parametric non-convex problem can be used in explicit formulations, which often requires quadratic costs.

- Investigate ideas of event-based predictive control schemes:

  One of the main challenges of avoidance strategies within the MPC framework lies in how the avoidance process could be less reactive and more tactical. MPC schemes become local by design as they are finite horizon strategies, meaning that control actions are obtained by looking only at a finite time window ahead. Therefore, as the prediction horizon is indexed in time, it limits the overall prediction capability that could be used for avoidance purposes. In this context, hybrid time-based and event-based predictive schemes could potentially provide better results in terms of avoidance capacity.

- Investigate the problem of avoidance in non-Euclidean space:

  For some applications, such as robotics, improved performance may be achieved if more suitable topological representations are considered. However, there is a clear limitation of the control strategies for avoidance proposed in this thesis when it comes to handling non-Euclidean space, since the optimal control problem formulated is Euclidean-based. Therefore, a whole new framework must be proposed to allow this problem to be solved in distinct topological spaces.

Bibliography

Alessandretti, A., Aguiar, A. P., & Jones, C. N. (2017). An input-to-state-stability approach to economic optimization in model predictive control. *IEEE Transactions on Automatic Control*, 62(12), 6081–6093.

Althoff, M. (2015). An introduction to cora 2015. In *Workshop on Applied Verification for Continuous and Hybrid Systems* (pp. 120–151).

Andersson, J. A. E., Gillis, J., Horn, G., Rawlings, J. B., & Diehl, M. (2019). CasADi – A software framework for nonlinear optimization and optimal control. *Mathematical Programming Computation*, 11(1), 1–36.

Angeli, D. & Mosca, E. (1999). Command governors for constrained nonlinear systems. *IEEE Transactions on Automatic Control*, 44(4), 816–820.

Bemporad, A. (1998). Reference governor for constrained nonlinear systems. *IEEE Transactions on Automatic Control*, 43(3), 415–419.

Bemporad, A. & Morari, M. (1999). Robust model predictive control: A survey. In *Robustness in identification and control* (pp. 207 – 226). Springer London.

Blanchini, F. & Miani, S. (2007). *Set-Theoretic Methods in Control*. Birkhauser Basel, 1st edition.

Bock, H. & Plitt, K. (1984). A multiple shooting algorithm for direct solution of optimal control problems. *IFAC Proceedings Volumes*, 17(2), 1603–1608.

Camacho, E. F. & Bordons, C. (2004). *Model Predictive Control*. Springer-Verlag London.

Campo, P. J. & Morari, M. (1987). Robust model predictive control. In *Proceedings of the American Control Conference* (pp. 1021–1026).

Castillo, P., Lozano, R., & Dzul, A. (2005). *Modelling and Control of Mini Flying Machines*. Springer-Verlag.

Chisci, L., Rossiter, J., & Zappa, G. (2001). Systems with persistent disturbances: predictive control with restricted constraints. *Automatica*, 37(7), 1019–1028.

Chisci, L. & Zappa, G. (2003). Dual mode predictive tracking of piecewise constant references for constrained linear systems. *International Journal of Control*, 76(1), 61–72.

Combastel, C. (2003). A state bounding observer based on zonotopes. In *Proceedings of the European Control Conference* (pp. 2589–2594).

Cotorruelo, A., Ramirez, D. R., Limon, D., & Garone, E. (2021). Nonlinear MPC for tracking for a class of nonconvex admissible output sets. *IEEE Transactions on Automatic Control*, 66(8), 3726–3732.

Darup, M. S. & Mönnigmann, M. (2018). Optimization-free robust MPC around the terminal region. *Automatica*, 95, 229–235.

Diehl, M., Amrit, R., & Rawlings, J. B. (2011). A Lyapunov function for economic optimizing model predictive control. *IEEE Transactions on Automatic Control*, 56(3), 703–707.

D'Jorge, A., Anderson, A., González, A. H., & Ferramosca, A. (2018). A robust economic MPC for changing economic criterion. *International Journal of Robust and Nonlinear Control*, 28(1), 1 – 20.

D'Jorge, A., Santoro, B. F., Anderson, A., González, A. H., & Ferramosca, A. (2020). Stochastic model predictive control for tracking linear systems. *Optimal Control Applications and Methods*, 41(1), 65–83.

Ellis, M., Durand, H., & Christofides, P. D. (2014). A tutorial review of economic model predictive control methods. *Journal of process control*, 24(1), 1156–1178.

Ferramosca, A. (2011). *Model Predictive Control for systems with changing setpoints*. PhD thesis, Universidad de Sevilla.

Ferramosca, A., González, A. H., & Limon, D. (2017). Offset-free multi-model economic model predictive control for changing economic criterion. *Journal of Process Control*, 54, 1–13.

Ferramosca, A., Limon, D., Alvarado, I., Alamo, T., & Camacho, E. (2009). MPC for tracking with optimal closed-loop performance. *Automatica*, 45(8), 1975–1978.

Ferramosca, A., Limon, D., Alvarado, I., Alamo, T., Castaño, F., & Camacho, E. (2011). Optimal MPC for tracking of constrained linear systems. *International Journal of Systems Science*, 42(8), 1265–1276.

Ferramosca, A., Limon, D., González, A., Alvarado, I., & Camacho, E. (2012). Robust MPC for tracking zone regions based on nominal predictions. *Journal of Process Control*, 22(10), 1966–1974.

Ferramosca, A., Limon, D., González, A., Odloak, D., & Camacho, E. (2010). MPC for tracking zone regions. *Journal of Process Control*, 20(4), 506–516.

Garone, E., Cairano, S., & Kolmanovsky, I. (2017). Reference and command governors for systems with constraints: A survey on theory and applications. *Automatica*, 75, 306–328.

Goldar, A., Romagnoli, R., Couto, L. D., Romero, A., Kinnaert, M., & Garone, E. (2020). MPC strategies based on the equivalent hydraulic model for the fast charge of commercial li-ion batteries. *Computers & Chemical Engineering*, 141, 1–10.

Hermans, B., Patrinos, P., & Pipeleers, G. (2018). A penalty method based approach for autonomous navigation using nonlinear model predictive control. *IFAC-PapersOnLine*, 51(20), 234–240.

Jacquet, M. & Franchi, A. (2022). Enforcing vision-based localization using perception constrained n-MPC for multi-rotor aerial vehicles. In *Proceedings of the International Conference on Intelligent Robots and Systems* (pp. 3621–3626).

Jiang, Z.-P. & Wang, Y. (2001). Input-to-state stability for discrete-time nonlinear systems. *Automatica*, 37(6), 857–869.

Jiang, Z.-P. & Wang, Y. (2002). A converse lyapunov theorem for discrete-time systems with disturbances. *System & Control Letters*, 45(1), 49–58.

Kamel, M., Alonso-Mora, J., Siegwart, R., & Nieto, J. (2017). Robust collision avoidance for multiple micro aerial vehicles using nonlinear model predictive control. In *Proceedings of the International Conference on Intelligent Robots and Systems* (pp. 236 – 243).

Kerrigan, E. C. (2000). *Robust Constraint Satisfaction: Invariant Sets and Predictive Control*. PhD thesis, University of Cambridge, Department of Engineering.

Kerrigan, E. C. & Maciejowski, J. M. (2000). Invariant sets for constrained nonlinear discrete-time systems with application to feasibility in model predictive control. In *Proceedings of the Conference on Decision and Control* (pp. 4951–4956).

Khalil, H. K. (2002). *Nonlinear systems*. Prentice-Hall, 3rd edition.

Kloeser, D., Schoels, T., Sartor, T., Zanelli, A., Prison, G., & Diehl, M. (2020). NMPC for racing using a singularity-free path-parametric model with obstacle avoidance. *IFAC-PapersOnLine*, 53(2), 14324–14329.

Kouvaritakis, B. & Cannon, M. (2016). *Model Predictive Control: Classical, Robust and Stochastic*. Springer International Publishing.

Langson, W., Chryssochoos, I., Rakovic, S. V., & Mayne, D. Q. (2004). Robust model predictive control using tubes. *Automatica*, 40(1), 125–133.

Le, V. T. H., Stoica, C., Alamo, T., Camacho, E. F., & Dumur, D. (2013). *Zonotopes: From Guaranteed State-estimation to Control*. John Wiley & Sons.

Lee, J. H. & Yu, J. (1997). Worst-case formulation of model predictive control for systems with bounded parameters. *Automatica*, 33(5), 763–781.

Limon, D., Alamo, T., Raimondo, D. M., de la Peña, D. M., Bravo, J. M., Ferramosca, A., & Camacho, E. F. (2009). Input-to-state stability: A unifying framework for robust model predictive control. In *Nonlinear Model Predictive Control* (pp. 1–26). Springer Berlin Heidelberg.

Limon, D., Alvarado, I., Alamo, T., & Camacho, E. (2008). MPC for tracking piecewise constant references for constrained linear systems. *Automatica*, 44(9), 2382–2387.

Limon, D., Alvarado, I., Alamo, T., & Camacho, E. (2010). Robust tube-based MPC for tracking of constrained linear systems with additive disturbances. *Journal of Process Control*, 20(3), 248–260.

Limon, D., Ferramosca, A., Alamo, T., González, A. H., & Odloak, D. (2012). Model predictive control for changing economic targets. In *Proceedings of the Nonlinear Model Predictive Control Conference* (pp. 384 – 391).

Limon, D., Ferramosca, A., Alvarado, I., & Alamo, T. (2018). Nonlinear MPC for tracking piece-wise constant reference signals. *IEEE Transactions on Automatic Control*, 63(11), 3735–3750.

Lucia, S., Subramanian, S., Limon, D., & Engell, S. (2020). Stability properties of multi-stage nonlinear model predictive control. *Systems & Control Letters*, 143, 1 – 9.

Luenberger, D. G. & Ye, Y. (2008). *Linear and Nonlinear Programming*. Springer.

Mayne, D., Rawlings, J., Rao, C., & Scokaert, P. (2000). Constrained model predictive control: Stability and optimality. *Automatica*, 36(6), 789–814.

Mayne, D. Q. (2014). Model predictive control: Recent developments and future promise. *Automatica*, 50(12), 2967–2986.

Mayne, D. Q., Raković, S. V., Findeisen, R., & Allgöwer, F. (2006). Robust output feedback model predictive control of constrained linear systems. *Automatica*, 42(7), 1217–1222.

Morari, M. & Maeder, U. (2012). Nonlinear offset-free model predictive control. *Automatica*, 48(9), 2059–2067.

Morato, M. M., Cunha, V., Santos, T. L. M., Normey-Rico, J., & Sename, O. (2023). A robust nonlinear tracking MPC using qLPV embedding and zonotopic uncertainty propagation. (pp. 1–31).

Nascimento, I. B. P., Ferramosca, A., Pimenta, L. C. A., & Raffo, G. V. (2019). NMPC strategy for a quadrotor UAV in a 3D unknown environment. In *Proceedings of the International Conference on Advanced Robotics* (pp. 179 – 184).

Nguyen, H.-N. (2014). *Constrained Control of Uncertain, Time-Varying, Discrete-time Systems: An interpolation-Based Approach*. Springer, 1st edition.

Pannocchia, G. & Kerrigan, E. C. (2005). Offset-free receding horizon control of constrained linear systems. *AIChE Journal*, 51(12), 3134–3146.

Paulson, J. A. & Mesbah, A. (2020). A low-complexity tube controller using contractive invariant sets. In *Proceedings of the Conference on Decision and Control* (pp. 1–7).

Pereira, J. C., Leite, V. J. S., & Raffo, G. V. (2019). Nonlinear model predictive control on SE(3) for quadrotor trajectory tracking and obstacle avoidance. In *Proceedings of the International Conference on Advanced Robotics* (pp. 155 – 160).

Pereira, J. C., Leite, V. J. S., & Raffo, G. V. (2021a). An ellipsoidal-polytopic based approach for aggressive navigation using nonlinear model predictive control. In *Proceedings of the International Conference on Unmanned Aircraft Systems* (pp. 827 – 835).

Pereira, J. C., Leite, V. J. S., & Raffo, G. V. (2021b). Nonlinear model predictive control on SE(3) for quadrotor aggressive maneuvers. *Journal of Intelligent & Robotic Systems*, 101(3), 1 – 15.

Pereira, L. A. A., Nunes, A. H. D., Rezende, A. M. C., Goncalves, V. M., Raffo, G. V., & Pimenta, L. C. A. (2021c). Collision-free vector field guidance and MPC for a fixed-wing UAV. In *Proceedings of the International Conference on Robotics and Automation* (pp. 176 – 182).

Raffo, G. V. (2011). *Robust Control Strategies for a Quadrotor Helicopter: An Underactuated Mechanical System*. PhD thesis, University of Seville.

Raffo, G. V., Ortega, M. G., & Rubio, F. R. (2011). Nonlinear $\mathcal{H}_\infty$ controller for the quad-rotor helicopter with input coupling. *IFAC-PapersOnLine*, 44(1), 13834–13839.

Raimondo, D. M., Marseglia, G. R., Braatz, R. D., & Scott, J. K. (2013). Fault-tolerant model predictive control with active fault isolation. In *Proceedings of the Conference on Control and Fault-Tolerant Systems*.

Raković, S. V., Zhang, S., Dai, L., Hao, Y., & Xia, Y. (2021). Convex model predictive control for collision avoidance. *IET Control Theory and Applications*, 15(9), 1270–1285.

Rao, C. V. & Rawlings, J. B. (1999). Steady states and constraints in model predictive control. *AIChE Journal*, 45(6), 1266–1278.

Rawlings, J. B. & Mayne, D. Q. (2009). *Model Predictive Control: Theory and Design*. Nob-Hill Publishing.

Sánchez, I., D'Jorge, A., Raffo, G. V., González, A. H., & Ferramosca, A. (2021). Nonlinear model predictive path following controller with obstacle avoidance. *Journal of Intelligent & Robotic Systems*, 102(1).

Santos, M. A., Ferramosca, A., & Raffo, G. V. (2021). Tracking nonlinear model predictive control for obstacle avoidance. In *Proceedings of the Latin American Robotics Symposium* (pp. 30 – 35).

Shim, D. H., Kim, H. J., & Sastry, S. (2003). Decentralized nonlinear model predictive control of multiple flying robots. In *Proceedings of the Conference on Decision and Control* (pp. 3621–3626).

Siciliano, B. & Khatib, O. (2016). *Handbook of Robotics*. Springer International Publishing.

Skokaert, P. & Mayne, D. (1998). Min-max feedback model predictive control for constrained linear systems. *IEEE Transactions on Automatic Control*, 43(1), 1136–1142.

Small, E., Sopasakis, P., Fresk, E., Patrinos, P., & Nikolakopoulos, G. (2019). Aerial navigation in obstructed environments with embedded nonlinear model predictive control. In *Proceedings of the European Control Conference* (pp. 3556–3563).

Spong, M. W., Hutchinson, S., & Vidyasagar, M. (2006). *Robot Modeling and Control*. John Wiley & Sons, Inc.

Tatjewski, P. (2008). Advanced control and on-line process optimization in multilayer structures. *Annual Reviews in Control*, 32(1), 71–85.

Thirugnanam, A., Zeng, J., & Sreenath, K. (2022). Duality-based convex optimization for real-time obstacle avoidance between polytopes with control barrier functions. In *Proceedings of the American Control Conference* (pp. 2239 – 2246).

Vidyasagar, M. (1993). *Nonlinear Systems Theory*. Prentice-Hall, 2nd ed. edition.

Vidyasagar, M. (2002). *Nonlinear Systems Analysis*. Society for Industrial and Applied Mathematics.

Wächter, A. & Biegler, L. T. (2005). Line search filter methods for nonlinear programming: Motivation and global convergence. *SIAM Journal on Optimization*, 16(1), 1–31.

Yu, S., Reble, M., Chen, H., & Allgöwer, F. (2014). Inherent robustness properties of quasi-infinite horizon nonlinear model predictive control. *Automatica*, 50(9), 2269–2280.

Zhang, X., Liniger, A., & Borrelli, F. (2021). Optimization-based collision avoidance. *IEEE Transactions on Control System Technology*, 29(3), 972–983.

A

Numerical Examples Models

For the sake of completeness, this Appendix describes with more details the models used in the numerical examples explored along the thesis.

A.1 Ball-on-plate

Consider the ball-on-plate system as described in Figure A.1. Based on a reference frame rigidly attached to the center of the plate, let p_1 and p_2 be the position of the ball along the axes of the reference frame and let θ_1 and θ_2 be the angle of the plate along those axes (see Figure A.1).

Thus, the mechanical system can be modeled as (Cotorruelo et al., 2021)

$$\begin{aligned}
\ddot{p}_1 &= \tfrac{m}{m+I_{ball}/r^2}(p_1\dot{\theta}_1^2 + p_2\dot{\theta}_1\dot{\theta}_2 + g\sin\theta_1),\\
\ddot{p}_2 &= \tfrac{m}{m+I_{ball}/r^2}(p_2\dot{\theta}_2^2 + p_1\dot{\theta}_1\dot{\theta}_2 + g\sin\theta_2),\\
\ddot{\theta}_1 &= a_1,\\
\ddot{\theta}_2 &= a_2,
\end{aligned} \tag{A.1}$$

with m, r, and I_{ball} being, respectively, the ball mass, radius, and inertia moment. Moreover, g is the gravitational acceleration.

Considering that the system is actuated through the desired angular acceleration of the plate, the state and input vectors can be defined, respectively, as $x = [p_1\ p_2\ \theta_1\ \theta_2\ \dot{p}_1\ \dot{p}_2\ \dot{\theta}_1\ \dot{\theta}_2]'$ and $u = [a_1\ a_2]'$. Further, the output of the system is the position of the ball $y = [p_1\ p_2]'$.

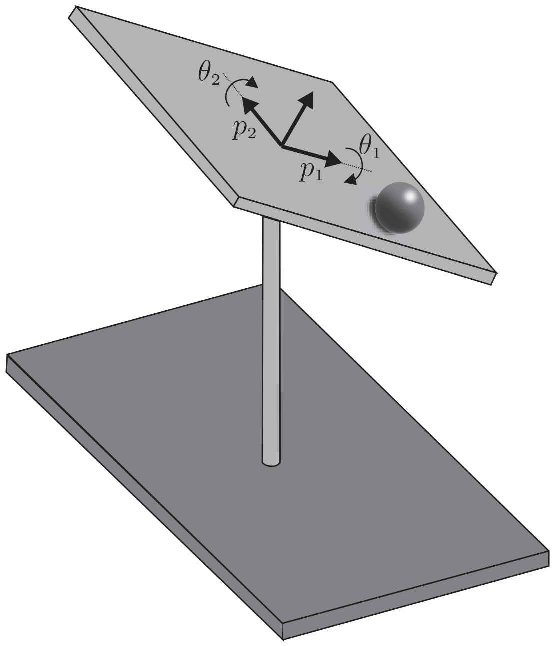

Figure A.1: Ball-on-plate system frames and variables definition.

The linear model can be obtained from (A.1) through the linearization around the equilibrium condition (x^{eq}, u^{eq}). Afterward, the linearized system is discretized considering first-order Euler approximation with sampling time T_s. The resulting discrete linear model is given by

$$\Delta x(k+1) = A_d \Delta x(k) + B_d \Delta u(k), \tag{A.2}$$

where $A_d = I_8 + T_s A$ and $B_d = T_s B$. Moreover, A and B are the Jacobians for the system $\dot{x} = f(x, u)$, i.e.,

$$A = \left.\frac{\partial f(x,u)}{\partial x}\right|_{\substack{x=x^{eq}\\u=u^{eq}}}, \quad B = \left.\frac{\partial f(x,u)}{\partial u}\right|_{\substack{x=x^{eq}\\u=u^{eq}}}. \tag{A.3}$$

Finally, the parameters considered for simulations are presented in Table A.1.

Table A.1: Ball-on-plate parameters.

Parameter description	**Parameter**	**Value**
Mass of the ball	m	0.05 [kg]
Ball radius	r	0.01 [m]
Moment of inertia around the ball axes	I_{ball}	$2.5 \cdot 10^{-6}$ [kgm^2]
Gravitational acceleration	g	9.81 [m/s^2]
Sampling time for discretization	T_s	0.25 [s]
Equilibrium condition for the states	x^{eq}	$O_{8,1}$
Equilibrium condition for the inputs	u^{eq}	$O_{2,1}$

A.2 Differential Mobile Robot

Consider an inertial frame, $\mathcal{I}$, and a moving frame, $\mathcal{B}$, rigidly attached to the robot center of rotation. The robot is considered to be actuated on the forward velocity, v, and the angular velocity, ω. Moreover, the generalized coordinates describing the robot in the workspace can be defined combining the robot position, x and y, and orientation, θ, with respect to the inertial frame. Figure A.2 illustrates the coordinated systems and variables considered.

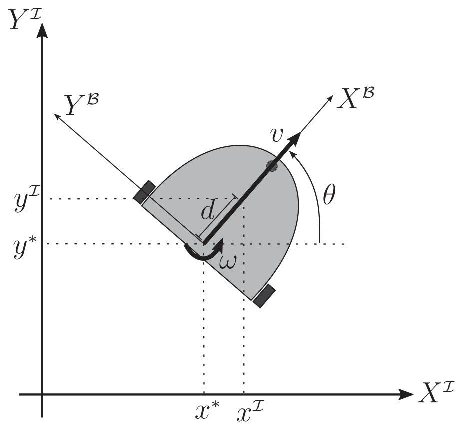

Figure A.2: Differential mobile robot with non-holonomic constraints frames and variables definition.

The kinematics can be described projecting the forward velocity in the $X^{\mathcal{I}}$-axis and $Y^{\mathcal{I}}$-axis, and defining the angular velocity equals to the orientation time derivative. Thus, the kinematic model can be written as (Siciliano & Khatib, 2016)

$$\begin{aligned} \dot{x}^* &= v\,\cos(\theta), \\ \dot{y}^* &= v\,\sin(\theta), \\ \dot{\theta} &= \omega. \end{aligned} \tag{A.4}$$

Further, it is possible to enhance the kinematic model (A.4) controllability defining the forward kinematics with respect to a point displaced from the rotation center by a distance d (see Figure A.2), which can be described as

$$\begin{aligned} x^{\mathcal{I}} &= x^* + d\,\cos(\theta), \\ y^{\mathcal{I}} &= y^* + d\,\sin(\theta). \end{aligned} \tag{A.5}$$

Taking the first time derivative of (A.5) and using equation (A.4), the modified kinematic model is given by

$$\begin{aligned} \dot{x}^{\mathcal{I}} &= v\,\cos(\theta) - d\omega\,\sin(\theta), \\ \dot{y}^{\mathcal{I}} &= v\,\sin(\theta) + d\omega\,\cos(\theta), \\ \dot{\theta} &= \omega, \end{aligned} \tag{A.6}$$

which can be expressed in the matrix form defining the state, input, and output vectors, respectively, as $x = [x^{\mathcal{I}}\ y^{\mathcal{I}}\ \theta]'$, $u = [v\ \omega]'$, and $y = [x^{\mathcal{I}}\ y^{\mathcal{I}}]'$, yielding to

$$\begin{aligned} \dot{x} &= \begin{bmatrix} \cos(\theta) & -d\,\sin(\theta) \\ \sin(\theta) & d\,\cos(\theta) \\ 0 & 1 \end{bmatrix} u, \\ y &= \begin{bmatrix} 1 & 0 & 0 \\ 0 & 1 & 0 \end{bmatrix} x. \end{aligned} \tag{A.7}$$

Finally, for simulation purposes, it is considered in this work $d = 0.1$.

A.3 Quadrotor UAV

The quadrotor can be seen as a rigid body described by a frame $\mathcal{B}$ rigidly attached to its center of rotation, a frame $\mathcal{C}$ rigidly attached to its center of mass, and an inertial frame $\mathcal{I}$ (see Figure A.3). The position of the body frame's origin represented in $\mathcal{I}$ is given by $\xi = [x^{\mathcal{I}}\ y^{\mathcal{I}}\ z^{\mathcal{I}}]'$ and its attitude by $\eta = [\phi\ \theta\ \psi]'$, considering the Euler angles with the ZYX convention about local axes. Figure A.3 shows the four propellers tilted towards the origin of $\mathcal{B}$ by an angle α, which is introduced, as explained in Raffo et al. (2011), to increase the controllability by allowing direct actuation on x and y without the necessity to employ augmented state vector nor cascade control strategies. On the other hand, it is worth noting that this procedure reduces the total lift force in the body Z-axis direction, thus, α is expected to be small aiming at a good trade-off between controllability and lifting power. Moreover, for modeling purposes, since the quadrotor is assumed to be a rigid body, then, the distance r between the frames $\mathcal{B}$ and $\mathcal{C}$ is constant. Thus, the generalized coordinates describing the quadrotor UAV motion can be chosen as $q = [\xi'\ \eta']'$. Finally, the system inputs are $u = [f_1\ f_2\ f_3\ f_4]'$, with f_i being the thrust force generated by the i-th rotor.

The dynamic model of the quadrotor UAV can be described by the Euler-Lagrange equations of motion as (Raffo, 2011)

$$M(q)\ddot{q} + C(q,\dot{q})\dot{q} + G(q) = B(q)u, \tag{A.8}$$

with $M(q) \in \mathbb{R}^{n\times n}$ denoting the inertia matrix, $C(q,\dot{q}) \in \mathbb{R}^{n\times n}$ denoting the Coriolis and centripetal forces matrix, $G(q) \in \mathbb{R}^n$ denoting the gravitational force vector, and $B(q) \in \mathbb{R}^{n\times m}$

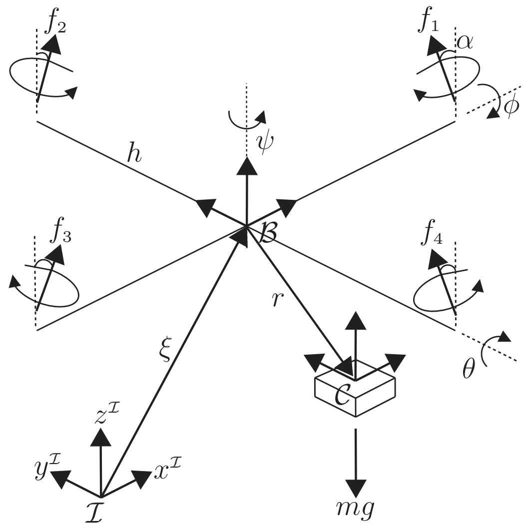

Figure A.3: Quadrotor UAV frames and variables definition.

denoting the force matrix.

The inertia matrix and the gravitational force vector can be written, respectively, as

$$M(q) = \begin{bmatrix} mI_3 & -mR_{\mathcal{B}}^{\mathcal{I}} S(r) W_\eta \\ -m(R_{\mathcal{B}}^{\mathcal{I}} S(r) W_\eta)' & J(\eta) \end{bmatrix}, \tag{A.9}$$

$$G(q) = \begin{bmatrix} 0 \\ 0 \\ mg \\ -mg\left(-r_y c_\theta c_\phi + r_z c_\theta s_\phi\right) \\ -mg\left(r_x c_\theta + r_y s_\theta s_\phi + r_z s_\theta c_\phi\right) \\ 0 \end{bmatrix}, \tag{A.10}$$

where $R_{\mathcal{B}}^{\mathcal{I}}$ denotes the rotation matrix between $\mathcal{B}$ and $\mathcal{I}$, $S(\cdot)$ denotes the skew symmetric matrix (Spong et al., 2006), $r = [r_x \ r_y \ r_z]'$, m is the UAV mass, g is the gravitational acceleration, I_3 represents an identity matrix with dimension $\mathbb{R}^{3\times 3}$, $s_{(\cdot)} = \sin(\cdot)$, and $c_{(\cdot)} = \cos(\cdot)$. Further, $J(\eta) = W_\eta' I_{UAV} W_\eta$, with I_{UAV} being the moment of inertia, and

$$W_\eta = \begin{bmatrix} 1 & 0 & -s_\theta \\ 0 & c_\phi & s_\phi c_\theta \\ 0 & -s_\phi & c_\phi c_\theta \end{bmatrix}.$$

Additionally, the Coriolis and centripetal forces matrix, $C(q, \dot{q})$, is obtained by using the Christoffel symbols of first kind (Spong et al., 2006).

The generalized force vector can be defined as

$$\begin{bmatrix} f_\xi \\ \tau_\eta \end{bmatrix} = B(q)u, \tag{A.11}$$

where $f_\xi = R_\mathcal{B}^\mathcal{I} f_a$ represents the translational force vector, and $\tau_\eta = W_\eta' \tau_a$ represents the total attitude moments, both expressed in the inertial reference frame.

Inspecting Figure A.3, it is easy to see that f_a and τ_a can be expressed as

$$f_a = \begin{bmatrix} s_\alpha (f_3 - f_1) \\ s_\alpha (f_4 - f_2) \\ c_\alpha \sum_{i=1}^{4} f_i \end{bmatrix}, \quad \tau_a = \begin{bmatrix} hc_\alpha (f_2 - f_4) \\ hc_\alpha (f_3 - f_1) \\ c_\alpha \sum_{i=1}^{4} \tau_{M_i} \end{bmatrix}, \tag{A.12}$$

where h is the distance between the rotors and the center of rotation, and τ_{M_i} is the motor torsion effort.

The lift force generated by each rotor can be approximated by $f_i = b\Omega_i^2$ and its torsion effort by $\tau_{M_i} = k_\tau \Omega_i^2$ (Castillo et al., 2005), with Ω_i being the angular velocity of the i-th rotor around its axis, b being the thrust coefficient, and $k_\tau > 0$ being a drag coefficient. Therefore, using equations (A.11) and (A.12), the force matrix $B(q)$ can be written as

$$B(q) = \begin{bmatrix} R_\mathcal{B}^\mathcal{I} & O_{3,3} \\ O_{3,3} & W_\eta' \end{bmatrix} \begin{bmatrix} -s_\alpha & 0 & s_\alpha & 0 \\ 0 & -s_\alpha & 0 & s_\alpha \\ c_\alpha & c_\alpha & c_\alpha & c_\alpha \\ 0 & hc_\alpha & 0 & -hc_\alpha \\ -hc_\alpha & 0 & hc_\alpha & 0 \\ \frac{k_\tau}{b} c_\alpha & -\frac{k_\tau}{b} c_\alpha & \frac{k_\tau}{b} c_\alpha & -\frac{k_\tau}{b} c_\alpha \end{bmatrix}. \tag{A.13}$$

After all terms of the equation (A.8) are obtained, it is possible to rewrite the equations of motion in the state-space representation, yielding to

$$\dot{x} = f(x,u) = \begin{bmatrix} \dot{q} \\ \ddot{q} \end{bmatrix} = \begin{bmatrix} \dot{q} \\ M^{-1}[Bu - C\dot{q} - G] \end{bmatrix}. \tag{A.14}$$

The presented dynamical model takes into account the coupling between translational and rotational dynamics due to the displacement between the quadrotor's geometric center and its center of mass. This complete model aims to better emulate the vehicle dynamics during the simulation; however, for control design purposes, this displacement is neglected, and a simplified version of the model is considered.

Additionally, for formulations requiring linear discrete representations, the model (A.14) can be linearized and discretized around an equilibrium condition. Therefore, we have

$$\Delta\dot{x} = A\Delta x + B\Delta u, \tag{A.15}$$

where

$$A = \left.\frac{\partial f(x,u)}{\partial x}\right|_{\substack{x=x^{eq} \\ u=u^{eq}}}, \quad B = \left.\frac{\partial f(x,u)}{\partial u}\right|_{\substack{x=x^{eq} \\ u=u^{eq}}}, \tag{A.16}$$

with x^{eq} and u^{eq} being the equilibrium states and inputs obtained considering $q^{eq} = [(\xi^{eq})' \ (\eta^{eq})']'$ and $u^{eq} = [f_1^{eq} \ f_2^{eq} \ f_3^{eq} \ f_4^{eq}]'$, with f_i^{eq} being the thrust required to keep the vehicle in hovering without external disturbances.

The discrete linearized model can be obtained after mapping (A.15) from the continuous-time to the discrete-time domain, yielding to

$$\Delta x(k+1) = A_d \Delta x(k) + B_d \Delta u(k), \tag{A.17}$$

with A_d and B_d being obtained after discretizing the model using the first-order Euler approximation with sampling time T_s.

Finally, the parameters considered for simulation are presented in Table A.2.

Table A.2: Quadrotor UAV parameters.

Parameter description	**Parameter**	**Value**
Mass of the Quadrotor UAV	m	2.24 [kg]
Distance between the mass center and the rotors	h	0.332 [m]
Gravitational acceleration	g	9.81 [m/s^2]
Thrust coefficient of the rotors	b	$9.5 \cdot 10^{-6}$ [Ns^2]
Drag coefficient of the rotors	k_τ	$1.7 \cdot 10^{-7}$ [Nms^2]
Tilt angle of the rotors	α	5 [°]
Moment of inertia around the x-axis	$I_{UAV,xx}$	0.0363 [kgm^2]
Moment of inertia around the y-axis	$I_{UAV,yy}$	0.0363 [kgm^2]
Moment of inertia around the z-axis	$I_{UAV,zz}$	0.0615 [kgm^2]
Position x of the center of mass expressed in $\mathcal{B}$	r_x	-0.00069 [m]
Position y of the center of mass expressed in $\mathcal{B}$	r_y	-0.0014 [m]
Position z of the center of mass expressed in $\mathcal{B}$	r_z	-0.0311 [m]
Sampling time for discretization	T_s	0.01 [s]
Equilibrium condition for the states	x^{eq}	$O_{12,1}$
Equilibrium condition for the inputs	u^{eq}	$5.5146 I_4$